AN ABSTRACT OF THE THESIS OF

Philip L. Barbour for the degree of Master of Science in Atmospheric Sciences presented on March 16, 1992.

Title: The Use of Conserved Variables in the Modeling and Parameterization of Shallow Cumulus Trade Wind Boundary Layers

Abstract approved: Redacted for Privacy

A time dependent model of the shallow, tropical convective boundary layer is developed and tested. To simplify the treatment of thermodynamic processes and return to first principles of physics, conserved quantities of entropy and total water density are used as primary model variables. In addition, a new shallow cumulus parameterization scheme is developed and is based on the use of a time dependent cloud kinetic energy equation combining local concepts of cloud processes with the use of a special buoyancy length scale. Two model simulations are performed in an attempt to assess the model's performance and the effectiveness of the parameterization scheme.

Results indicate that the model does a reasonable job in both representing the equilibrium structure of a shallow convective boundary layer and in generating a realistic boundary layer structure from an initial state consisting of a shallow moist layer with dry air aloft. The cumulus parameterization scheme appears to adequately represent the transport of thermodynamic quantities associated with convective activity and the use of conserved variables provides an effective way of representing the boundary layer structure and treating the mixing processes associated with cloud processes.

This work illustrates the usefulness of generalized conserved variables,

particularly entropy and total water density, and indicates that the general approach of using a time dependent cloud kinetic energy equation may be effective for representing thermodynamic processes in the tropical boundary layer.

The Use of Conserved Variables in the Modeling and Parameterization of Shallow Cumulus Trade Wind Boundary Layers

By

Philip L. Barbour

A THESIS

submitted to

Oregon State University

in partial fulfillment of
the requirements for the
degree of

Master of Science

Completed March 16, 1992

Commencement June 1992

APPROVED:

Redacted for Privacy

Professor of Atmospheric Sciences, in charge of major

Redacted for Privacy

Head of department of Atmospheric Sciences

Redacted for Privacy

Dean of G[illegible]

Date thesis presented March 16, 1992

Thesis Prepared by Philip L. Barbour

TABLE OF CONTENTS

TABLE OF CONTENTS (CONT.)

List of Figures

The Use of Conserved Variables in the Modeling and Parameterization of Shallow Cumulus Trade Wind Boundary Layers

1. INTRODUCTION

The tropical oceans cover an extensive region of the globe and receive a large proportion of the Earth's incoming solar radiation. Much of this radiation is returned to the atmosphere as sensible or latent heat that is eventually transported equatorward in the low level flow of the easterly trades. Riehl and Malkus (1957) showed that the transport of this sensible and latent heat is an important element in supplying energy to fuel the deep disturbances of the Inter-Tropical Convergence Zone and in providing energy to help maintain the tropical Hadley circulation. By regulating the exchanges of heat and moisture across the ocean surface, the tropical Convective Boundary Layer (CBL) plays an important role in determining the structure of the general circulation in the tropics.

Early studies of trade wind regions concentrated on this downstream moistening and warming process (Riehl et al.1951; Malkus 1956). These studies showed that the tropical CBL possesses an extremely persistent and characteristic vertical structure of temperature and moisture. This structure is made up of a series of well defined layers including a *surface boundary layer* characterized by a strong wind shear instability and a weak gravitational instability, a *subcloud mixed layer* where the temperature decrease is near adiabatic and the moisture profile is constant, a slightly stable *transition layer* where the moisture content decreases, a conditionally unstable *cloud layer* dominated by convective processes and a *trade inversion* characterized by an increase in temperature and a sharp decrease in humidity. The cloud layer typically contains a number of shallow non-

precipitating cumulus clouds that rise to various levels before dissipating.

Once the importance of the tropical CBL was recognized, an attempt was made to understand in greater detail the processes involved in maintaining its uniform and persistent structure. The Atlantic Trade-Wind Experiment (ATEX) and the Barbados Oceanographic and Meteorological Experiment (BOMEX) were conducted in 1969 in an attempt to quantify the magnitudes of the CBL processes acting on space and time scales indicative of boundary layer processes. Holland and Rasmusson (1973) used the BOMEX data to compute the mean heat, moisture and momentum budgets for a five day period of undisturbed convection and to obtain estimates of the magnitudes of subgrid-scale processes. The study emphasized the existence of subsidence over the entire depth of the CBL and led to the determination that the characteristic trade inversion is not a material boundary but rather the result of interactions between several physical processes. A study by Nitta and Esbensen (1974) showed similar results for the same undisturbed period. Evidence of a moisture source and heat sink in the upper portion of the cloud layer was also presented and thought to be a result of evaporative cooling associated with decaying cumulus cells. The magnitude of the convective scale processes were estimated to be large enough to maintain the inversion against the warming and drying effects of large scale subsidence. Using idealized concepts of cloud processes in a simple layered model, Betts (1973) also showed that the cooling and moistening associated with detraining cumulus elements was sufficient to maintain the characteristic trade wind inversion structure. The importance of these studies was to introduce the concept of an equilibrium balance between the convective processes of the CBL and the large scale processes of the tropics.

The cloud layer is seen to play a major role in maintaining this equilibrium balance and yet, to date, few attempts have been made to obtain reliable measurements of cloud layer heat and moisture fluxes. This is due in part to instrumentation problems associated with making in-cloud measurements of temperature and moisture (see Blyth et al., 1988). Temperature and humidity

sensors often become wet and unreliable when used at high speeds inside clouds. They also have response times too slow to be useful in computing eddy correlation quantities. The lack of reliable measurements is also partly due to the relatively small fraction of area occupied by clouds at any given time. It is difficult to obtain a sufficient sampling to produce statistically reliable values.

In the absence of experimental data, diagnostic and prognostic models of cloud populations have been developed to provide an internally consistent interpretation of CBL processes. These models differ significantly in assumptions and complexity but have the common goal of interpreting the role and magnitude of convective and other sub-grid scale processes. Diagnostic models generally attempt to diagnose the magnitude of convective processes using observed heat and moisture budgets as constraints. Convective properties are then analysed using simple conceptual cloud models. For example, Betts (1975) used a simple one dimensional parametric model to interpret the magnitude and structure of convective processes during BOMEX. His parametric model included a single cloud type that entrained and detrained at all levels. Applying this cloud model to the BOMEX heat and moisture budgets he found that the diagnosed cloud detrainment rates were substantially larger than the entrainment rates, leading to the conclusion that cloud detrainment may be the dominant process in the cloud layer under shallow convective conditions. Nitta (1975) used the spectral cloud model of Arakawa and Schubert (1974) to obtain a similar interpretation of the BOMEX convective transports and observed that most clouds detrained below the trade inversion. This detrainment was responsible for the cooling and moistening of the upper cloud layer. Esbensen (1978) used separate cloud models to represent deep and shallow convection to further examine the BOMEX budgets. What he found was that the convective buoyancy of shallow cumulus are much less than for deeper convection and illustrated that the important processes for each case may be distinct different and must be represented differently

Time dependent models have also been used to interpret convective boundary

layer processes by integrating a set of prognostic equations over time until an equilibrium state of the model is reached. Convective properties appear as terms in the prognostic equations that must be parameterized in terms of the mean model variables. Albrecht et al. (1979) for example developed a simple layered model of the convective boundary layer that has been used to interpret boundary layer structures and to study the downstream variation in the trades (Albrecht 1984). This model consists of separate prediction equations for thermodynamic quantities at various levels of the model and also includes a prediction equation for the height of the inversion. This model has been used to obtain estimates of the equilibrium structure of the trades.

A variety of other budget models have been used to study the equilibrium structure of the tropical CBL. Among these are models by Ogura (1977), Albrecht (1979), Sarachik (1978), Betts and Ridgway (1987) and Betts (1989). Each of these are important in that they illustrate the complex balance between the various physical processes involved. For example Sarachik (1978) coupled a one dimensional model to the sea surface temperature, reasoning that only a fully coupled model was capable of determining the full equilibrium structure of the CBL. This work implied that the equilibrium structure of the CBL was not only dependent upon the local forcing but also on the time scales over which these forcing mechanisms act. Betts and Ridgway (1987) and Betts (1989) used their diagnostic model to study the interactions and adjustments on several different time scales ranging from two days to 100 days and noted the importance of radiation in helping maintain the equilibrium structure of the trades.

In other work, Betts (1982,1987) has shown that cloud layer profiles of temperature and moisture can be represented using saturation point analysis. This process consists of defining a saturation point for each level of the sounding that represents a conserved property of that level. Betts found that all of the saturation points through the cloud layer lie nearly on a straight line drawn between the

saturation points for air directly above the trade inversion and air in the subcloud layer. Using BOMEX and ATEX data, Betts (1986) interpreted this to mean that the equilibrium structure of the cloud layer can be considered the net result of a simple mixing process between mid tropospheric air and sub cloud mixed layer air. The actual interactions between the processes involved may be extremely complex but the net effect can be represented by a simple mixing line structure. This concept has become the basis for a shallow convective adjustment scheme.

Another important aspect of the work by Betts (1982,1987) and of the work of Paluch (1979), Raymond and Blyth (1986) and Blyth et. al. (1988) is the use of conserved variables and conserved variable diagrams when dealing with cloud mixing processes. Conserved variables provide an extremely convenient way of representing the state of any system especially when mixing processes are involved.

In spite of the effort that has been put towards studying the trade wind boundary layer, many aspects are still not fully understood. For example, very little is known about the exact nature of boundary layer clouds and how they act to transport heat and moisture. There is also very little information about the interaction between the cloud layer and the subcloud mixed layer. The purpose of the research in this thesis is to examine a few of these unknown areas and to take a slightly different approach at constructing a model to obtain the equilibrium structure of the tropical convective boundary layer.

This thesis concentrates on three topics. The first deals with the use of conserved variables in the development and testing of a one dimensional time dependent model of the tropical convective boundary layer. By using conserved variables, many of the traditional assumptions used in treating thermodynamic processes can be reexamined and in some cases eliminated. The second aspect is the description and results of a new scheme for parameterizing the transports of thermodynamic quantities associated with shallow convection. This method is based on some assumed physical properties of clouds and is rooted in the assumption that

local balance arguments are sufficient to characterize cloud scale transports of heat and moisture. The third element of this work examines the interaction between the cloud layer and the subcloud mixed layer. Little is known about the interaction between these two layers and certain features of this model should provide insight into some elements of their interaction.

2. THE MODEL

One component of this thesis involves the construction of a one-dimensional, time-dependent, hydrostatic model designed to explore the equilibrium structure that exists between the tropical CBL and larger scale forcing processes. To accomplish this, a unique modeling approach is taken that involves the direct use of the first principles of physics in the governing equations. The method has been proposed by Ooyama (1990), and consists of a return to first principles as a means of separating the role of thermodynamics from the role of dynamics in the governing equations. This achieves two main goals. First, the separation allows the thermodynamic state of the system to be determined solely through thermodynamic considerations rather than through a combination of thermodynamics and dynamics; and secondly, it allows the model to be developed in a modular fashion that provides an easy method of transition between hydrostatic and non-hydrostatic approaches.

A variety of approaches have been developed to model different aspects of the atmosphere. Hydrostatic models in pressure and sigma coordinates have been used successfully to model large-scale atmospheric motions (Phillips, 1957) and tropical cyclones (Rosenthal, 1978) and non-hydrostatic models using geometric height (z) coordinates have been used to study mesoscale convective systems (Klemp and Wilhelmson, 1977). For all the differences that exist in these approaches, a few common elements are present. The first has to do with the treatment of moist thermodynamic processes. For the most part these models do not begin with laws that conservatively treat the phase changes of water. For example, most models contain separate equations for moisture and liquid water content, making the transition between an unsaturated state and a saturated state clumsy and often poorly represented. Secondly, once a set of equations is obtained using the hydrostatic assumption, the configuration cannot be changed without

writing a new set of equations. A third common element of these models is that they generally determine pressure through dynamical arguments. While pressure does influence the dynamics of a system, it is also a state variable. If pressure is predicted, as in many non-hydrostatic models, then the thermodynamics are determined by the dynamics of the system and not explicitly defined in terms of the thermal and chemical state.

The use of a method that conservatively treats the phase change of water is of particular interest in modeling atmospheric systems. This is especially true in the tropics where the release of latent heat plays a major role in maintaining the large scale Hadley circulation. Even small errors in treating surface evaporation and moisture properties can have a tremendous impact on the amount of energy available to drive circulation patterns.

The above points are not meant as a condemnation of past modeling approaches, but rather serve as the basic motivation behind the approach taken in this thesis. It is important to note that applying assumptions early in the development stage may provide computational advantages but may also restrict a model to a narrowly specified purpose.

2.1) Prognostic Equations

The prognostic equations used in this model follow directly from work done by Ooyama (1990) and are based on the conservation laws of mass, momentum and energy. For the moist atmosphere, continuity equations can be written for both the density of dry air ($\xi = m_a/V$) and total airborne water ($\eta = m_v/V$). The total airborne water includes both water vapor and the portion condensate that moves with the air. Moist entropy density ($\sigma = \rho S$) will be used to represent the conservation of energy and the two components of the horizontal momentum equation (U,V) will be used to represent momentum conservation. This particular

combination of variables is well suited for atmospheric modeling for two reasons. First, each of the five variables is conserved for moist adiabatic motions and can be expressed in terms of the first principles of physics. Secondly, a natural separation is made between the equations representing the thermodynamic properties of the system and those representing the dynamic properties. Equations for these variables may then be written in flux form as

$$\frac{\partial \xi}{\partial t} + \nabla \cdot (\xi \mathbf{v}) + \frac{\partial}{\partial z}(\xi w) = 0 \qquad (2.1a)$$

$$\frac{\partial \eta}{\partial t} + \nabla \cdot (\eta \mathbf{v}) + \frac{\partial}{\partial z}(\eta w) = 0 \qquad (2.1b)$$

$$\frac{\partial \sigma}{\partial t} + \nabla \cdot (\sigma \mathbf{v}) + \frac{\partial}{\partial z}(\sigma w) = Q_{\sigma_R} \qquad (2.1c)$$

$$\frac{\partial \mathbf{V}_H}{\partial t} + \nabla \cdot (\mathbf{V}_H \mathbf{v}) + \frac{\partial}{\partial z}(\mathbf{V}_H w) + f\mathbf{k}\times\mathbf{V}_H + \nabla P = 0 \qquad (2.1d)$$

The only non-adiabatic effects to be included are those associated with radiation and, because entropy is the only variable influenced by radiative properties, a Q term has been included in the equation for entropy density and will be treated in a later section. In this model, hydrostatic balance will be used as a separate constraint to derive a diagnostic equation for vertical velocity that is consistent with the above equations.

In a frictionless, adiabatic system the global integration of ξ, η and σ are conserved. However, they are not necessarily conserved for processes acting within the system. For example, because of the density factor involved σ is not conserved following a rising parcel of air. To treat adiabatic motions within the system, the correct variable to use would be specific entropy (s) rather than entropy density (σ). The variables that will be used to conservatively treat these interior processes will be the specific entropy (s) and the total water mixing ratio (r).

If it were necessary to relax the hydrostatic assumption and convert this

system to a non-hydrostatic framework, an additional prognostic equation for vertical velocity could be included. No changes are necessary in the other prognostic equation greatly simplifying the transition between a hydrostatic and non-hydrostatic approach is greatly simplified.

To apply this set of equations within a one-dimensional framework we will separate each variable into a zonal mean and perturbation part. Because of the nontraditional nature of the variables used here, care will be taken when applying the usual Reynolds averaging approximations. To illustrate the steps that are needed to obtain a working set of model equations, the derivation of the entropy equation will be used. The derivation of other model variables follow in a similar manner.

After separating variables into zonal mean and perturbation parts and after applying the Reynolds averaging assumptions we obtain an equation of the form

$$\frac{\partial[\sigma]}{\partial t} = -\nabla_H\cdot[\sigma][\mathbf{v}_H] - \frac{\partial[\sigma][w]}{\partial z} - \nabla_H\cdot[\sigma^*\mathbf{v}_H^*] - \frac{\partial[\sigma^* w^*]}{\partial z} + [Q_{\sigma_D}] \qquad (2.2)$$

In this study, the mean scale velocity components $[\mathbf{v}_H]$ and $[w]$ will be partitioned into a steady planetary scale component that will be imposed and a time dependent, explicitly resolved component. The time-dependent vertical velocity acts as an adjustment term that continually acts to restore hydrostatic balance. After separating the vertical velocity components into two parts $[w] = [w_s] + [w]$ we arrive at an expression for the time rate of change of entropy density in the form

$$\frac{\partial[\sigma]}{\partial t} = -[\sigma]\left(\nabla_H\cdot[\mathbf{v}_H] + \frac{\partial[w_s]}{\partial z}\right) - [\mathbf{v}_H]\cdot\nabla_H[\sigma] - [w_s]\frac{\partial[\sigma]}{\partial z} - \frac{\partial[w\sigma]}{\partial z}$$

$$- \nabla_H\cdot[\sigma^*\mathbf{v}_H^*] - \frac{\partial[\sigma^* w^*]}{\partial z} + [Q_{\sigma_P}] \qquad (2.3)$$

We now introduce several approximations into (2.3). The first approximation is that horizontal variations of explicitly resolved model quantities can be considered small and can be represented as being locally homogeneous in the horizontal. As a

consequence, the advective terms in the prognostic equations are neglected. The two terms representing the vertical transport of mean-scale specific entropy are considered to be the combination of two effects. The first of these involves the vertical transport associated with the imposed, steady large-scale subsidence. The second effect is the transport of specific entropy that results from the explicitly calculated vertical motion. Because of the hydrostatic nature of this model, this term represents the small adjustment necessary to keep the system in hydrostatic balance in the presence of the various mechanisms that force the system from hydrostatic balance.

The subgrid-scale diffusion terms that emerge from this averaging process also need to be explored in order to ensure that the conserved properties are maintained. For entropy, the vertical diffusion term in (2.3) takes the form

$$\frac{\partial \sigma}{\partial t}\Big|_D = -\frac{\partial}{\partial z}[\sigma^{\cdot} w^{\cdot}]$$

At the level of approximation considered here, eddy transports involving factors of density will be neglected. To remove the density portion, it is necessary to express the flux quantity above in a slightly different manner. This involves using the definition of entropy to separate it as

$$\sigma = \rho s = [\rho]([s] + s^{\cdot})$$
$$[\sigma] = \quad = [\rho][s]$$

leaving an expression for the entropy perturbation of the form

$$\sigma^{\cdot} = \sigma - [\sigma] = [\rho]s^{\cdot}$$

When this is substituted into the above diffusion expression, the result is one term of the form

$$= -\frac{\partial}{\partial z}([\rho][w^{\cdot}s^{\cdot}]) \qquad (2.4)$$

This expression represents the sub-grid scale transport of entropy. This model will consider that contributions to this transport are made from both boundary layer diffusive processes and convective processes. These processes will be considered separately and in greater detail in a later section. To simplify the

notation here we will let

$$Q_{\sigma_D} = -\frac{\partial}{\partial z}([\rho][\overline{w's'}]) \quad \text{Diffusion}$$

$$Q_{\sigma_C} = -\frac{\partial}{\partial z}([\rho][\overline{w's'}]) \quad \text{Convection}$$

and group these forcing terms together in a single Q term as

$$Q_\sigma = Q_{\sigma_R} + Q_{\sigma_D} + Q_{\sigma_C}$$

Using similar simplifications for the other prognostic variable and after dropping brackets, we obtain a complete set of equations of the form

$$\frac{\partial \xi}{\partial t} = -\xi\left(\nabla_H \cdot v_H + \frac{\partial w_s}{\partial z} + \frac{w_s}{\xi}\frac{\partial \xi}{\partial z} \right) - \frac{\partial}{\partial z}(w\xi) + Q_\xi \qquad (2.5a)$$

$$\frac{\partial \eta}{\partial t} = -\eta\left(\nabla_H \cdot v_H + \frac{\partial w_s}{\partial z} + \frac{w_s}{\xi}\frac{\partial \xi}{\partial z} \right) - \xi w_s \frac{\partial r}{\partial z} - \frac{\partial w\eta}{\partial z} + Q_\eta \qquad (2.5b)$$

$$\frac{\partial \sigma}{\partial t} = -\sigma\left(\nabla_H \cdot v_H + \frac{\partial w_s}{\partial z} + \frac{w_s}{\xi}\frac{\partial \xi}{\partial z} \right) - \xi w_s \frac{\partial s}{\partial z} - \frac{\partial w\sigma}{\partial z} + Q_\sigma \qquad (2.5c)$$

$$\frac{\partial U}{\partial t} = -U\left(\nabla_H \cdot v_H + \frac{\partial w_s}{\partial z} + \frac{w_s}{\xi}\frac{\partial \xi}{\partial z} \right) - \xi w_s \frac{\partial u}{\partial z} - \frac{\partial wU}{\partial z} + fV + Q_U \qquad (2.5d)$$

$$\frac{\partial V}{\partial t} = -V\left(\nabla_H \cdot v_H + \frac{\partial w_s}{\partial z} + \frac{w_s}{\xi}\frac{\partial \xi}{\partial z} \right) - \xi w_s \frac{\partial v}{\partial z} - \frac{\partial wV}{\partial z} - fU - \frac{\partial P}{\partial y} + Q_V \qquad (2.5e)$$

The term in brackets is common to each of the equations and represents the effects of the large-scale horizontal and vertical dry-air mass balance. The one-dimensional framework of this model does not allow the spatial gradients of the horizontal momentum terms to be determined, therefore using an assumption of quasi-incompressibility, the bracketed terms will be considered negligible and neglected in the current model.

This quasi-incompressibility assumption implies that changes in dry air density can only come about as a result of the explicitly resolved vertical motion of the model and that the large scale effects of subsidence and horizontal divergence have no net effect on the underlying dry-air density structure. In a completely dry

atmosphere, this assumption of quasi-incompressibility would reduce to the usual assumption of incompressibility used in many models. The approach taken here is adopted in part to overcome our inability to determine horizontal gradients. It is also a way of maintaining consistency between the mass balance of the model and the use of the hydrostatic equation as a constraint to diagnose the model resolved vertical velocity.

As a result of neglecting the terms in brackets from Eqs. (2.5a-e) a simplified set of equations can be obtained and take the form

$$\frac{\partial \xi}{\partial t} = -\frac{\partial}{\partial z}(w\xi) + Q_\xi \tag{2.6a}$$

$$\frac{\partial \eta}{\partial t} = -\xi w_s \frac{\partial r}{\partial z} - \frac{\partial w\eta}{\partial z} + Q_\eta \tag{2.6b}$$

$$\frac{\partial \sigma}{\partial t} = -\xi w_s \frac{\partial s}{\partial z} - \frac{\partial w\sigma}{\partial z} + Q_\sigma \tag{2.6c}$$

$$\frac{\partial U}{\partial t} = -\xi w_s \frac{\partial u}{\partial z} - \frac{\partial wU}{\partial z} + fV + Q_U \tag{2.6d}$$

$$\frac{\partial V}{\partial t} = -\xi w_s \frac{\partial v}{\partial z} - \frac{\partial wV}{\partial z} - fU - \frac{\partial P}{\partial y} + Q_U \tag{2.6e}$$

Ideally, this quasi-incompressibility assumption is not necessary. It should be possible to include a specified divergence profile and use the hydrostatic maintenance condition to diagnose a vertical velocity that represents combined effects of both the planetary-scale and model resolved vertical velocities. However, even small errors in this diagnosed vertical velocity would lead to a large-scale mass budget imbalance and could result in a systematic change in the density structure of the model. Because of the uncertainties involved in defining a divergence profile, an imbalance is very possible and could have a tremendous impact on the model's ability to treat boundary layer properties.

The effects of imposed large-scale subsidence in Eqs. (2.6b-e) comes through as an advection of specific entropy and total water mixing ratio. These terms play a major role in determining the structure of the tropical convective boundary layer. The pressure gradient and coriolis terms have been retained in the horizontal

momentum equations to enable a specified forcing to be included to drive the horizontal winds. The sub-grid scale transport terms and the effects of radiation have been combined and represented as a single Q term. The parameterization of these terms is discussed in section 2.3.

The Q term was retained for symmetry in (2.6a) and will be set to zero for our calculations. The only way that dry air density can change is as a result of the hydrostatic adjustment process and depends on the magnitude of the model resolved vertical velocity. In this way, the dry air density equation plays an active role in maintaining hydrostatic balance in the model.

2.2) Diagnostic Variables

Using the five prognostic variables $\{U,V,\xi,\eta,\sigma\}$, it is possible to diagnose both the thermodynamic state of the system and the vertical velocity. The thermodynamic state can be defined by obtaining values for the temperature and the pressure from the predicted values of $\{\xi,\eta,\sigma\}$, while the vertical velocity can be determined diagnostically using the hydrostatic equation in conjunction with the hydrostatic maintenance approximation. The determination of these variables depends on several assumptions about the thermodynamics of the system. These assumptions include

- There exists within each volume element a chemical and thermal equilibrium between the various phases of water. This implies that the temperature is the same for each component of a mixture of phases and rules out any occurrence of super-cooled droplets.
- The volume occupied by any condensate is negligible compared to the volumes of water vapor and dry air.
- Dalton's law of partial pressures holds, allowing separate gas laws to be

written for the water vapor and dry air.

- In the absence of ice, all specific heat values are assumed constant with respect to temperature.

2.2a) Temperature Functions

There are several temperature dependent functions and laws that must be defined and calculated to compute the temperature and pressure of the system.

$E(T)$ The saturation vapor pressure is considered only a function of temperature and will be computed using tabulated values compiled from the Goff-Gratch formulas.

$\eta^*(T) = E(T)/(R_v T)$ The saturation vapor density or the density of water vapor under saturated conditions. This is used primarily for determining the saturation condition of the system.

$L(T)$ The latent heat of vaporization/evaporation is computed using the integrated Kirchoff law assuming constant specific heats.

$dE(T)/dT = (L(T)E(T)) \ / \ (R_v T)$ The Clausius-Clapeyron equation.

2.2b) Temperature Diagnosis.

To determine the temperature diagnostically, an equation defining entropy must be obtained that includes the prognostic variables of the system. It is necessary to derive two separate equations, one for a mixture of dry air and water vapor below saturation and one for saturation conditions that includes condensed water. This is the approach taken by Ooyama 1990. It may be possible to develop a single equation that could be used for both conditions, (Emanuel and Rotuno 1989) but the present approach involves fewer approximations in the moist thermodynamics.

To derive the equations defining the entropy of the system, we use Gibbs

theorem. Gibbs theorem states that the total entropy of a given volume containing one or more phases of a given substance is the sum of the partial entropies of the individual phases assuming they are mixed under reversible conditions (Iribarne and Godson, 1981). As long as phase changes occur isentropically, there is no change in entropy due to mixing. In this way the two forms of total entropy may be written as

$$dS_1 = dS_a + dS_v \qquad \text{for unsaturated conditions}$$

$$dS_2 = dS_a + dS_v + dS_c \qquad \text{for saturated conditions.}$$

where the subscripts a,v,c represent the phase components of dry air, water vapor and condensate. Since the formation of ice is not included in the current model formulation, the condensate will be water drops only but the c will be maintained to help generalize the expressions. The total differential expansion of entropy for a single constituent is

$$dS_i = \frac{\partial S_i}{\partial T})_{P,m} + \frac{\partial S_i}{\partial P})_{T,m} + s_i dm_i \qquad (2.7)$$

where the i will represent either a, v or c.

To obtain the desired form of the total entropy equation it is necessary to integrate over the change from a reference state to a final state. The choice of a reference state is somewhat arbitrary and several approaches have been taken in the past. In order to simplify the integration and put it on a physically meaningful foundation, a reference state is chosen that consists of water vapor and dry air with a total pressure P_0 and temperature T_0 at the point of marginal saturation. The integration is then performed from this reference state to the final temperature and pressures to obtain a complete equation for S. A common approach is to take the reference state as a combination of dry air and pure condensate with no vapor and integrate this over the change. The final integrated form should be the same, yet the use of an initial state consisting of pure liquid and dry air with no vapor seems counter-intuitive and somewhat confusing. A more detailed derivation of the entropy equations may be found in appendix 2. The final forms of the equations

represented in the form of entropy density are

$$\sigma_1 = \xi\left(C_{v_a}\ln\frac{t}{t_0} - R_a\ln\frac{\xi}{\xi_0}\right) + \eta\left(C_{v_v}\ln\frac{T}{T_0} - R_v\ln\frac{\eta}{\eta_0}\right) \qquad (2.8)$$

for unsaturated conditions, and

$$\sigma_2 = \xi\left(C_{v_a}\ln\frac{T}{T_0} - R_a\ln\frac{\xi}{\xi_0}\right) + \eta^*\frac{L(T)}{T} - \eta\frac{L(T_0)}{T_0} + \eta C_c\ln\frac{T}{T_0} \qquad (2.9)$$

for saturated conditions.

The process of obtaining the temperature consists of first solving (2.8) analytically to obtain an unsaturated temperature estimate T_1. Using this temperature, the saturation condition

$$\eta < \eta^*(T_1)$$

is checked using the computed value of $\eta^*(T_1)$. If this condition is satisfied then the system is unsaturated and the temperature is T_1. No additional computations are necessary. If, however, the condition is not satisfied then the system is saturated and the second form of the equation must be used. Because of the presence of several functions of temperature in (2.9) the solution for the saturated temperature, T_2 must be found using iterative techniques. The form of this iterative technique may be found in Appendix 3

It may be of importance to note that at the point of marginal saturation, Eqn (2.8) and (2.9) are equal and would therefore give the same temperature. This is important for maintaining a consistency while using two forms of an equation.

2.2.3). Pressure Diagnosis.

The complete description of the thermodynamic state of the system depends on the pressure as well as the temperature. The thermal and chemical equilibrium assumptions stated at the begining of section 2.2 make it possible to consider that the temperature is the same for each component of a mixture of phases. Because of

this, it is possible to write separate equations of state for dry air and for water vapor. Using these equations, the temperature obtained from the process described in the previous section and a knowledge of the saturation condition, the determination of the system's total pressure is a simple matter.

The equation of state for the dry air component may be written as $P_a = \xi R_v T$ The dry air pressure can then be easily obtained by using the computed temperature and the predicted value of ξ. Obtaining the vapor pressure of the system depends on the saturation condition. If the system is saturated the vapor pressure is simply the saturation vapor pressure E(T). If unsaturated, then the gas law for the vapor phase can be used to determine P_v. The total pressure is then $P = P_a + P_v$.

Knowing the densities of dry air, water vapor and condensate, the temperature and the partial pressures of the system allows all other thermodynamic variables of interest to be computed using their definitions.

2.2.4) Vertical Velocity.

To complete the set of prognostic equations it is necessary to obtain the vertical velocity as a function of height. The determination of w will depend on the assumption that over time the vertical velocity will act dynamically to maintain hydrostatic balance. Using this maintenance condition it is possible to obtain a diagnostic equation for the vertical velocity.

If we write the hydrostatic equations as

$$\frac{\partial P}{\partial z} + \rho g = \varepsilon \qquad (2.10)$$

then ε represents any imbalance that might exist over a spatial domain. To maintain hydrostatic balance in a prognostic model it is necessary to satisfy the condition that over time $\varepsilon=0$. Under this approach the maintenance condition

becomes

$$\frac{\partial}{\partial t}(\varepsilon) = \frac{\partial}{\partial t}\left(\frac{\partial P}{\partial z} + \rho g\right) = 0. \tag{2.11}$$

After rearranging the order of integration, this becomes

$$\frac{\partial}{\partial t}(\varepsilon) = \frac{\partial}{\partial z}\left(\frac{\partial P}{\partial t}\right) + g\frac{\partial \rho}{\partial t} = 0. \tag{2.12}$$

Pressure is not a prognostic variable yet it changes in time as a function of the prognostic variables. The time derivative of the total pressure can be expressed in terms of the prognostic variables as

$$P = P(\xi,\eta,\sigma)$$
$$P_t = P_\xi\frac{\partial \xi}{\partial t} + P_\eta\frac{\partial \eta}{\partial t} + P_\sigma\frac{\partial \sigma}{\partial t} \tag{2.13}$$

Because pressure is a diagnostic variable, these p-coefficients are themselves diagnostically determinable. Using the prognostic equations (Eqs. 2.6a-2.6c), the time variations can be eliminated and the diagnostic equation for w becomes

$$-\frac{\partial}{\partial z}\left[\rho c_N^2\frac{\partial w}{\partial z}\right] - \frac{\partial}{\partial z}[\varepsilon w] + F(Q) = 0 \tag{2.14}$$

where

$$F(Q) = \frac{\partial}{\partial z}[P_\xi Q_\xi + P_\eta Q_\eta + P_\sigma Q_\sigma] + g[Q_\xi + Q_\eta] \tag{2.15}$$

Assuming that the model is initially in hydrostatic balance this can be simplified by eliminating the terms that combine to form ε and its derivatives. With this simplification the vertical velocity equation becomes

$$\frac{\partial}{\partial z}\left[\rho c_N^2\frac{\partial w}{\partial z}\right] = F(Q) \tag{2.16}$$

where

$$\rho c_N^2 = \xi P_\xi + \eta P_\eta + \sigma P_\sigma$$

and c_N represents the speed of sound in a Newtonian fluid. This equation is solved numerically using a Galerkin approach described in Appendix 3.

2.3. Forcing Terms

One of the greatest challenges in large-scale atmospheric modelling is in the treatment and parameterization of the physical and dynamical processes that cannot be explicitly resolved. These effects are represented by the Q terms in the governing equations and represent the source and sink of model variables due to outside and subgrid-scale influences. In the current model approach the processes influencing model variables include the effects of sub-grid scale diffusion, longwave radiation, subsidence and convection in both the cloud and subcloud layers. The treatment of these physical processes is an essential ingredient in bringing a model to life yet, methods of parameterization vary from model to model and in many cases the physical process itself in not well understood. In the current approach each of these physical processes is treated in a comprehensive manner, while at the same time maintaining a simplicity that will allow the computational advantages of using a one-dimensional model to be realized. The methods used to parameterize turbulent diffusion, radiation and subsidence will be examined here. Convective processes will be treated in section 3.

2.3.1) Sub-Grid Scale Eddy Diffusion

The eddy diffusion terms that emerge from the averaging process of Eqs. (2.1a-2.1e) are treated using the first-order closure method of Troen and Mahrt (1986). In this approach the turbulent flux of any quantity can be expressed in terms of the local gradient of that variable and an exchange coefficient that represents the strength of the turbulent eddies. Under unstable conditions , a counter-gradient correction factor γ is included in the thermodynamic terms to compensate for the enhanced diffusion when thermal or dry convective processes are present. Following this approach the vertical turbulent flux of any thermodynamic variable c can be expressed in the form

$$[w^*c^*] = -\left(k\frac{\partial c}{\partial z} - \gamma_c \right) \tag{2.17}$$

while the turbulent flux of each momentum component v can be expressed as.

$$[w^*v^*] = -\left(k\frac{\partial v}{\partial z} \right) \tag{2.18}$$

The counter gradient correction term is necessary to compensate for the fact that convective or thermal elements are not related to the local gradient and in fact can exist in the absence of any local gradient. The range over which these elements can transport momentum is limited by pressure effects so no counter gradient term is used for the two momentum equations.

To obtain the diffusion coefficients, subroutines were obtained from the from the OSU 1-D Planetary Boundary Layer model of Ek and Mahrt (1990). All computations were performed using fields of potential temperature, specific humidity and horizontal winds. The resulting coefficients for heat and momentum were transported for use in computing the diffusion effects on the current model variables.

The final form of the diffusion coefficient for momentum is computed in the form

$$K_M = w_s hk\frac{z}{h}\left(1-\frac{z}{h}\right)^P \tag{2.19}$$

where w_s is the velocity scale of the mixed layer, k the Von Karmen constant and h the depth of the mixed layer. The mixed layer is considered to be the layer over which turbulent processes are observed and is formulated to represent all of those turbulent processes over portions of the spatial domain where phase changes of water do not occur. The velocity scale of this layer is defined as

$$w_s = u_*\phi_m^{-1}\left(\frac{z_s}{L}\right) \tag{2.20}$$

Here, u_* is the surface friction velocity, L is the Monin-Obukov length, z_s is the height of the surface layer (set to 0.1h), and ϕ_m is a non-dimensional profile function. The diffusion coefficient for heat is used for the thermodynamic

quantities of entropy and total water density, and is related to the coefficient for momentum by a non-dimensional Prandtl number of the form

$$K_H = K_m Pr^{-1} \tag{2.21}$$

The Prandtl number is defined in terms of the non-dimensional profile functions as

$$Pr^{-1} = \frac{\phi_n\left(\frac{z_s}{L}\right)}{\phi_m\left(\frac{z_s}{L}\right)} + ck\frac{z_s}{h} \tag{2.22}$$

With this formulation, the counter-gradient term is incorporated into the Prandtl number and as a result does not explicitly appear in the diffusion term. A more detailed description of the profile functions can be found in Holtslag (1988).

The mixed layer height h is diagnosed using the method of Troen and Mahrt (1986) and is used here in the form

$$h = Ri_c \frac{\theta_{0v} | \mathbf{V}(h) - \mathbf{V}_0 |^2}{g[\theta_v(h) - \theta^*_{0v}]} \tag{2.23}$$

where Ri_c is the critical Richardson, number θ_{0v} the surface virtual potential temperature, $\theta_v(h)$ the virtual potential temperature at level h and θ^*_{0v} the surface potential temperature enhanced under unstable conditions. This enhancement is included to provide a more accurate diagnosis of mixed layer height under unstable conditions and has been shown to work well in approximating the growth of the daytime mixed layer. This term takes the form

$$\theta^*_{0v} = \begin{cases} \theta_{0v} & \text{stable} \\ \theta_{0v} + C\frac{[w^*\theta^*_v]_s}{w_s} & \text{unstable} \end{cases}$$

With this formulation, the time rate of change of model variables due to eddy scale diffusion can be expressed as

$$Q_{U_D} = \frac{\partial U}{\partial t}\Big|_D = -\frac{\partial}{\partial z}\left([\rho][w^* u^*] \right) = -\frac{\partial}{\partial z}\left(-\rho K_M \frac{\partial u}{\partial z} \right) \tag{2.24a}$$

$$Q_{V_D} = \frac{\partial V}{\partial t}\Big|_D = -\frac{\partial}{\partial z}\left([\rho][w^* v^*]\right) = -\frac{\partial}{\partial z}\left(-\rho K_M \frac{\partial v}{\partial z}\right) \qquad (2.24b)$$

$$Q_{\xi_D} = \frac{\partial \xi}{\partial t}\Big|_D = 0 \qquad (2.24c)$$

$$Q_{\eta_D} = \frac{\partial \eta}{\partial t}\Big|_D = -\frac{\partial}{\partial z}\left([\xi][w^* r^*]\right) = -\frac{\partial}{\partial z}\left(-\xi K_H \frac{\partial r}{\partial z}\right) \qquad (2.24d)$$

$$Q_{\sigma_D} = \frac{\partial \sigma}{\partial t}\Big|_D = -\frac{\partial}{\partial z}\left([\xi][w^* s^*]\right) = -\frac{\partial}{\partial z}\left(-\xi K_H \frac{\partial s}{\partial z}\right) \qquad (2.24e)$$

2.3.2) Surface Flux

The surface fluxes of thermodynamic quantities also play an important role in the structure of the trade wind convective boundary layer. The surface fluxes of entropy and moisture are parameterized following Ek and Mahrt (1989). This method consists of computing a surface exchange coefficient for heat and moisture and relating this to the difference between the lowest model level and an assumed surface state. This assumed surface state of the air is saturated and remains fixed with time at the specified sea surface temperature. The exact form of the surface exchange coefficients can be found in Ek and Mahrt (1989)

Using this representation, the surface flux of moisture and entropy takes the form

$$[w^* \sigma^*]_s = [\xi][w^* s^*] = \xi C_h (s_s - s_0) \qquad (2.25a)$$

$$[w^* \eta^*]_s = [\xi][w^* r^*] = \xi C_h (r_s - r_0) \qquad (2.25b)$$

where the s subscript represent the assumed surface values and the 0 subscripts represent the state of the first model level.

2.3.3) Subsidence.

Large-scale subsidence is an essential feature in helping maintain the equilibrium structure of the trade wind convective boundary layer. The strength

of subsidence is related to the low-level horizontal divergent flow in the equatorial branch of the Hadley circulation. The expressions representing the effects of subsidence emerged from the derivation of the model prognostic variables in section 2.1. For the purposes of this model, the large-scale vertical velocity or subsidence velocity will be a prescribed quantity and will remain fixed with time. The subsidence forcing terms take the form

$$Q_{\sigma_s} = \frac{\partial \sigma}{\partial t}\Big|_{Sub} = -[\xi w_{Sub}] \frac{\partial [s]}{\partial z} \tag{2.26a}$$

$$Q_{\eta_s} = \frac{\partial \eta}{\partial t}\Big|_{Sub} = -[\xi w_{Sub}] \frac{\partial [r]}{\partial z} \tag{2.26b}$$

where $[w_{Sub}]$ represents the mean subsidence rate. It can be seen from these expressions that the warming and drying effects of subsidence are due to large scale vertical motions acting on the local gradient of the conservative thermodynamic variables.

2.3.4) Radiation.

The radiative properties of water vapor and liquid water also play an important role in maintaining the equilibrium structure of the CBL. The cooling that results due to a net outward flux of longwave radiation helps maintain the convective instability of the tropical troposphere. The radiative cooling effect also plays a significant role in the maintenance of the characteristic inversion structure. Because energy must be conserved, any net flux of radiative energy between layers in the atmosphere must result in heating or cooling. This concept can be expressed by the first law in the form

$$ds\Big|_{Rad} = \frac{\delta Q\Big|_{Rad}}{T} \tag{2.27}$$

By expressing the heating rate in terms of the net flux of radiation, an approximation to this equation can be written that relates the net flux to the time

rate of change of entropy.

$$Q_{\sigma_R} = \frac{\partial \sigma}{\partial t}\Big|_{Rad} = \frac{-1}{T}\frac{\partial F}{\partial z} \tag{2.28}$$

To compute the net radiative fluxes, a method used by Sommeria (1978) is used. This approach treats the layer above and below a level z as isothermal and the net flux is computed as simply the difference between the upward and downward fluxes. The upward fluxes take the form

$$\uparrow F_v(z) = B(0)[1 - A_v(0,z)] + B(z)A_v(0,z) \tag{2.29a}$$

$$\uparrow F_l(z) = -B(0)A_l(0,z) + B(z)A_l(0,z) \tag{2.29b}$$

where the subscripts v and l are for vapor and liquid, B(0) and B(z) are the blackbody emisivities at the surface and at level z and A(0,z) is the absorption function for the region below level z. Similarly, the downward fluxes can be written in the form

$$\downarrow F_v(z) = A_v(z,T)B(z)$$

$$\downarrow F_l(z) = A_l(z,T)B(z)$$

where $A_v(z,T)$ and $A_l(z,T)$ are the total absorptivities of water vapor and liquid water for the region from level z up to the top of the atmosphere. These absortivities are given by

$$A_v(0,z) = 1 - \tau_v(u_{v0})$$

$$A_v(z,T) = 1 - \tau_v(u_{vT})$$

for water vapor, and

$$A_l(0,z) = 1 - \tau_l(u_{l0})$$

$$A_l(z,T) = 1 - \tau_l(u_{lT})$$

for liquid water where τ_v, τ_l represent transmission functions for vapor and liquid water and u_{v0}, u_{vT} are the total amounts of water vapor and liquid water above and below level z. The transmission functions are obtained using the formulations of Yamamoto et al.(1970) and Sasamori (1972) assuming an average over the entire spectrum. These transmission functions take the form

$$\tau_v = 0.381 - 0.240 \log (u + 0.01) \qquad (2.30a)$$

$$\tau_l = \exp (-3.0 \times 10^3 u) \qquad (2.30b)$$

where u is in units of g/cm^3 . Because the model domain does not extend to the top of the atmosphere, prescribed values for u must be set for the region above the model domain. For this region, u_l is chosen to be zero while u_v is chosen according to the standard values computed by Sasamori(1972).

2.4 Numerical Procedures:

2.4.1) Solution Methods

The numerical procedures used in this model are a one-dimensional version of the two-dimensional nested-grid hurricane prediction model developed by Ooyama (1985). The numerical procedures were developed with the objective of producing quantitatively accurate results that can easily accommodate the model's physics and boundary conditions. The method expands any physical variable u(z) in the form

$$u(z) = \sum_{m=1}^{M} a_m \phi_m(z) \qquad (2.31)$$

where $\phi_m(z)$, m=1,2,3...M are linearly independent basis functions and a_m, m=1,2,3...M are amplitudes. M represents the total number of nodal intervals over the domain. In this model, cubic B-splines are chosen as the basis functions primarily because they have the advantage of being continuously differentiable at second order (piecewise differentiable at third) and can accommodate a variety of boundary condition types. The cubic B-splines are smoothly joined cubic polynomial segments rather than analytic functions and can be represented in the form

$$\phi_m(z) = B[(z - z_m)/\Delta z]$$

where

$$B(z) = \begin{cases} 0 & |z| \geq 2 \\ \frac{1}{4}(2-|z|)^3 & 2 \geq |z| \geq 1 \\ \frac{1}{4}(2-|z|)^3 - (1-|z|)^3 & |z| \leq 1 \end{cases}$$

In this approach, spatial fields can be fitted by minimizing the least square norm with a derivative constraint in the form

$$\int_D \{ (u-\hat{u})^2 + \alpha_j D_j[u]^2 \} dz \qquad (2.32)$$

where $u-\hat{u}$ is the difference between the actual and fitted values and α_j is a filter weight used to smooth the fitted profile. Substituting Eqn. 2.31 into this, we can obtain a linear system of equations that can be written in matrix notation as

$$[\tilde{P} + \alpha\tilde{Q}]\,\tilde{a} = \tilde{b} \qquad (2.33)$$

where

$$P = P_{mn} = \int_D \phi_m(z)\,\phi_n(z)\,dz$$

$$Q = Q_{mn} = \int_D \phi_m'(z)\,\phi_n'(z)\,dz$$

$$b = b_m = \int_D \phi_m(z)\,\hat{u}(z)\,dz$$

This approach provides a convenient and efficient way of integrating the prognostic equations in time. This is done by first computing the spline amplitudes associated with the forcing of model variables (a_m). If f(z) represents this forcing, (the terms on the right hand side of the prognostic equations), then the amplitudes a_m can be obtained for this forcing by solving (2.33) with

$$\hat{b}_m = \int_D f(z)\,\phi(z)\,dz \qquad (2.34)$$

These amplitudes are then used to advance the state of the model in time. To do this the leap-frog method will be used and takes the form

$$a_m^{t+2} = a_m^t + 2\Delta t\,\hat{a}_m$$

The variable of interest can then be obtained using Eqn. (2.31) with the new amplitude.

By choosing cubic B-splines over more orthogonal basis functions such as chapeau functions, some computational efficiency is sacrificed. The coefficient matrix in (2.33) becomes a seven diagonal banded matrix as compared to the tridiagonal matrix that would arise from the use of an orthogonal basis function. However, because the coefficient matrix remains constant in time, an efficient recursive algorithm may be utilized to to solve the matrix system. Any added computational time is compensated for by the accuracy of the method and the ease to which boundary conditions can be treated.

2.4.2) Boundary Conditions

In the framework of a one-dimensional column model, the lower boundary must be treated as a material Surface. A closed set of basis functions is utilized that makes it possible to easily choose a boundary condition that specifies either the value of a variable or its first or second derivative. This is accomplished by matching the shape of the basis function at the nodal points nearest to the boundary to the choice of boundary condition type. If a first derivative boundary condition is specified for a variable, then the basis elements near the boundary will be different than if a second derivative condition is specified. By defining the basis functions in this way, a great deal of flexibility is added to the choice of model boundary conditions.

In addition, it is possible to include an inhomogeneous time dependent boundary condition. If we let the lower boundary be represented by z=1, and express the boundary condition in the form

$$u(z=1) = u'(z=1) + \hat{\gamma}(z=1) \qquad (2.35)$$

then $u'(z=1)$ represents the homogeneous portion of the boundary condition and $\hat{\gamma}(z=1)$ the inhomogeneous portion. The condition at the boundary may then be set as

$$\hat{g}(z=1) = u_j(z=1)$$

where j is the order of the specified derivative, { j = 0,1,2}. The inhomogeneous term is included in an adjustment term in the form

$$\hat{a}(z=1) = \hat{g}(z=1)/\phi_j(z=1) \qquad (2.36)$$

This adjustment term is applied to the $\hat{b}$ term of Eqn. 2.33 before the matrix system is solved so that

$$\hat{b}_1 = \hat{b}_1 - \hat{a}(z=1) \cdot [\text{ first element of matrix } P+\alpha Q]$$

The choice of boundary conditions in this model has been partially guided by expectations of its eventual use. As a model to help test parameterization schemes and to diagnose subgrid scale heat, moisture and momentum properties for a larger scale model, it is important to be able to represent the boundary layer characteristics of these properties. It is not necessary to explicitly resolve the model profiles through the lowest surface layer. In fact, the physics to do this have not been included. What we wish to concentrate on is providing a boundary condition that will maintain a fairly neutral profile at the surface, one that won't produce any extreme or unrealistic values. To do this, the homogeneous condition

$$u_{zz}(1) = 0$$

is specified for each of the prognostic variables. This condition provides a mechanism by which the model is free to set the first derivative, the slope of the profile, to a value that is related to the profile above the surface layer. Thus, the surface layer profiles are linked to the atmosphere conditions above the surface rather than matched to surface boundary layer profiles that cannot be resolved by the basis functions.

One of the most important processes driving the convective boundary layer is the flux of water vapor and heat across the lower surface. This is a physical condition that must be treated. Conventionally these effects would appear as an inhomogeneous boundary condition on the total water density and entropy terms but here they will be included in a slightly different manner. This is done partially for

the reasons given above but also because the model numerics provide a simple and convenient way in which the surface fluxes may be included. The surface flux of water vapor and entropy are included as the lower limits of integration when the diffusive forcing terms are integrated by parts during the solution process. The diffusion term for the lowest model node is can be written as

$$\hat{b}_d = \int_D \phi_1 \frac{\partial}{\partial z}[F_\eta]\, dz = \phi_1 f_\eta \Big|_1^{z_t} - \int_D F_\eta \phi'_m\, dz \qquad (2.37)$$

where F_η is the flux of total water. For the lowest model level this flux is simply the surface flux and is expressed using the ideas presented in section 2.3d as

$$F_\eta = [w^* \eta^*] = C_H(\eta - \eta_s) \qquad (2.38)$$

In this way the surface flux is dependent upon the surface gradient while at the same time the specified boundary condition is maintaining a smooth transition through the surface layer. This same approach is taken for dealing with the flux of entropy.

3 CUMULUS PARAMETERIZATION

The general objective of any shallow cumulus parameterization scheme is to provide a way of estimating the magnitude and structure of subgrid-scale convective transports and their effect on mean model variables. Because the exact physical nature of clouds are not sufficiently understood, this often requires that assumptions be made about either the important physical processes involved or about the bulk effects of these processes. In the parameterization scheme presented here an attempt has been made to rely primarily on physical arguments to motivate the current method, with the hope that by maintaining a physically-based system it will be much simpler to interpret the model results.

In searching for a cumulus parameterization scheme we have settled on a modified eddy-diffusion approach. This approach was chosen in part because of its simplicity and in part to accommodate current boundary-layer approaches. It was also believe that an eddy-diffusion approach can be based on physically realistic assumptions of cloud scale mixing and at the same time help ensure that model variables are mixed conservatively. While not much is known about the processes responsible for cloud scale transports, the eddy-diffusion approach will provide a simple means by which several physical concepts can be applied.

The implementation of an eddy diffusion scheme requires the definition of a cloud mixing coefficient (K_c). With this coefficient the subgrid-scale transports of conserved quantities through the cloud layer can be expressed as

$$[w^{*}M^{*}] = -K_c \frac{\partial M}{\partial z} = L_c w_c \frac{\partial M}{\partial z} \qquad (3.1)$$

where w_c and L are characteristic velocity and length scales that can be used to represent convective mixing and $\frac{\partial M}{\partial z}$ represents the gradient of any conserved variable. This basic approach has been used with some success to parameterize shallow convection in the ECMWF model with a constant value for the cloud mixing coefficient K_c (Tiedtke et. al. 1988).

The characteristic length and velocity scales are inherent properties of the cumulus clouds themselves. To obtain these values, it is necessary to define the principal physical properties that influence shallow convective motions. To do this, the assumption is made that the physical processes contributing to mixing in shallow clouds are local in nature and that they are best described by considering a local balance between the properties that generate and dissipate convective motions. This local approach is taken because it is believed that the characteristic length scale for shallow convection is short enough so that mixing across the local gradient can account for the majority of the convective mixing. This characteristic is only believed to be valid for shallow convection and a distinct separation is believed to exist between the properties that govern shallow and deep convection. While shallow cumulus are generally free of precipitation and develop as a result of weak vertical motions, deep convection is characterized by strong updrafts and large undilute parcels that may mix over deep layers regardless of the local gradient.

The biggest obstacle to determining the characteristic properties of shallow cumulus clouds comes from the lack of experimental evidence of their true nature. Because instruments are not capable of accurately measuring temperature and humidity inside clouds and because it is nearly impossible to sample on sufficient time and space scales to obtain statistically meaningful measurements within the cloud layer, our knowledge is insufficient to describe fully the physics involve in convective scale transports. For this reason, the parameterization methods discussed here will rely only partially on the experimental evidence from several trade wind boundary layer studies. In addition, results from several three-dimensional (3-D) modeling studies will be used to examine possible links between turbulent fluxes and mean model variables and results from several studies of continental cumulus clouds will be examined to explore several cloud mixing concepts that may be relevant to tropical cloud systems.

Several field studies of the trade wind boundary layer have been conducted over the past few decades. The BOMEX and ATEX studies conducted in the late 1960s were primarily used to compute large-scale budgets while the Puerto Rico and GATE studies concentrated on aircraft measurements of the lower boundary layer. Although these experimental studies don't reveal a great deal about the physical characteristics of the cloud layer, they do provide some insight into the possible mechanisms responsible for the generation of shallow convective activity. Shallow cumulus are believed to be associated with weak, low level convergence of heat and moisture in the subcloud-layer. Whether this convergence is due to large scale processes or to the accumulation of heat and moisture associated with surface processes is unclear. What is apparent is that the large mass flux and buoyancy flux associated with deep clouds is not found in regions of shallow cumulus (Yanai et. al., 1976). Using GATE data, Nichols and LeMone (1980) examined the subcloud layer for any signs of cloud signature. What they found was a distinct moistening of the subcloud-layer under convective conditions. They also found only a weak enhancement of both the vertical velocity variance and buoyancy flux below shallow clouds. Previous work by LeMone and Pennell (1976) showed a slightly different structure for a strong-wind case of the Puerto Rico experiment. Here, a distinct turbulent enhancement was observed up to 300m below the cloud base. What these studies suggest is that the structure of the subcloud layer has a strong influence on the cloud layer and therefore any parameterization of convective transports must include both elements of the subcloud layer structure and the enhancement of fluxes below cloud base.

The degree to which cloud-layer properties depend on the subcloud layer is uncertain. Clearly, for saturation to occur at a particular level in a convective region, air must be lifted from below and have sufficient moisture content for saturation. This air must also have sufficient energy to reach its level of saturation. Yet little evidence exists to suggest how the mixed layer influences the formation and strength of convective turbulence.

Further clues that will help in characterizing the nature of convective transports can be found in a series of 3-D modelling studies of the tropical CBL. Sommeria (1976) adapted the large eddy simulation model of Deardorff (1972) to include non-precipitating convection. Different versions of this model have been used to simulate a number of trade wind cases. Because this model contains second-order closure assumptions, the evolution of convective fluxes are readily available for inspection as well as the terms of the turbulent kinetic energy budget.

Results of model simulations were compared to observations taken during both the Puerto Rico experiment (Sommeria and LeMone, 1978, Beniston and Sommeria, 1980) and to observations during a single period of GATE (Nichols et al. ,1982). In all cases cloud activity was seen to cycle through periods of both strong and weak activity where substantial variations could be seen in the mean turbulent structure. Figures 3.1 and 3.2 show the modelled and observed terms of the turbulent kinetic energy budget for the two cases. These quantities are for the cloud layer as a whole and not simply the regions where active clouds are found. These figures show the relative importance of the various terms in the budget equation. Sommeria and LeMone (1978) suggested that the cloud layer can be divided into two layers; a lower layer where the buoyant production of turbulent kinetic energy is strong and an upper portion where the buoyant production becomes weak and turbulent transport from below is strong.

The significance of turbulent transport in these figures suggests that a strict local balance between production and dissipation of cloud kinetic energy is perhaps too simplistic and that some non-local effects must also be included. This would seem to be particularly true in the lower region of the inversion layer where the local production effect is essentially zero yet turbulent kinetic energy is observed.

Another interesting element of these model simulations is that they consistently underestimate the variances of moisture and temperature. The recognition of this fact has led to speculation that mesoscale eddies on scales larger than the model can resolve, may be important in determining the low level

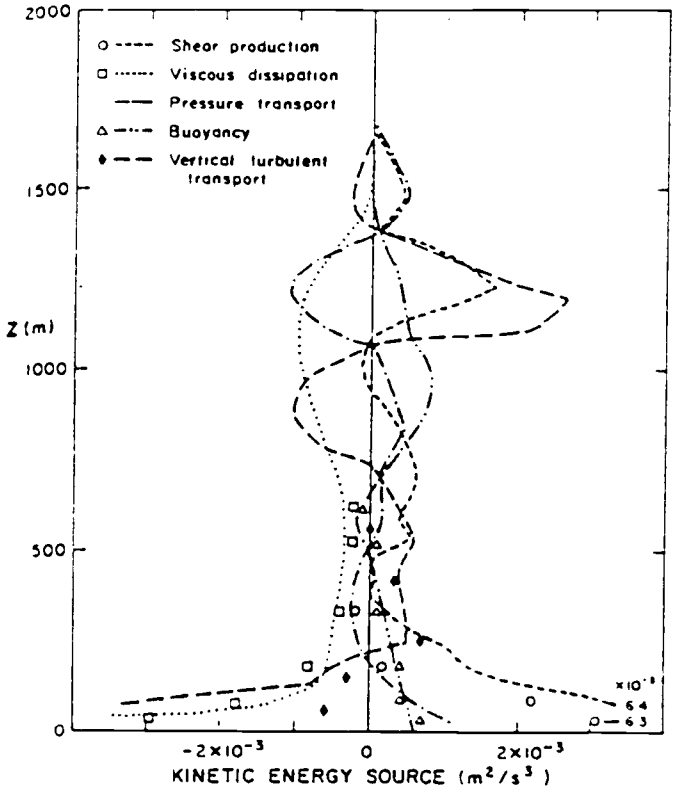

Fig 3.1 Terms of the turbulent kinetic energy budget for a 3-D simulation of the Puerto Rico experiment. (from Sommeria and LeMone 1978)

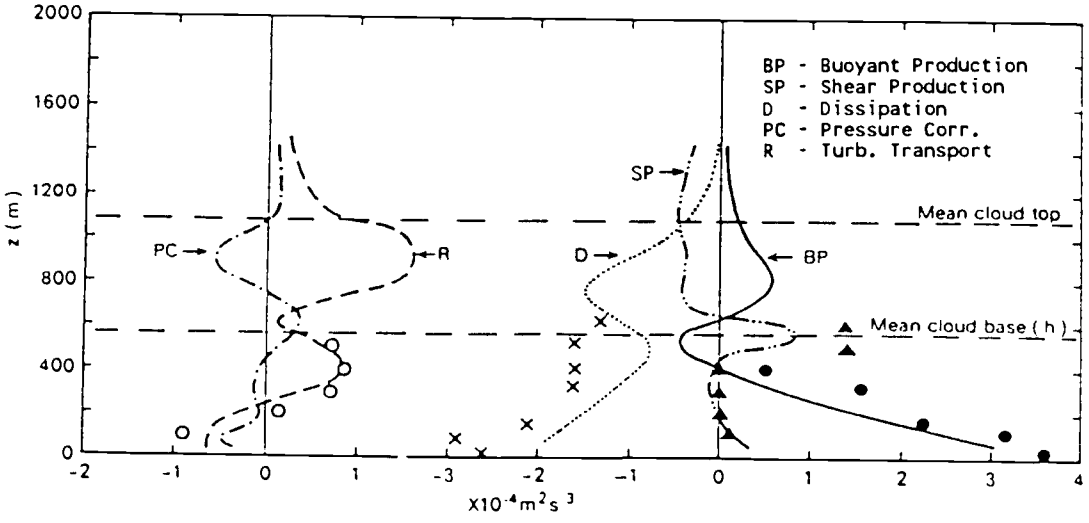

Fig 3.2 Terms of the turbulent kinetic energy budget for a 3-D simulation of the Gate (from Nichols and LeMone 1978).

moisture convergence that is found during periods of convective activity (Cotton and Anthes, 1989). It was also determined that the vertical velocity spectrum and the cospectrum between vertical velocity and moisture both exhibited peaks at about 700m. One implication of this is that the disturbances responsible for producing clouds and contributing to the enhancement of model variances may scale vertically on the order of either the boundary layer depth or the depth of the subcloud layer.

Additional evidence of the length and velocity scales relevant to convective transports can be found in some recent studies involving conserved variable analysis of individual continental cumulus clouds. Conserved variables have been used to diagnose the mixing structure of individual clouds by Paluch(1979), Raymond and Blyth (1986), Taylor and Baker(1991), and Blyth et. al.(1988). By examining the thermodynamic properties in and around clouds, it is possible to determine a great deal about both the mixing structure of the cloud being examined and about the characteristic scales involved in this mixing.

Using aircraft measurements obtained from small non-precipitating clouds during the CCOPE and HIPLEX experiments, Blyth et. al. (1988) examined the entrainment structure of small continental clouds and developed a conceptual model of rising cumulus elements. While direct measurements of in-cloud fluxes were not obtained, conserved variables were used to trace the source regions of entrained air and to diagnose the structure of the mixing. Their analysis suggests the use of a "shedding thermal" representation of cumulus clouds where cumulus transports would occur on two distinct scales. The first of these would be the scale of the potentially undilute cloud core as it rises through the cloud layer and generates buoyant kinetic energy . The second scale would represent the transports associated with mixtures of cloud and environmental air as they rise or sink to their level of neutral buoyancy. In this representation the processes of entrainment and detrainment can be thought of as a single process. Air is entrained into the cloud along the edges where it acts to evaporate portions of the cloud liquid

water into the relatively dry environmental air. This has the effect of reducing the size of the cloud. This view is also consistent with the kinetic energy budgets of the 3-D simulations discussed previously. In those cases the buoyancy generation was larger in the lower portion of the cloud layer and less in the upper cloud layer. This could be the result of the decreasing size of the undilute core region as it rises through the cloud layer and continuously detrains.

In the course of deriving closure assumptions for this parameterization scheme it became apparent that a relaxation of the local closure approach was necessary to account for convective penetration into the inversion layer. This became necessary because a strict balance between the production and dissipation of turbulent kinetic energy would not allow for a source of kinetic energy in the inversion layer where the local stable stratification would prevent production of any energy through buoyancy. In order to maintain the equilibrium structure of the boundary layer, the convective activity must have the capacity to mix moisture into the inversion layer.

To circumvent this problem two approaches were considered. The first involved the development of a two scale mixing model that closely resembled the shedding thermal view of cloud processes. In this approach two scales would be used to compute the mixing intensity and obtain a cloud mixing coefficient. One scale would represent the mixing by undilute parcels that would be capable of penetrating into the inversion and the other would represent the more local mixing associated with the smaller scale elements. This is the basic approach taken by Raymond and Blyth (1986) except here, the parcel arguments would be used to obtain estimates of cloud mixing intensity rather that the fluxes themselves. A second approach involved the development of a prognostic equation for the cloud turbulent kinetic energy that could include terms to represent the production and dissipation of kinetic energy associated with buoyancy, turbulent transport molecular dissipation and any other effects believed to be important. The cloud

mixing coefficient could be obtained using the predicted cloud turbulent kinetic energy. This second approach was chosen for several reasons. First, it is not clear if the shedding thermal concept directly pertains to tropical cloud systems where cloud parcels are rising through relatively humid air and are not driven by a substantial or sustained surface forcing. In this case it would seem that parcels would have a difficult time generating the buoyancy required to overcome mixing through the cloud layer and penetrate into the inversion. Secondly, a prognostic formulation would provide a much simpler means of including the physical processes that seem important without making any further or unnecessary assumptions.

The cloud turbulent kinetic energy equation developed here is essentially an extension of the diagnostic approaches discussed previously only a turbulent transport term has been included that should enable more turbulent mixing in the lower portion of the inversion layer. The velocity scale characterizing cumulus transports will be computed using this predicted kinetic energy. The three fundamental relationships used in this approach can be expressed in the form

$$\frac{\partial E}{\partial t} = w_c A - \frac{E}{\tau} - \frac{\partial w_c E}{\partial z} \tag{3.2}$$

$$A = A_p - A_R \tag{3.3}$$

$$E = \alpha (w_c)^2 \tag{3.4}$$

where E represents the cloud mean kinetic energy per unit mass, A represents the net buoyancy produced, w_c is the cloud vertical velocity scale, τ is a kinetic energy dissipation rate and α is a constant of proportionality. Eqn (3.2) represents the cloud kinetic energy budget. The first term on the right hand side of this equation represents the generation of kinetic energy resulting from buoyancy effects, the second term is the dissipation of kinetic energy resulting from the effects of turbulent processes and the third term represents turbulent transport of cloud kinetic energy. Eqn (3.2) is a simple diagnostic representation of the net buoyancy produced at each model level and is a result of two terms: the production

of buoyancy associated with the ascent of an undilute saturated parcel and the reduction in this amount associated with entrainment of unsaturated environmental air. Together this set of equations is conceptually very similar to the set of equations used in the cumulus ensemble model of Arakawa and Shubert (1974) except here, instead of a cloud work function defined by large scale processes and properties of the cloud layer as a whole, we define a diagnostic buoyancy function based on local properties in the cloud layer.

The left hand side of equation 3.3 represents the net production of buoyancy as a parcel rises through a layer and can be expressed as the balance between two processes. The first process can be thought of as a potential buoyancy or the amount of buoyancy a saturated parcel would generate if lifted adiabatically over a layer. This is the maximum amount of buoyancy that can be generated and will be expressed in terms of the local measure of conditional instability. Along these lines, the production of buoyancy can be expressed following Holton (1979) as

$$A_p = g\frac{\theta_{v_a} - \theta_{v_e}}{\theta_{v_e}} = \frac{-L_c\, g\, \partial\theta_{ES}}{\theta_{ES}\, \partial z} \qquad (3.5)$$

The second process is a correction factor that can be applied to this potential buoyancy in order to compensate for the effects of entrainment and other processes that act to reduce a parcel's buoyancy. The amount by which the buoyancy is reduced depends upon the size of the parcel, its temperature and liquid water content ,and the relative humidity of the air surrounding the parcel. The drier the air being mixed at the cloud boundaries, the greater the potential for evaporation of cloud liquid water and the larger the reduction in parcel buoyancy.

This correction factor will involve the use of a buoyancy length scale (l), representing the characteristic length over which an eddy is capable of producing buoyant kinetic energy. The fundamental principal behind the use of this length scale is presented in Fig. 3.3. If L_c is the length scale of a characteristic convective eddy, then this eddy must lift a parcel a distance Z^* to bring it to saturation. The remainder of the distance $l = L_c - Z^*$ represents the distance over which this

individual parcel will generate buoyancy through the process of condensation. Used in this way, Z^* is analogous to the saturated deficit pressure used by Betts (1982,1986). If the air at a particular level is moist, then Z^* will be small and more buoyant kinetic energy will be produced. If the air is somewhat drier, then Z^* will be large and the net amount of buoyancy produced will be relatively small. If Z^* is greater than L_c then it would be assumed that the conditions are such that although conditional instability may exist, there is insufficient moisture to produce clouds. Another way of looking at this is that by using this buoyant length scale, we are only considering eddies that have the potential to become saturated. Dry convection in the mixed layer will be treated separately.

With this approximation, the net buoyancy term can be expressed as

$$A = C_1 \frac{-l\, g}{\theta_{ES}} \frac{\partial \theta_{ES}}{\partial z} \qquad (3.6)$$

where the basic difference between (3.6) and (3.5) is that Eqn (3.5) represents the total production of cloud kinetic energy and Eqn. (3.6) represents the net production. Different length scales are used to accomplish this difference.

The turbulent dissipation term is treated in a much more conventional manner. The turbulent dissipation rate is defined by first making a substitution using (3.3) and then relating the convective time scale to the characteristic length and velocity scales ($\tau = L/w_c$). The result of this is that the dissipation rate takes the form

$$\varepsilon = c \frac{w_c^3}{L} \qquad (3.7)$$

In this expression, L has been used rather than the buoyancy length scale because it is more representative of the length over which dissipation will act in a typical convective element. A similar approach has been taken by Bougeault (1981) in a higher order closure model. No simplifications for the turbulent transport term are needed in order for it to be included.

With these changes, the full convective turbulent kinetic energy equation can

be written as

$$\frac{\partial E}{\partial t} = c_1 \frac{l\, g}{\theta_{ES}} \frac{\partial \theta_{ES}}{\partial z} w_c - c_2 \frac{w_c^3}{L_c} - \frac{\partial (w_c E)}{\partial z} \qquad (3.8)$$

To use Eqn. (3.8), several factors must still be determined. Perhaps the most difficult of these is the length scale L that characterizes the convective elements. It is quite probable that clouds contain elements that mix on many scales simultaneously and the use of a single value may be inappropriate. However, there is some evidence to suggest that the characteristic length scale is determined by the scale of the disturbance that helps generate the cloud (Cotton and Anthes 1989). This scale would then be less than or equal to the mixed layer height in regions away from the convective elements. In the approach developed here the length scale will be set to the height of the mixed layer as described in section 2.3a. The length scale has two main functions in Eqn. (3.8). First, it appears in the buoyancy production term and helps set a limit that determines if convection is possible. In shallow mixed layers, there must be a greater amount of moisture in order to produce convective turbulence. This comes about because of the buoyant length scale that is used $l = L_c - Z^*$. The second ues of L_c is in the turbulent dissipation term. Here L represents the length over which turbulence can be seen to dissipate. For shallow mixed layers it means that the same amount of turbulence would be dissipated over a shorter length leading to a dissipation rate that is larger.

The end purpose of devising a method to determine the characteristic length and velocity scales of shallow convection is to be able to use these quantities in estimating the transports of thermodynamic quantities. The form for representing these transports was given in Eqn. (3.1) One change, however, must be made to this formulation. The method described here leads to a determination of convective properties and represents the transports that would occur in the immediate vicinity of the cumulus clouds. In the trade wind boundary layers this may be only a small fraction of the total area. For this reason a simple fractional cloud cover parameter will be included when calculating the thermodynamic fluxes. This is a

fraction of the total area. For this reason a simple fractional cloud cover parameter will be included when calculating the thermodynamic fluxes. This is a common feature of parameterization schemes and leads to a flux formulation of the form

$$[w^*M^*] = -k_c \frac{\partial M}{\partial z} = \sigma_c L w_c \frac{\partial M}{\partial z} \qquad 3.7$$

In the current approach, σ_c will be a specified parameter of the model.

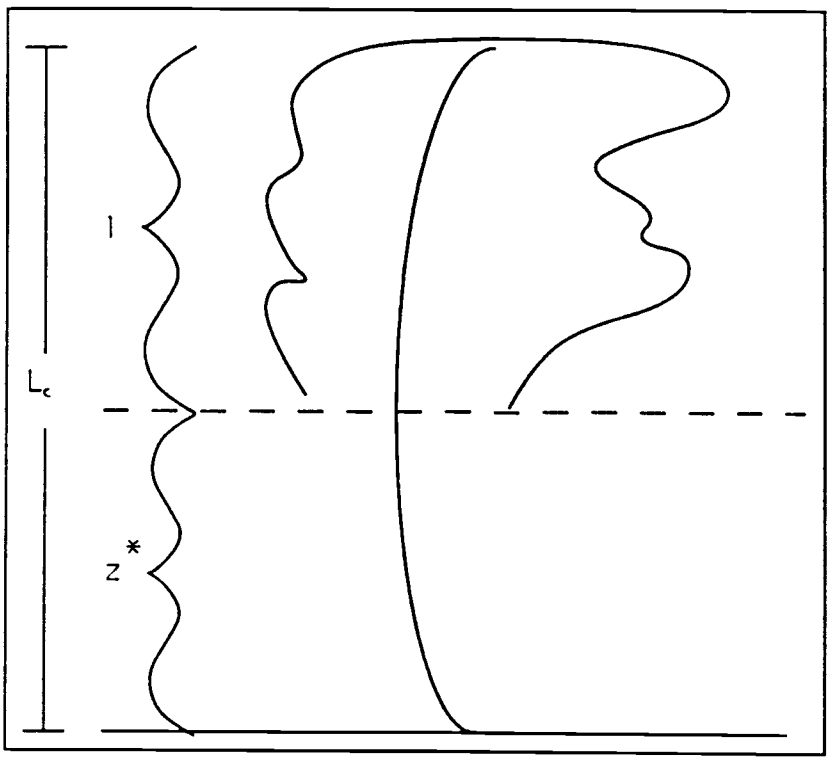

Fig 3.3: Sketch of relevant length scales used in the cumulus parameterization scheme presented here.

4. MODEL SIMULATIONS

To validate the model presented here, two separate simulations are performed and the results used to assess the model's usefulness in parameterizing shallow, convective trade-wind boundary layers. The first simulation is designed to explore the model's ability to maintain a given equilibrium trade-wind structure. The equilibrium state of a model depends on the interaction between the individual forcing elements. By examining the equilibrium state, it is possible to gain a better understanding of the role of each individual element. The results will be interpreted primarily to gage the effectiveness of the convective mixing scheme developed here. The second simulation is designed to test the model's ability to produce a cloud layer given an initially dry, unstable atmospheric profile over an unstable mixed layer. This is an important test of the models ability to respond in a physically realistic manner, to a specified set of physical forcing mechanisms. The results of these simulations will be used to explore some of the strengths and weaknesses of the model presented here.

4.1) Case I

In in effort to examine the models ability to maintain an equilibrium trade wind structure, initial profiles of model variables were constructed from a three day undisturbed period of BOMEX. This data source was chosen in part because of its availability and in part because previous studies of BOMEX will provide a strong basis for comparison (Holland and Rasmusson, 1973; Nitta and Esbensen, 1974; and Betts 1975). Of particular interest is the conserved variable analysis of the BOMEX structure performed by Betts and Albrecht 1987.

Profiles used to initialize the model for case 1 are Presented in Figs. 4.1, 4.2

and 4.3. Because of the non-traditional nature of these quantities, they are used here only as a matter of reference. To avoid confusion, more traditional variables will be used when interpreting model results. One exception to this will be the use of specific entropy (s) and a more detailed discussion of this quantity will be found in section 4.3. Specific entropy is used in conjunction with the total water mixing ratio (r) because it provides a convenient way of illustrating mixing processes. Two additional variables used for analysis purposes are equivalent potential temperature (θ_E) and saturation equivalent potential temperature (θ_{ES}). These two variables provide an excellent means of interpreting the layered structure of the trade wind boundary layer and provide a simple way of illustrating buoyancy concepts. The initial profiles of these quantities are presented in Figs 4.4 and 4.5

By examining these initial profiles, the characteristic structure of the trade wind boundary layer is clearly seen. A distinct mixed layer is visible up to about 500m where s and r are constant and θ_{ES} is nearly unstable for dry air. Just above this layer is a conditionally unstable cloud layer reaching up to about 1500m. In this region r decreases almost linearly with height and s increases nearly linearly. Above this is the inversion layer, diagnosed by the changing slope of s and r and the increase of θ_{ES}. The base of the inversion can be diagnosed as the point where θ_{ES} changes sign.

In initializing the model this way one basic simplification has been necessary. This involves neglecting liquid water in the initial computations of both total water density and entropy density. Both of these quantities include contributions due to the amount of total liquid water. However, any attempt to include some estimate would be in error. It was decided that allowing the model to reach an equilibrium on its own was preferable to including erroneous measures of cloud liquid water.

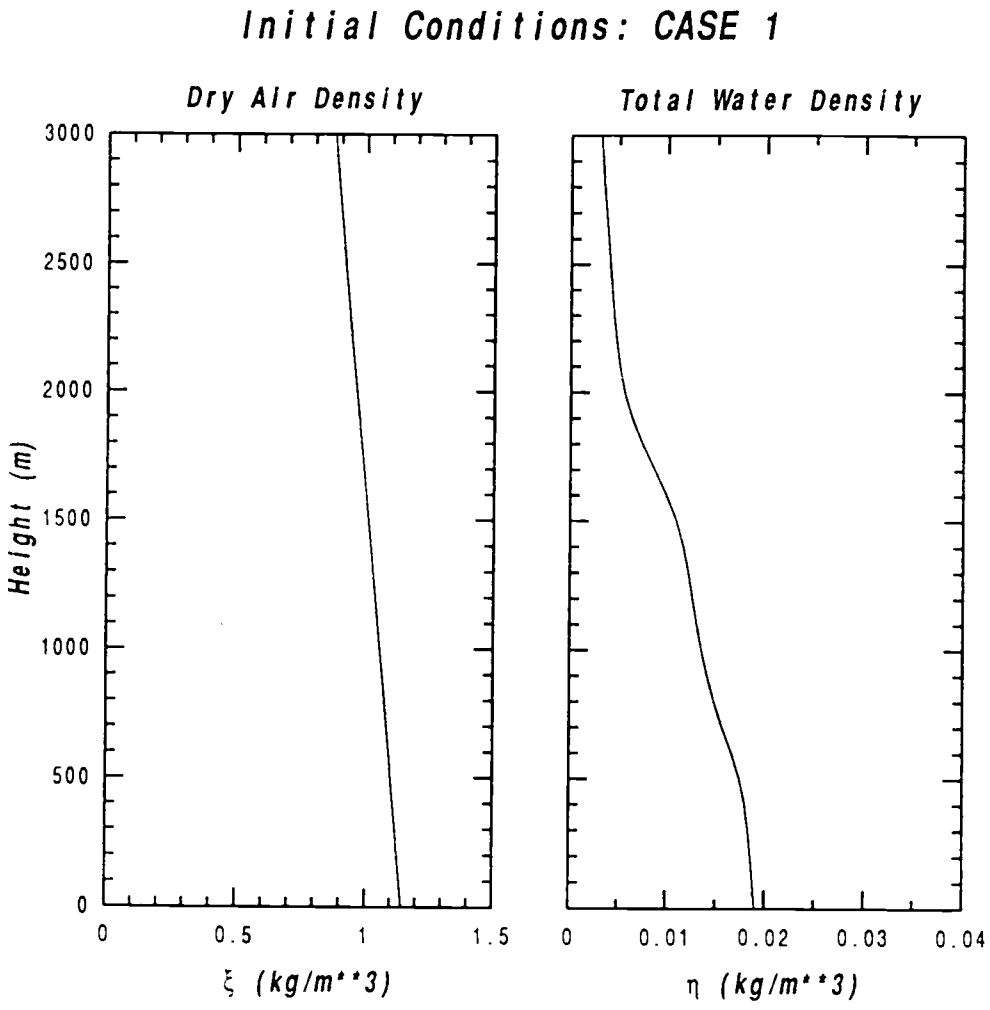

Fig. 4.1 Initial conditions for case I: (a) dry-air density and (b) density of total water substance.

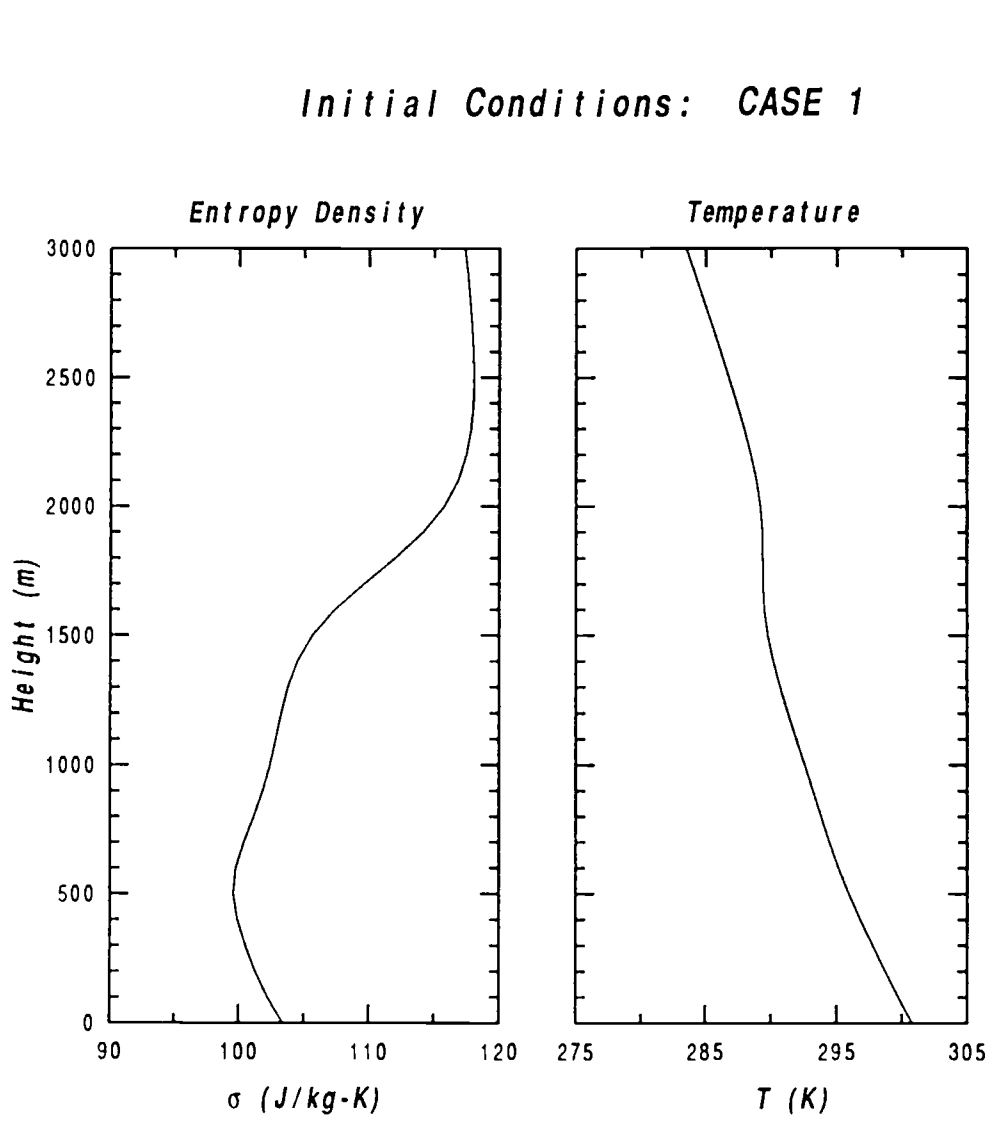

Fig. 4.2 Initial conditions for case I: (a) moist entropy density (b) temperature.

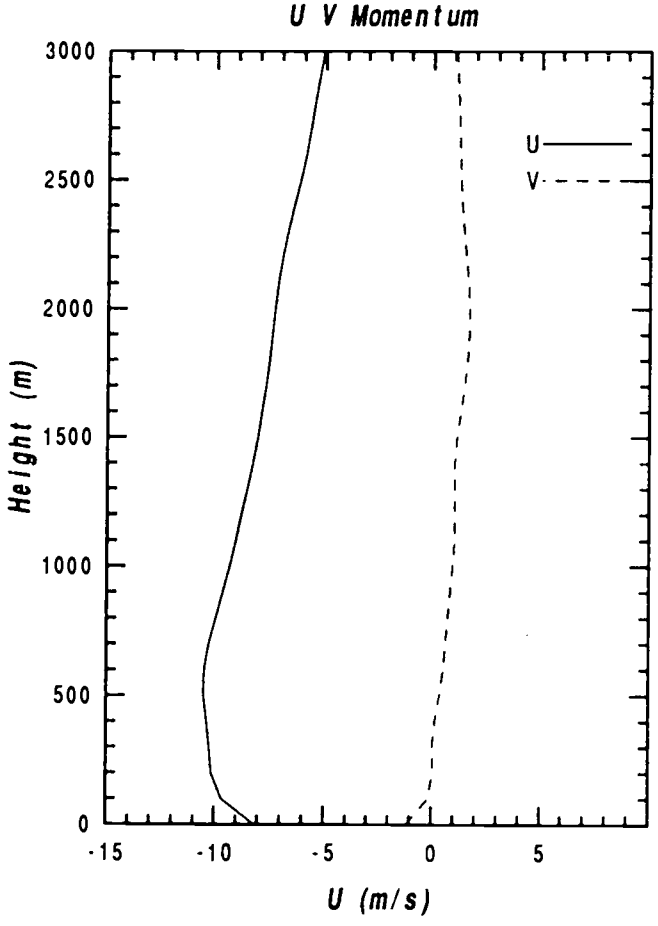

Fig. 4.3 Initial conditions for case I: two horizontal components of momentum

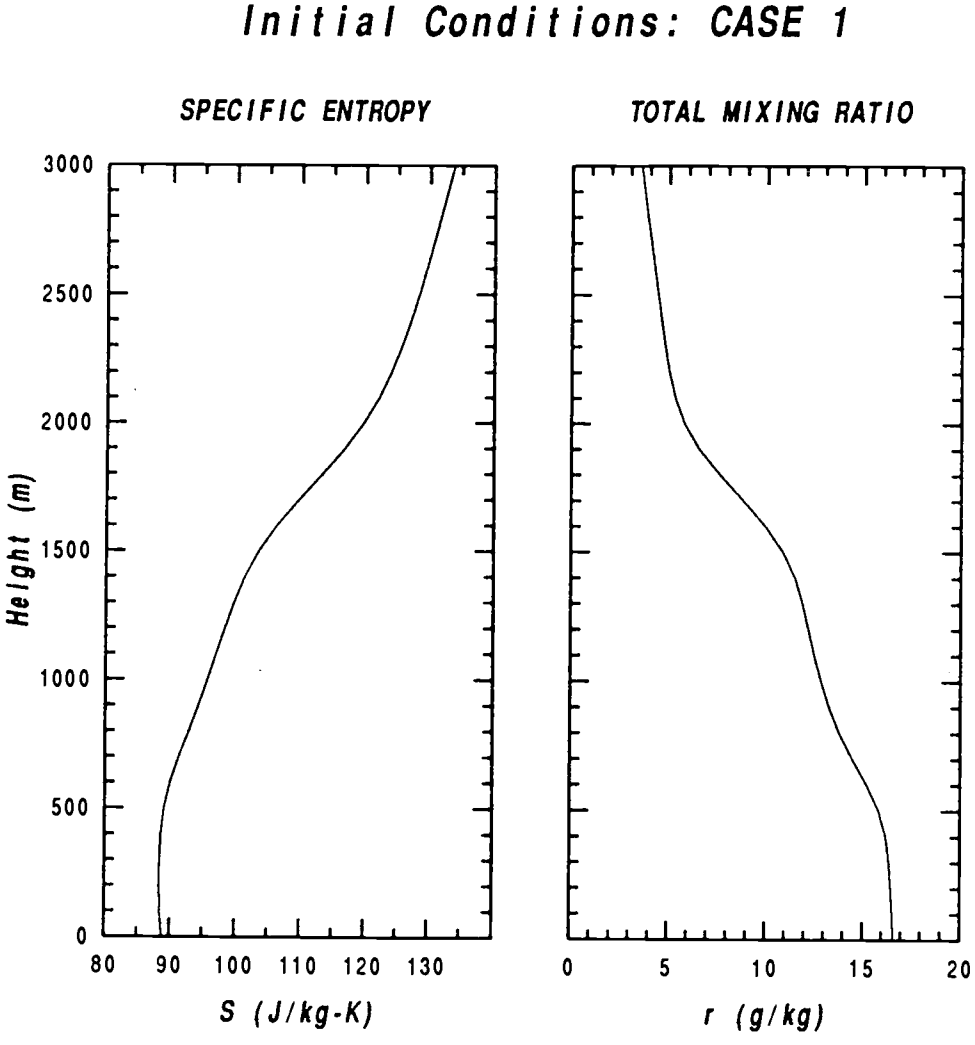

Fig. 4.4 Initial conditions for case I: (a) specific entropy and (b) total water mixing ratio.

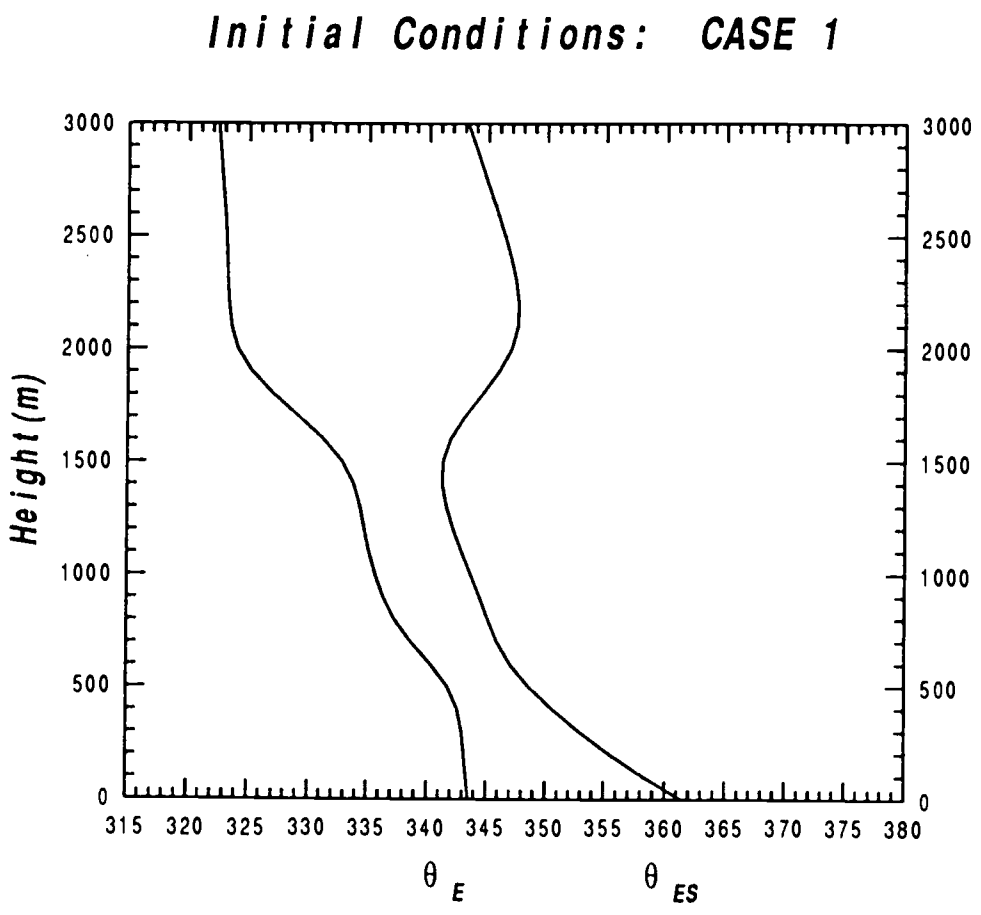

Fig. 4.5 Initial conditions for case I: equivalent potential temperature and saturation equivalent potential temperature

In addition to the model profiles presented in Figs. 4.1 through 4.5, several other quantities are necessary for this simulation. Of particular importance to trade-wind studies is the profile of subsidense used to simulate the large-scale sinking motion of the tropics. Presented in Fig. 4.6 is the subsidence profile used for this simulation. It is derived from estimates made by Holland and Rasmusson (1973) and is treated as a fixed quantity throughout this simulation. Two additional quantities that must be specified prior to this simulation are the sea surface temperature and the fractional cloud cover. A sea surface temperature of 300.8K is believed to correspond to the undisturbed period of BOMEX and a cloud cover of 0.1 has been chosen to represent the average area covered by clouds during this experiment. While several methods exist to obtain estimates of fractional cloud cover, these estimates may be off by as much as a factor of two. At this stage, it is preferred to include this as a designated parameter and concentrate on the physics of the model at hand.

The initial conditions of the cloud kinetic energy term are also important to the cumulus parameterization. To avoid introducing any unnecessary perturbations, this quantity is initially set to zero. Convective mixing will then depend on the ability of the production term to react to the conditional instability of the cloud layer to produce kinetic energy.

To examine the model's ability to maintain a trade-wind structure, the model is initialized and run for a simulation of 48 hours. This is believed to be a sufficient amount of time to illustrate both the evolution of model variables and the interactions between individual forcing terms. Because our interest lies primarily in the thermodynamic effects, the horizontal momentum terms will remain fixed at their initial values. The model is run with a time increment of 60 seconds using a standard leapfrog prediction scheme with a nodal spacing of 100m. The results of this simulation are presented in section 5.1

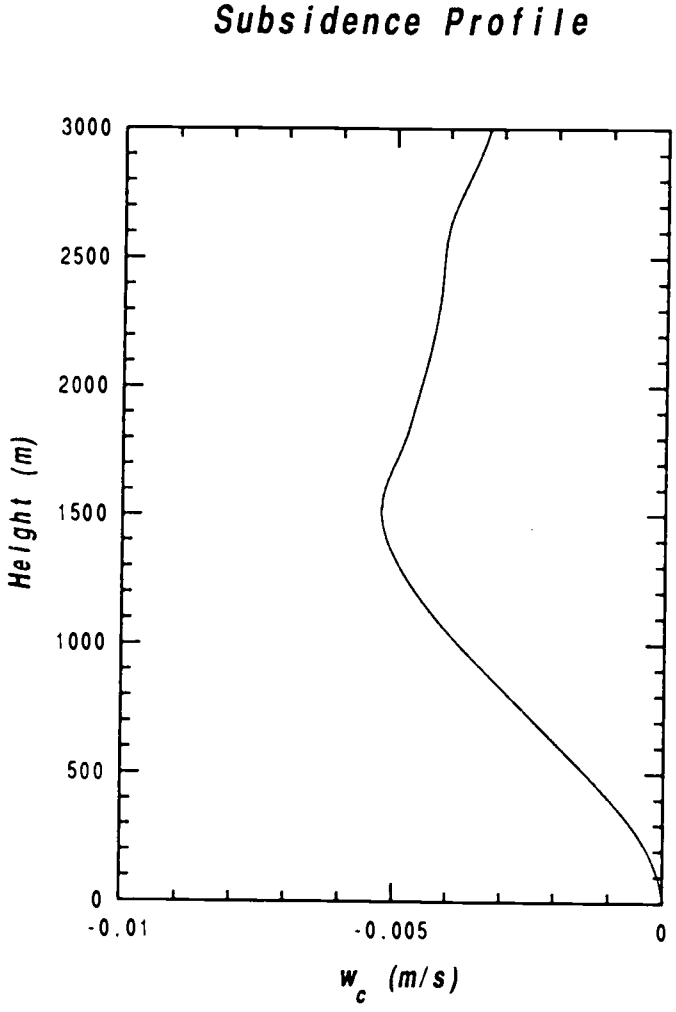

Fig. 4.6 Initial conditions for case I: subsidence profile.

4.2) Case II

The main purpose of this second simulation is to provide a way of examining the model's ability to produce a cloudy boundary layer given initially dry conditions. This is important because it illustrates the response of the model to a specific external forcing mechanism, in this case surface latent heat flux. To run this simulation only a few changes are made from case 1. First, the initial conditions are changed to represent a relatively dry boundary layer structure (Figs. 4.7-4.10). These profiles have been created simply for this purpose and are not meant to represent a physical situation that might occur in the tropics. The second change involves removing the effects of subsidence to allow the boundary layer to grow without any inhibiting factors.

Other than these differences, this simulation is much like case 1. In order to illustrate the necessary points, it was necessary only to run the model for a 24 hour simulation rather than the 48 hours used in case1. Results of this simulation can be found in section 5.2.

4.3) Entropy Discussion

Entropy has been used regularly for thermodynamic computations in the atmospheric sciences. However, it is not typically use to interpret atmospheric structures. Other conserved variables are used more commonly, including potential temperature, equivalent potential temperature and liquid water potential temperature. Because entropy is a primary variable used in this model, a brief discussion of its structure is useful and will help in interpreting model results.

The unsaturated form of the entropy equation as derived in section 2.2b takes the form

$$\sigma = \xi\left(C_{v_a} \ln\frac{T}{T_0} - R_a \ln\frac{\xi}{\xi_0} \right) + \eta\left(C_{v_v} \ln\frac{T}{T_0} - R_v \ln\frac{\eta}{\eta_0} \right) \qquad (4.1)$$

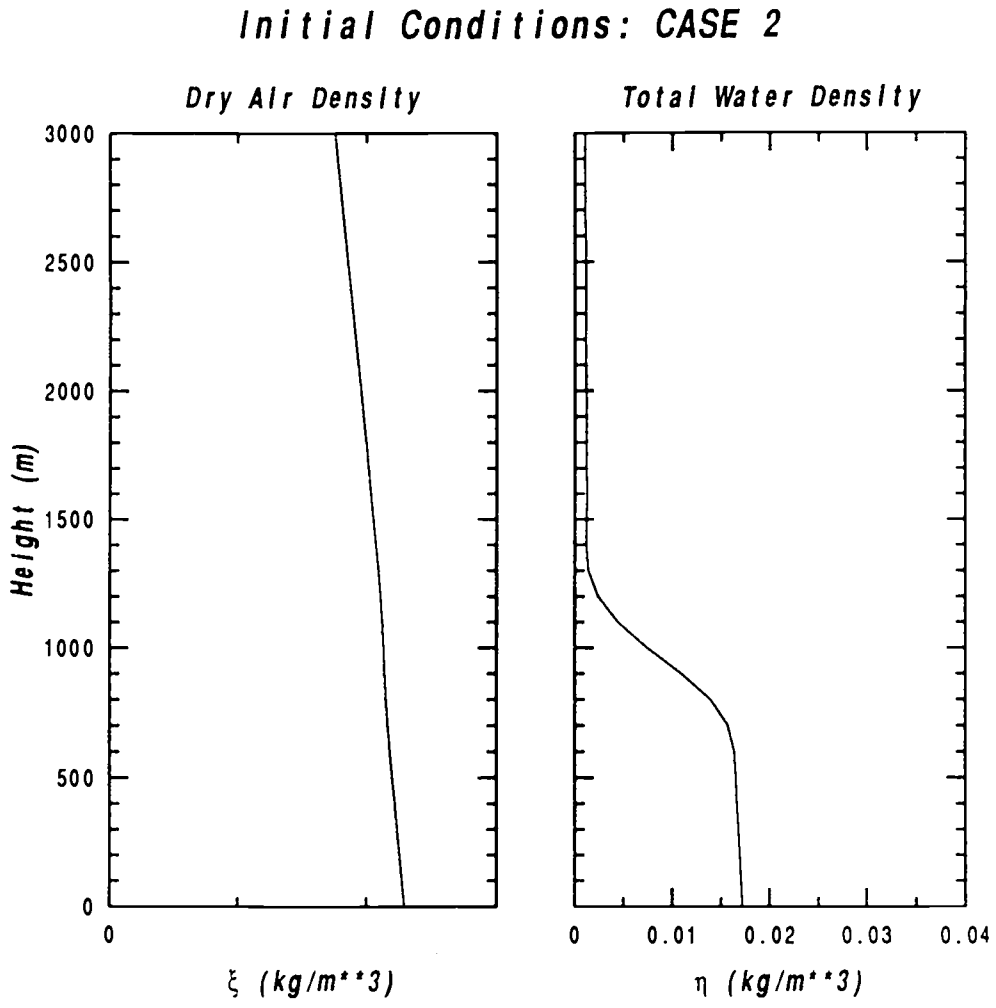

Fig. 4.7 Initial conditions for case II: (a) dry-air density and, (b) density of total water substance.

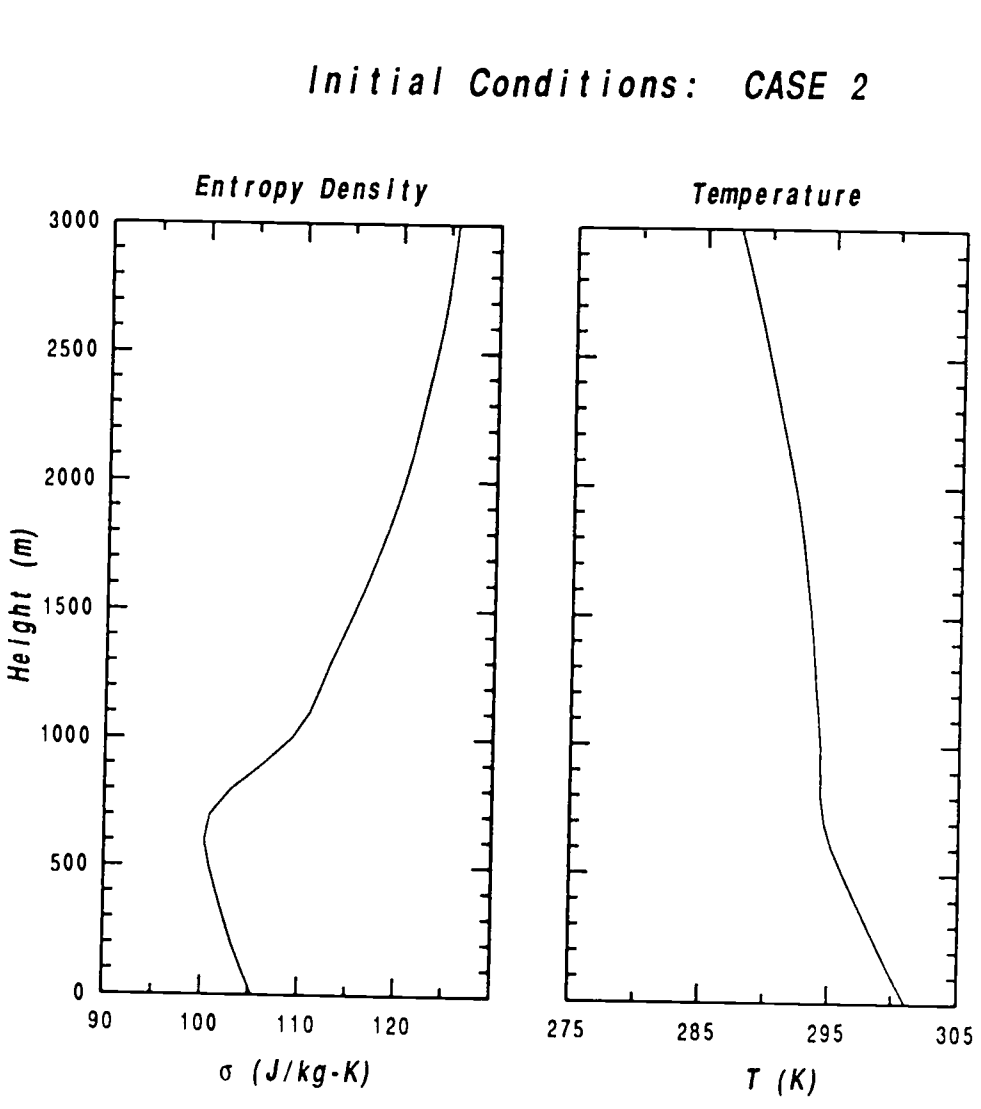

Fig. 4.8 Initial conditions for case II: (a) moist entropy density and (b) temperature.

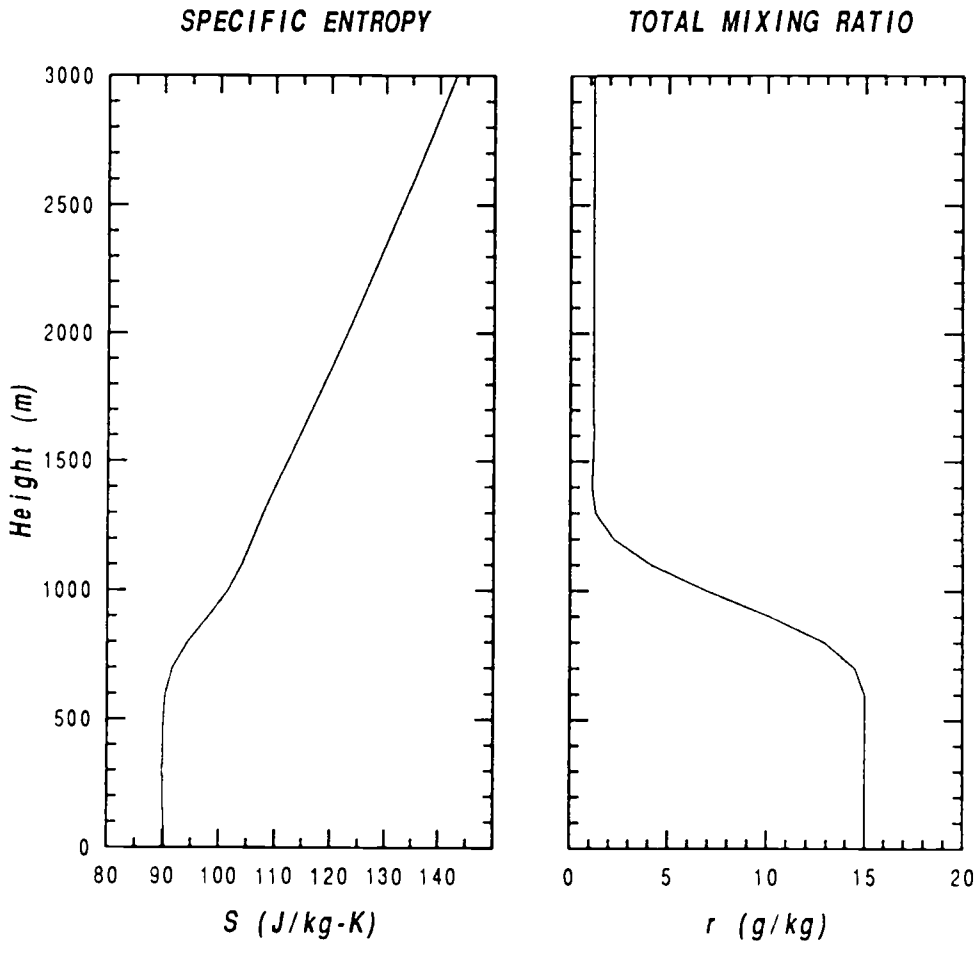

Fig. 4.9 Initial conditions for case II: (a) specific entropy and, (b) total water mixing ratio.

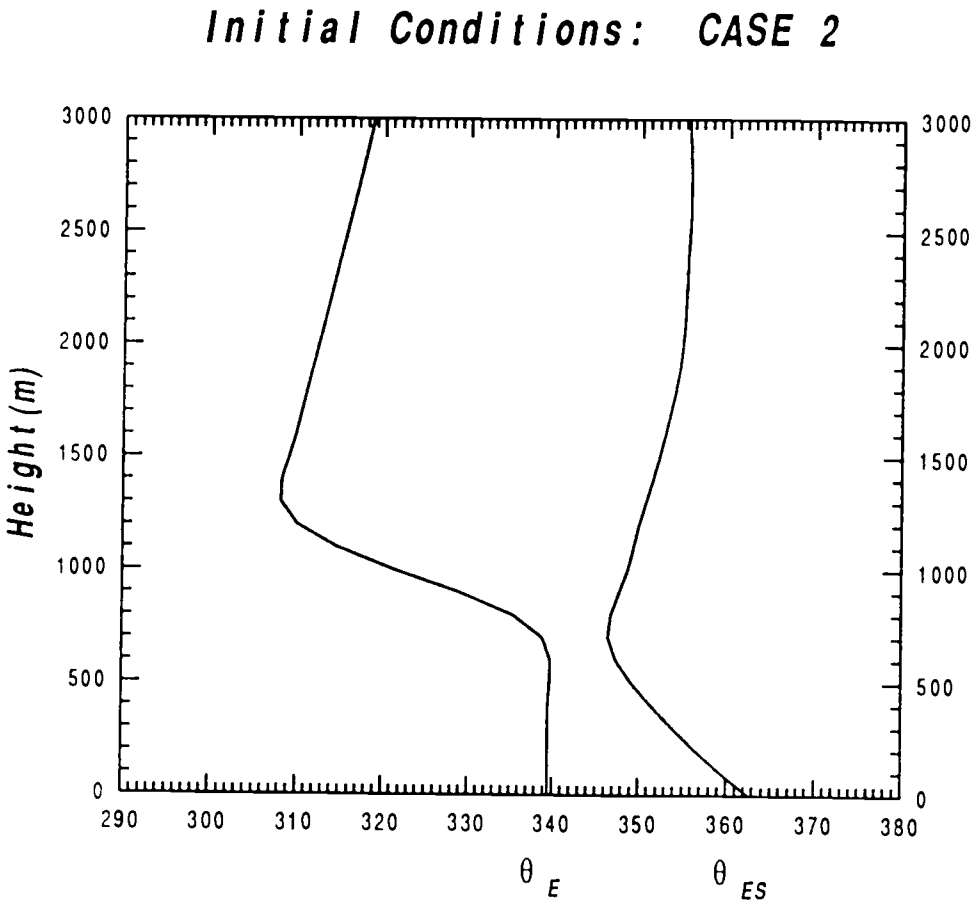

Fig. 4.10 Initial conditions for case II: equivalent potential temperature and saturation equivalent potential temperature

This equation can be rewritten as a specific quantity by substituting the definition for total water mixing ratio ($r = \eta/\xi$), and dividing by the density of dry air. In so doing we obtain an expression for dry specific entropy (s_D) that takes the form

$$s_D = C_{v_a} \ln\frac{T}{T_0} - R_a \ln\frac{\xi}{\xi_0} + r\left(C_{v_v} \ln\frac{T}{T_0} - R_v \ln\frac{\xi}{\xi_0} - R_v \ln\frac{r}{r_0} \right) \qquad (4.2)$$

For a completely dry atmosphere r=0 and this expression simplifies to

$$s_D = C_{v_a} \ln\frac{T}{T_0} - R_a \ln\frac{\xi}{\xi_0} \qquad (4.3)$$

The term dry specific entropy does not mean that no moisture is present but merely that the entropy has been divided by the dry air density rather than the total density. In a dry atmosphere only two terms contribute to the magnitude of the dry specific entropy and both of these depend upon the choice of the reference values used in deriving the initial expressions. A complete discussion of the variation of this quantity with differing reference conditions is beyond the scope of this discussion. The concern here will be in understanding the structure of entropy given the conditions presented in this model.

The reference conditions used in the current model formulation are for a parcel of air at the point of marginal saturation with at temperature of 273.15K and a total pressure of 1000 mb. This results in a reference dry air density of 1.267 kg/m^3. Over the conditions relevant to the tropical boundary layer, the dry-air density will always be less than this reference quantity ($\xi/\xi_0 < 1.0$) and as a result, the second term in (4.3) will always be negative. In addition, because density decreases with height, this term will not only remain negative but will increase in magnitude with height. Similarly, the thermodynamics considered in this model have dealt only with temperatures of 273.15K or greater and the first term will also always remain positive. The first term, however, will decrease with height as (T/T_0) goes to 1.0. When combined, the increase of the second term with height outweighs the decrease in the first, resulting in a profile of dry specific entropy that increases with height.

The relationship between temperature and specific entropy is somewhat

complicated by the presence of density terms. This relationship can be somewhat simplified by examining the variations of these two quantities when the dry-air density is held constant. This is illustrated in Fig. 4.11 and shows that temperature varies almost linearly with specific entropy along lines of constant density. This is significant because the dry-air density varies little with time and can be thought almost as a height coordinate. For example, if a process was seen to warm the atmosphere at a certain level then we would expect to see a similar rise in the dry specific entropy.

To illustrate the variation of the dry specific entropy with height, the initial conditions for Case 1 described in section 4.1 were used to construct the dry specific entropy as a function of dry air density. This relationship is presented in Fig. 4.12 and represents the dry specific entropy of this particular atmospheric profile with all the moisture removed. The increase of s_D with height is apparent and elements of the mixed layer, the cloud layer and the inversion layer can be seen. These features are visible because of variations in temperature through these layers.

To consider the change in dry specific entropy when moisture is included, Eqn. (4.2) can be rewritten in the form

$$s_D = (C_{v_a} + rC_{v_v}) \ln\frac{T}{T_0} - (R_a + rR_v) \ln\frac{\xi}{\xi_0} - rR_v \ln\frac{r}{r_0} \qquad (4.4)$$

With moisture present, r is no longer zero as was the case in the previous discussion. Because the mixing ratio under even the most tropical conditions rarely exceeds values of about .02kg/kg, the first two terms in brackets are influenced very little by the presence of moisture. In addition, the increase in the first term is partly overcome by the reduction in the second. The third term however exerts a significant influence. This is partly due to the fact that under the reference condition chosen for this model, (η/η_0) is generally positive and large at the surface where larger quantities of moisture are present. What this shows is that addition of moisture in significant amounts will act to reduce the magnitude of

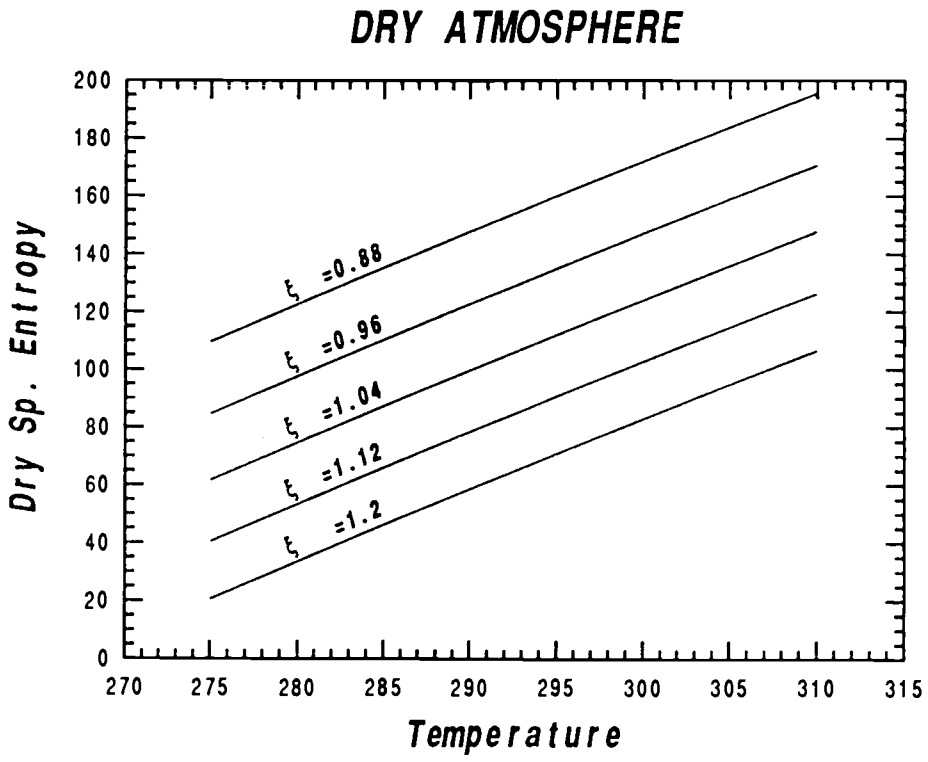

Fig. 4.11. Plot of dry specific entropy vs. temperature for dry air conditions, along lines of constant dry air density.

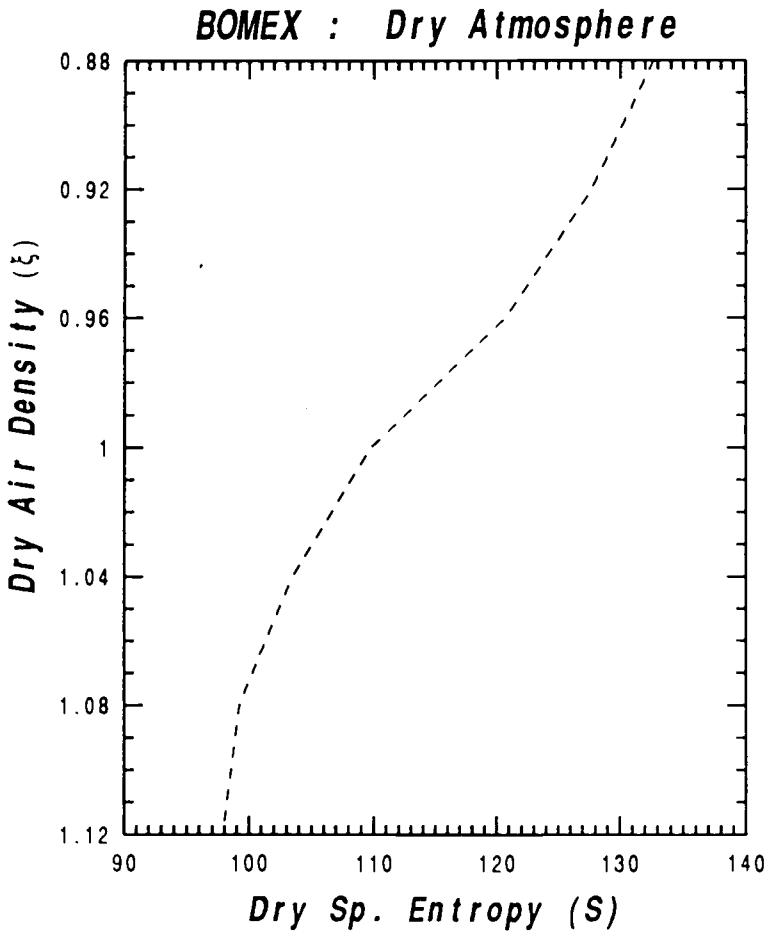

Fig. 4.12 Variation of dry specific entropy with dry air density for a dry atmosphere.

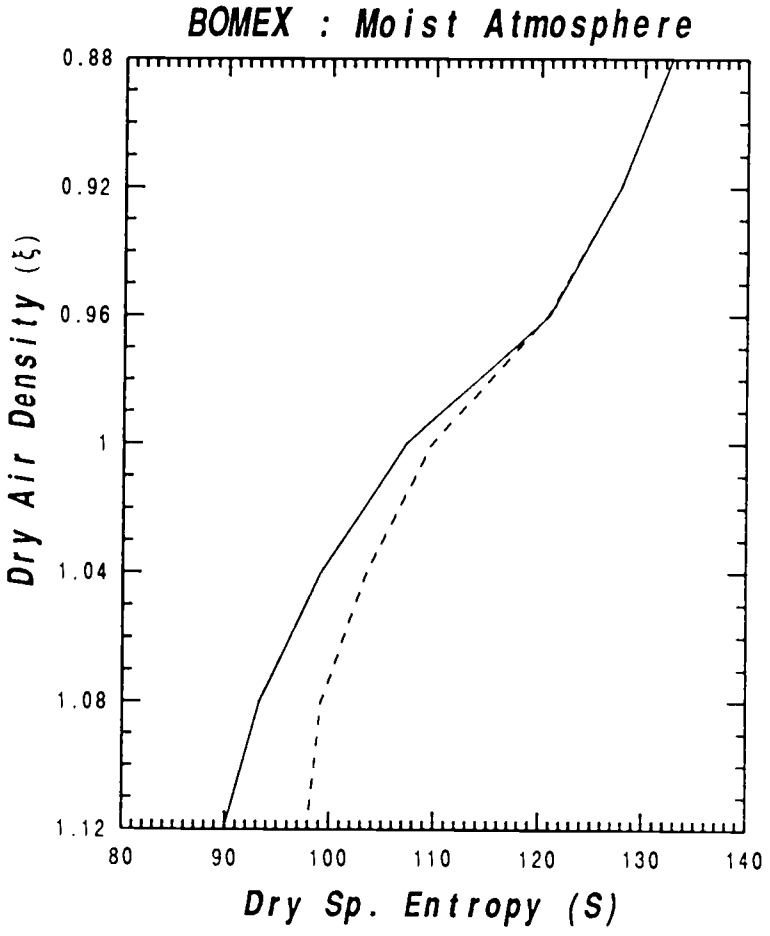

Fig. 4.13 Variation of dry specific entropy with dry air density for both a moist atmosphere (solid line) and a dry atmosphere (dashed line).

the dry specific entropy.

Figure 4.13 shows the effect of including moisture on the structure of the dry specific entropy. As would be expected, the decrease is greater near the surface where more moisture is present and near zero in the upper levels where the moisture content is extremely small.

This discussion of entropy is important when interpreting the surface and convective fluxes of the model. From the previous discussion, it is clear that a positive moisture flux across the lower surface corresponds to a negative surface flux of entropy. Similarly, when clouds transport moisture vertically, we would expect to observe a negative entropy flux. For processes that do not include moisture such as radiation and to some extent subsidence, we would expect to see a change in entropy that revolves around the thermal exchange properties: radiation will lead to cooling and a reduction in entropy and subsidence leads to warming and an increase in entropy.

5. MODEL RESULTS

In this section the results from two model simulations are presented and discussed. Special attention is placed on interpreting the results to gain insight into both the effectiveness of the applied cumulus parameterization scheme and the consequences of various assumptions used in it's development. The fundamental assumption used here is that shallow cumulus clouds are dominated by local processes and as a result, the intensity of convective mixing can be parameterized in terms of local measures of both the conditional instability and relative humidity. While the two simulations presented here will not provide a sufficient basis for a complete test of the models abilities, they do present the model with some of the fundamental challenges that must be met by any model of the convective boundary layer.

5.1) Case I

The purpose of case 1 is to examine the models ability to maintain the equilibrium trade wind structure discussed in section 4.1. To accomplish this a general balance must be reached between all of the forcing mechanisms involved. The heat and moisture added at the surface must be distributed upward over a sufficient depth to allow it to be balanced by the effects of radiation and subsidence. The ability to redistribute moisture is a fundamental test of any cumulus parameterization scheme. By examining the change from a given equilibrium structure it is possible to assess how well the parameterizations scheme represents this process.

Presented in Figs. 5.1 and 5.2a-b are the profiles of important model variables and their evolution over the 48 hour simulation. These figures show several important features of the models performance and illustrate the boundary layer structure that resulted from this simulation. First, although it is apparent that significant changes from the initial state occurred, the general layered

structure of the boundary layer is preserved. The fact that the model maintains the layered structure characteristic of the tropical boundary layer is encouraging. It indicates that at least in a general sense, each of the physical forcing mechanisms are being qualitatively well represented, but their magnitudes may be in error. For example, the growth of the inversion layer illustrates that subsidence is acting as it should, to warm and dry the upper layer. The continuation of near constant profiles of s and r near the surface indicates that mixing is occurring in the lowest layer above the surface and the presence of linear profiles of s and r above this illustrates that the convective processes are maintaining a convectivly well-mixed cloud layer.

Although the layered structure of the boundary layer is preserved, several departures from the initial state are apparent. Two of the most dramatic of these are the strong enhancement of the inversion layer and the moistening of the cloud and subcloud layers. Both of these changes can be attributed to the performance of the cumulus parameterization scheme and can be illustrated by examining Figs. 5.3-5.6. The curves in these figures represent the forcing terms of the prognostic Eqns. (2.6a-c) and show the effects of the individual physical processes being considered. It is fairly clear from these figures that the downward growth of the inversion layer is a result of a strong imbalance in the region above the inversion base. In this region the cloud effects go rapidly to zero while the subsidence terms are at their peak. For a balance to be achieved, the convective influences would have to reach much further into the inversion layer to a height of about 2000m. However, this is at the top of the inversion layer and it is questionable whether shallow clouds would be found to penetrate to this level. During BOMEX, this balance may have been achieved as a result of mesoscale variations in the boundary layer structure or in the presence of a limited number of deep convective cells

A second feature of interest is the initial jump and gradual increase of the

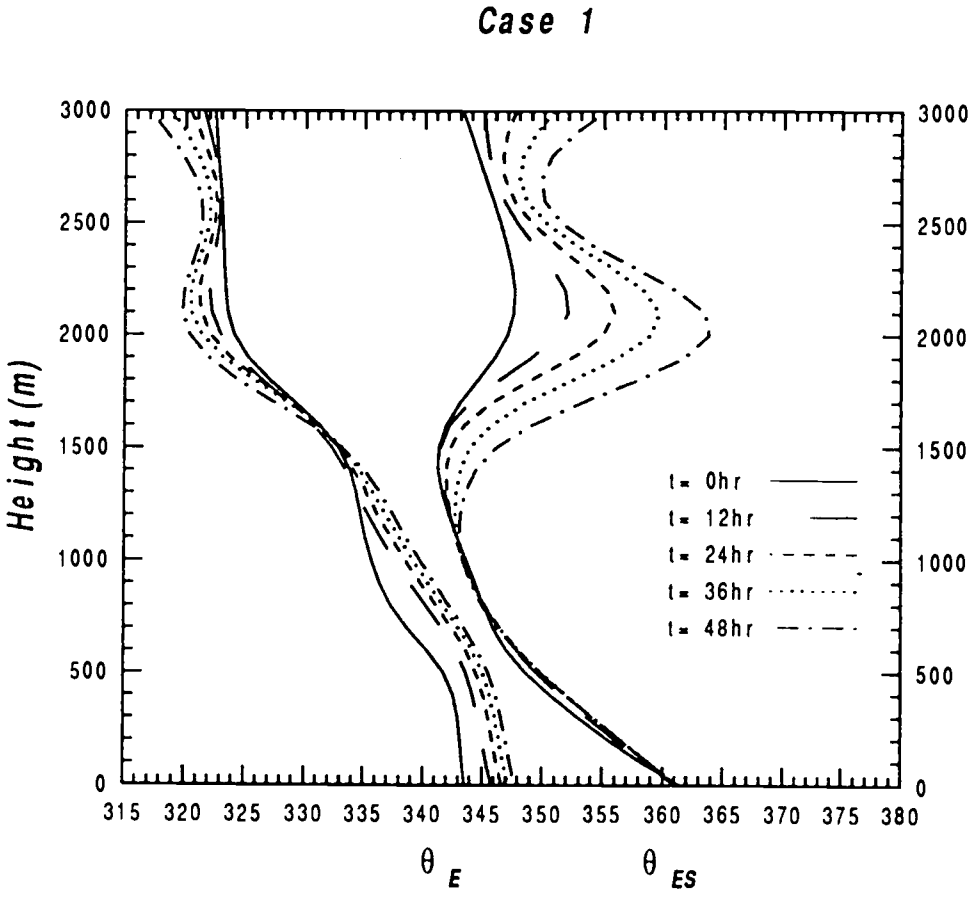

Fig. 5.1 Evolution of equivalent potential temperature and saturation equivalent potential temperature profiles over 48 hours of simulated time.

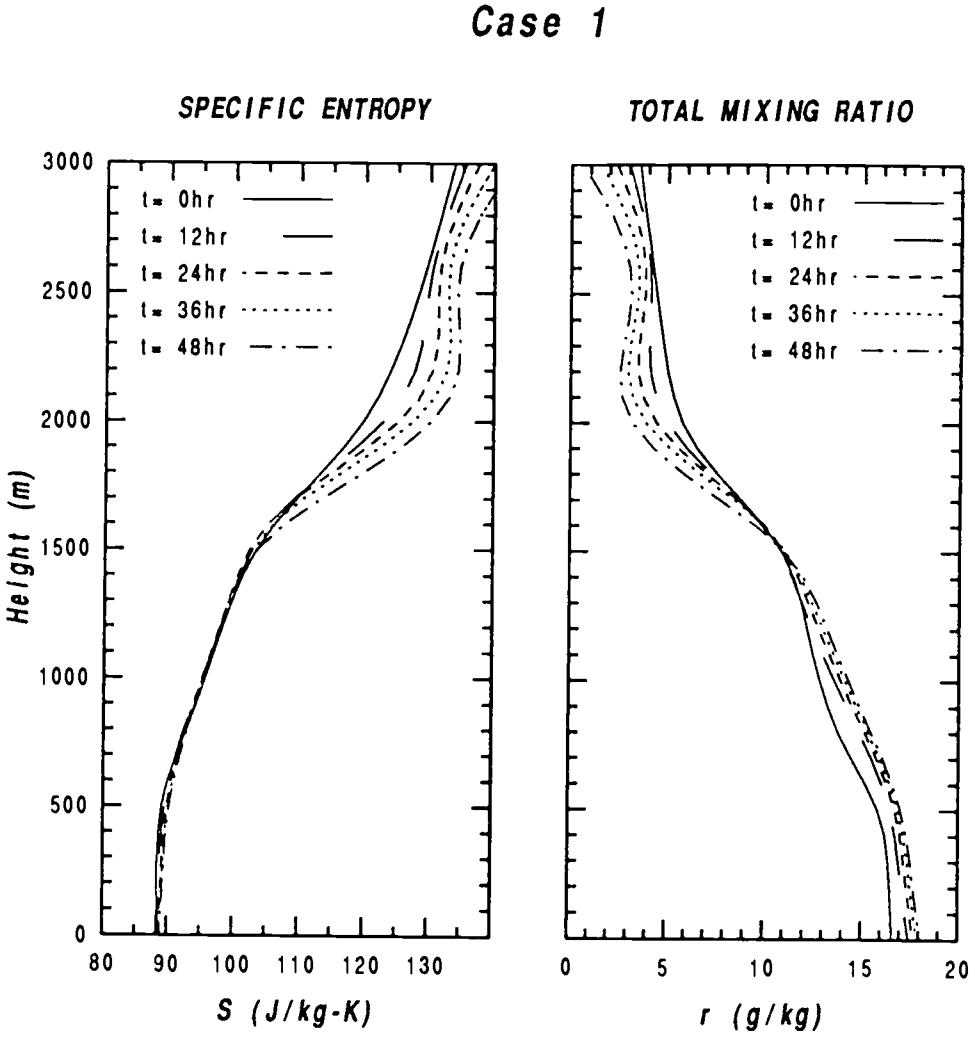

Fig. 5.2a,b Evolution of specific entropy and total water mixing ratio profiles with time.

total water mixing ratio below the inversion layer. This accumulation of moisture is a response to the interaction of several processes. First, there is basically an imbalance between the amount of moisture entering the model domain at the surface and what is being removed. For a balance to be achieved this moisture would have to be distributed over a deeper layer where it can counteract the effects of subsidence. Again, this would be achieved if the convective effects were found to penetrate much further into the inversion layer.

These changes from the initial mean conditions and the imbalance that exists in the forcing terms indicate that this convective parameterization scheme may not be accurately predicting the height to which cumulus effects are exerted. This suggests that the local buoyancy concept upon which this method is based is insufficient to explain completely the relevant physics involved, especially in the region of the inversion layer. However, several other explanations are also possible. For example it is quite possible that during the BOMEX period some degree of deep convection was present and would account for much of the imbalance in the upper inversion layer and above. Shallow clouds by definition will not penetrate to such heights and some degree of imbalance is inevitable unless deep convection occurs periodically.

Another explanation revolves around uncertainties in the initial profiles themselves. Upon examination of other studies of BOMEX it appears that differences exist in interpretation of the moisture structure. Tests of the convective adjustment scheme proposed by Betts and Miller (1986) also showed this tendency for the boundary layer to moisten. The reason given for this was that a correction is needed to adjust BOMEX soundings to account for diurnal variations (Holland and Rasmusen, 1973). A subsequent study by Betts and Albrecht (1988) contains profiles of BOMEX that are on the order of 1-2 g/kg greater at all levels than the initial conditions used here. The history of the current data set is unclear. However, it appears that the model is at least consistent with other studies.

The resulting model profiles appear to be in better agreement with the profiles studied by Betts (1988) than the initial conditions used here. If some errors were present in the initial moisture values, this could have a influence on the behavior of the convective parameterization scheme. Because this scheme depends upon the local moisture content of the air, low moisture values would produce weaker convective mixing throughout the cloud layer, and would also limit the height to which the convective processes are allowed to act. The use of a corrected moisture profile then, may help the cloud layer limit the strong downward growth of the inversion layer.

To explore this further, a second model simulation was performed after increasing the moisture profile of the initial profiles to more closely resemble those found in Betts and Albrecht (1988). The exact correction used by Betts is not known but amounted here to an increase of near 1.5 g/kg at all levels. The results of this simulation appear to be very similar to the uncorrected case (Fig. 5.7) with only a few exceptions. First, the increase in moisture below the inversion level is much weaker and remains closer to the initial profile (Fig. 4.5). Secondly, the depth of the cloud layer is slightly greater due to the increase of moisture and the downward growth of the inversion layer is slightly weakened by the cloud effects in the upper layer. However, the downward growth of the inversion layer is still strong and would eventually lead to a saturated boundary layer. Because only small changes were detected between the corrected and uncorrected cases and because the uncorrected case perhaps represents a greater challenge for the cloud scheme, the rest of the analysis concentrates on the uncorrected case.

The problem with the initial moisture content is perhaps why the profiles of entropy and total water mixing ratio behave so differently over time. Both are conserved variables, the forcing mechanisms are being parameterized in similar manners and both have similar vertical gradients through the model domain.

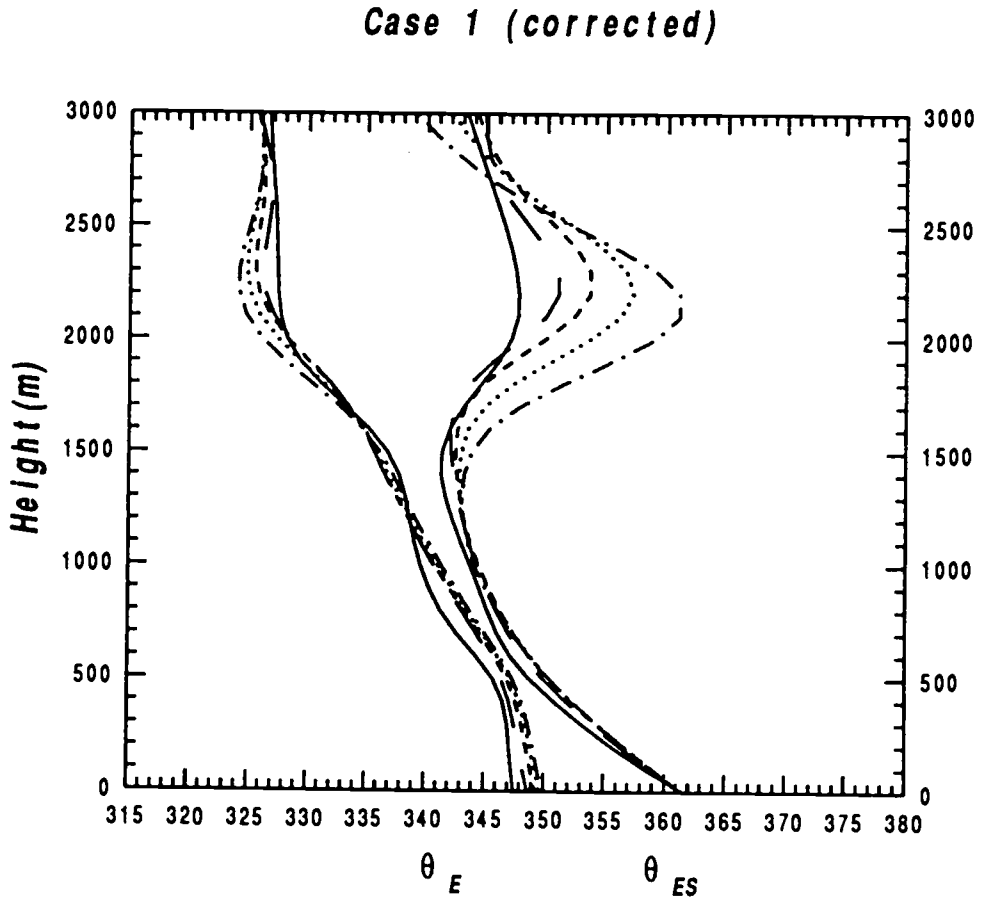

Fig 5.3. As in Fig 5.1 except with the moisture profile corrected.

However, the moisture grows while entropy appears to be nearly balanced. The only real difference is that entropy has one extra forcing mechanism representing the effects of radiation. Radiation has no direct effect on the moisture term and therefore does not enter the balance discussion for moisture. The specific entropy profile that results from this model simulation indicates that below the inversion a balance is achieved between the surface flux and the effects of radiation and subsidence. If the convective effects were to penetrate to a much higher level, it is possible that an imbalance in the entropy would occur. However, it is also likely that as entropy is transported upward, the surface flux would increase to help maintain the present balance.

The surface flux is an important element of the model and plays a strong role in balance structure of the boundary layer. Table 5.1 shows the surface flux quantities of moisture, and entropy initially and at 24 and 48 hours of the model run. Also included are computed values of sensible and latent heat flux . It is clear that as the moisture content of the boundary layer increases over the time span of the model run, the moisture flux decreases in response. The fact that the sensible and latent heat fluxes decrease over time is most likely due to the failure of the cloud portion of the model to penetrate to higher levels. More surface flux would be required to maintain a balance over a deeper layer.

Table 5.1: Model and observed surface flux values for BOMEX

	BOMEX	Model		
		t=0.0	t= 12hr	t= 24hr
Moisture (x10-4 m/s)		0.686	0.589	0.519
Entropy (W/m**2-K)		-0.047	-0.039	-0.037
Sensible Heat (W/m**2)	15	14.1	11.7	11.2
Latent Heat (W/m**2)	169	171	147	129.7

Several other quantities are also important to understanding the cloud scheme used here. These include the terms of the cloud turbulent kinetic energy equation, the computed cumulus velocity scale, the buoyancy length scale and the cloud

mixing coefficient used in computing the convective fluxes.

By examining Figs. 5.4-5.7 it is apparent that the cumulus forcing terms (dashed lines) are characterized by a peculiar two layer structure. This two layered structure is also apparent in the turbulent transport terms of the cloud kinetic energy equation presented in Figs. 5.8-5.9 and consist of a lower positive moisture peak near the 1000m level, a second positive peak near cloud top (1500m) and two negative moisture peaks located at 600m and 1300m. The lower negative moisture peak seems reasonable and is consistent with the notion of clouds removing moisture from the mixed layer. The upper negative peak, however seems unrealistic and inconsistent with our knowledge of convective processes. This pattern is also found in the convective forcing of entropy; only the signs are reversed.

The fact that this two layered structure shows up in the terms of the cloud turbulent kinetic energy equation implies that some element of the cloud scheme is responsible. Figures 5.10a-c contain the profiles of the convective buoyancy length scale, the cumulus velocity scale and the model derived cloud mixing coefficient. Examination of the convective length scale shows the presence of this two layer structure and its enhancement over time. Variations of this length scale is a function of the local moisture content alone and it can be seen from figure 5.2b that a slight change in the slope of the mixing ratio can be seen through the cloud layer. Because this length scale is a local property, the non-linear nature of the profile through the cloud layer is propagated over time. In fact, this two layer pattern is present in profiles from the first few time steps on.

In spite of this two layered pattern, the terms of the kinetic energy budget appear reasonable and qualitatively resemble those in figures 3.1 and 3.2. The production term goes from zero at the surface to a peak near cloud base where it levels off and goes to zero near 800m. It then becomes negative in the lower region of the inversion layer where the saturation equivalent potential temperature

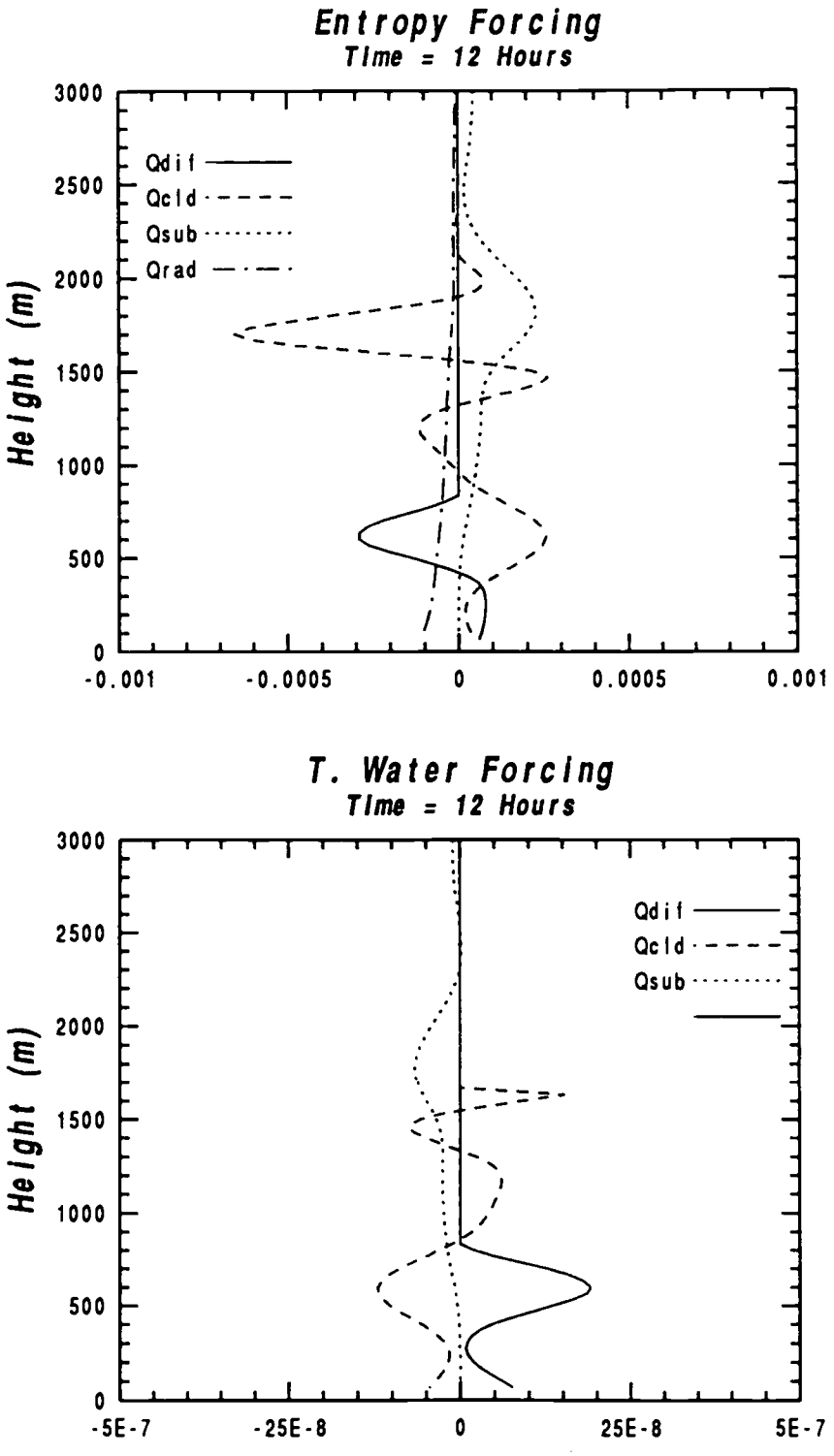

Fig 5.4a-b Parameterized forcing terms of the prognostic equations after 12 hours of simulated time.

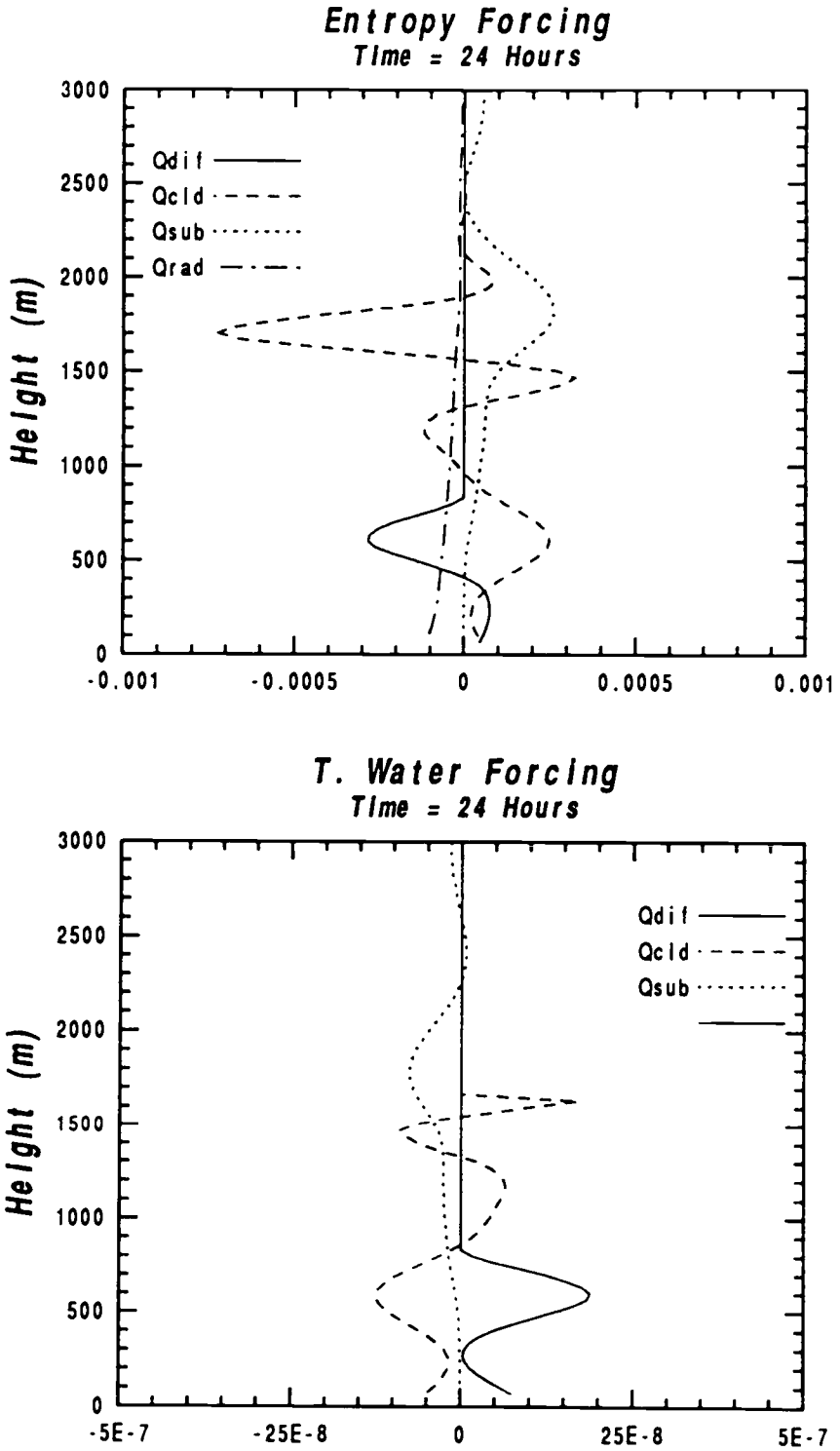

Fig 5.5a-b Parameterized forcing terms of the prognostic equations after 24 hours of simulated time.

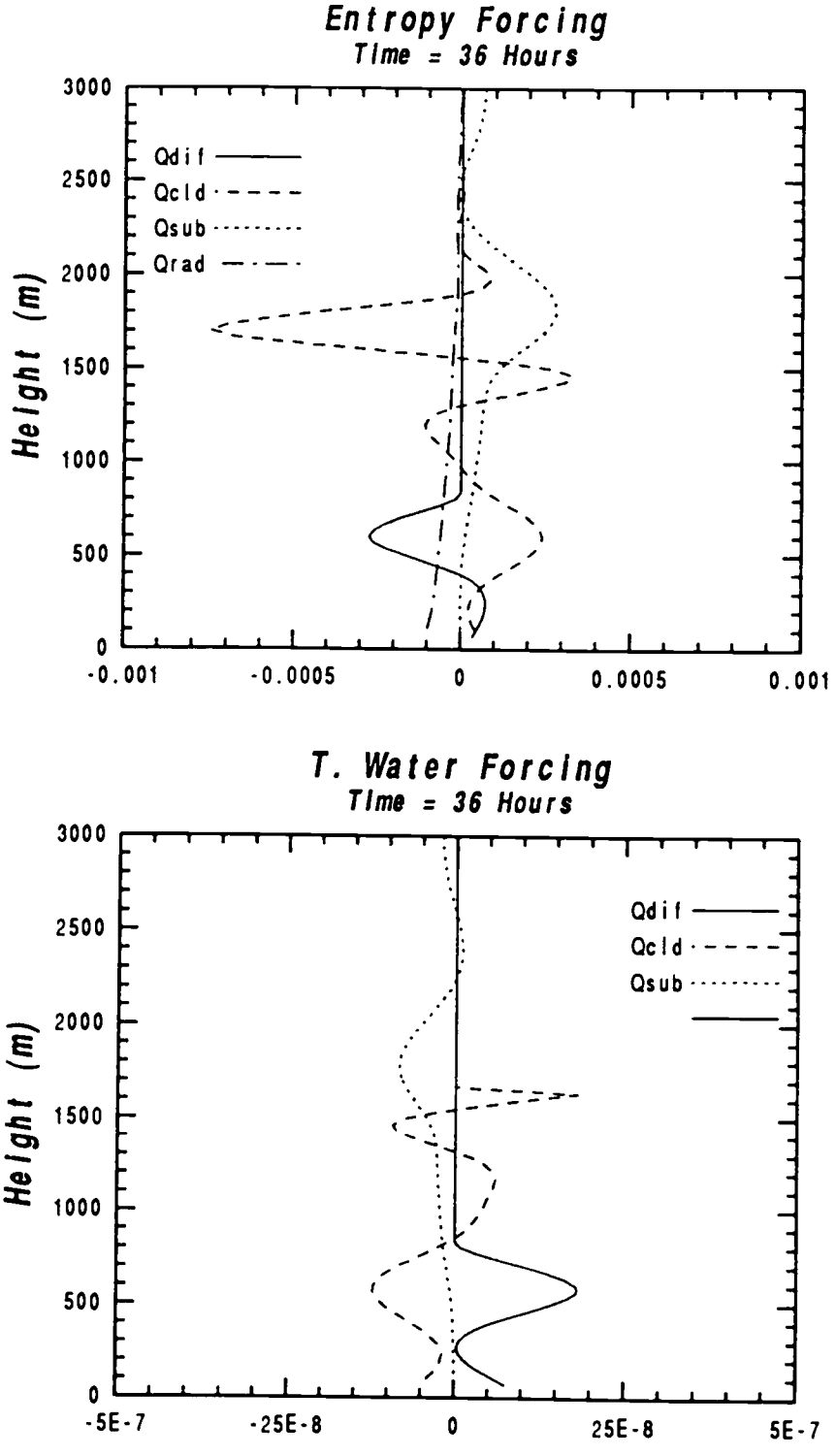

Fig 5.6a-b Parameterized forcing terms of the prognostic equations after 36 hours of simulated time.

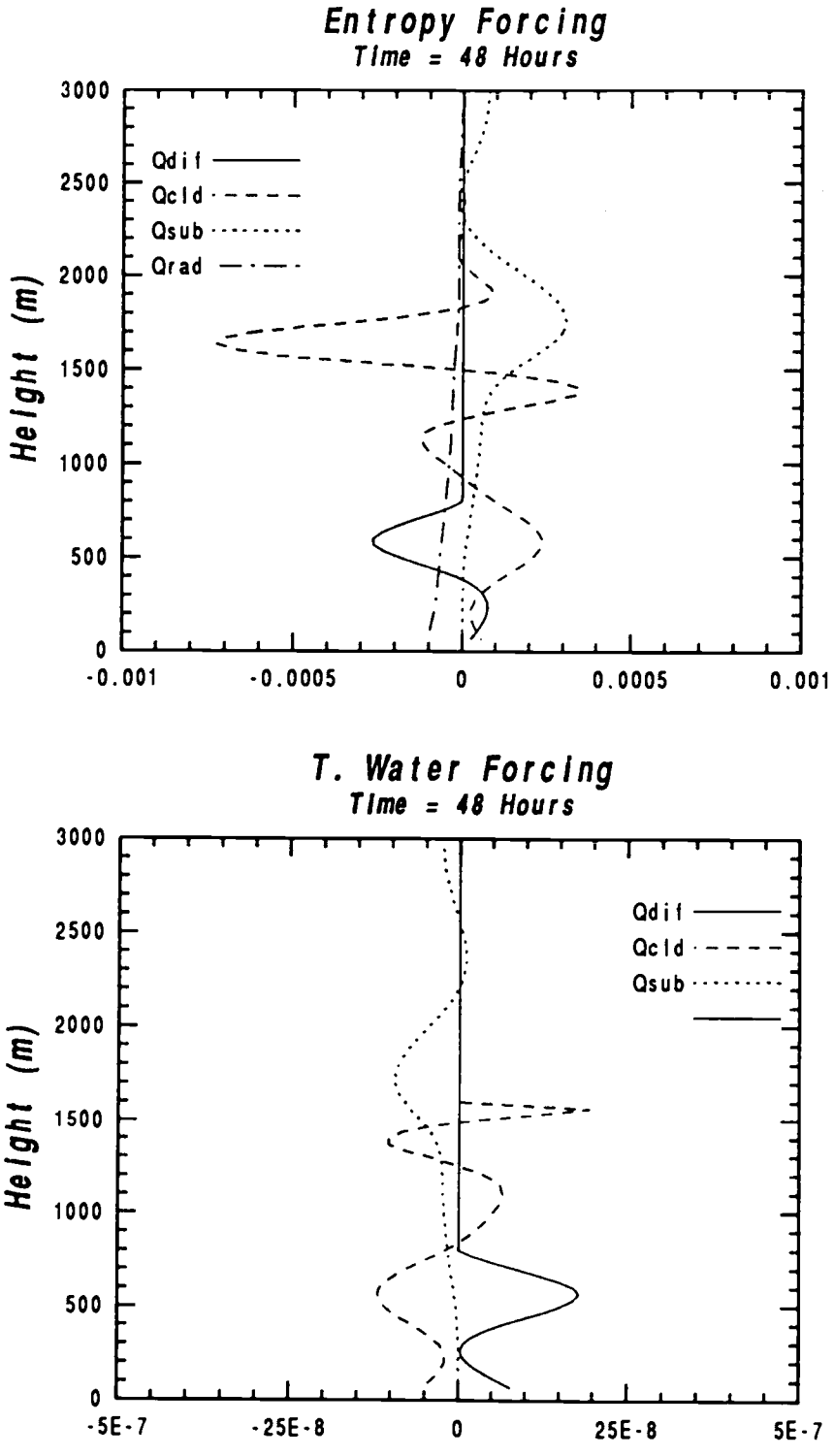

Fig 5.7a-b Parameterized forcing terms of the prognostic equations after 48 hours of simulated time.

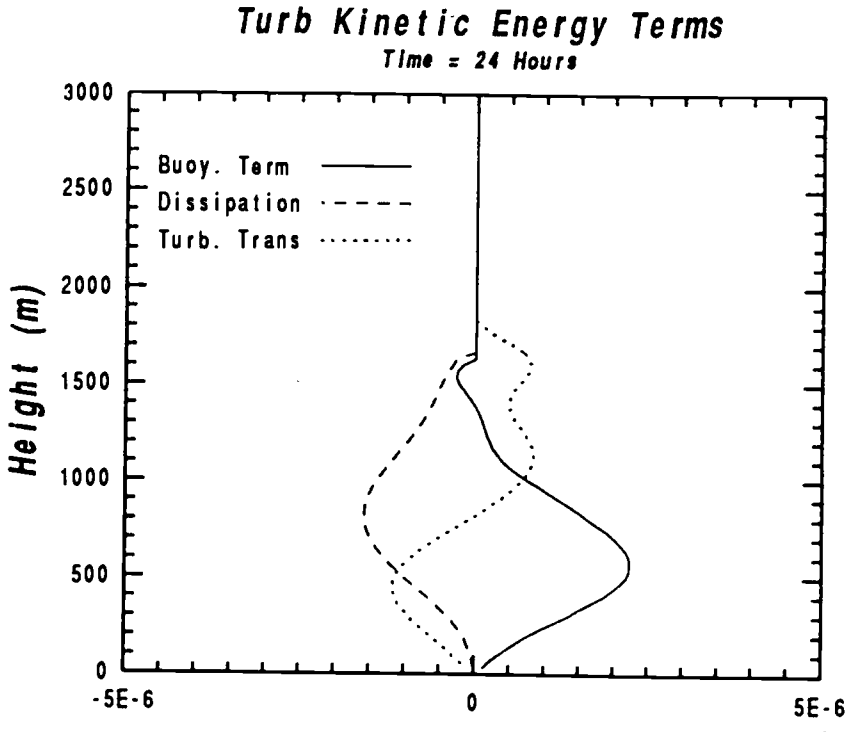

Fig 5.8 Terms of the cloud turbulent kinetic energy equation.

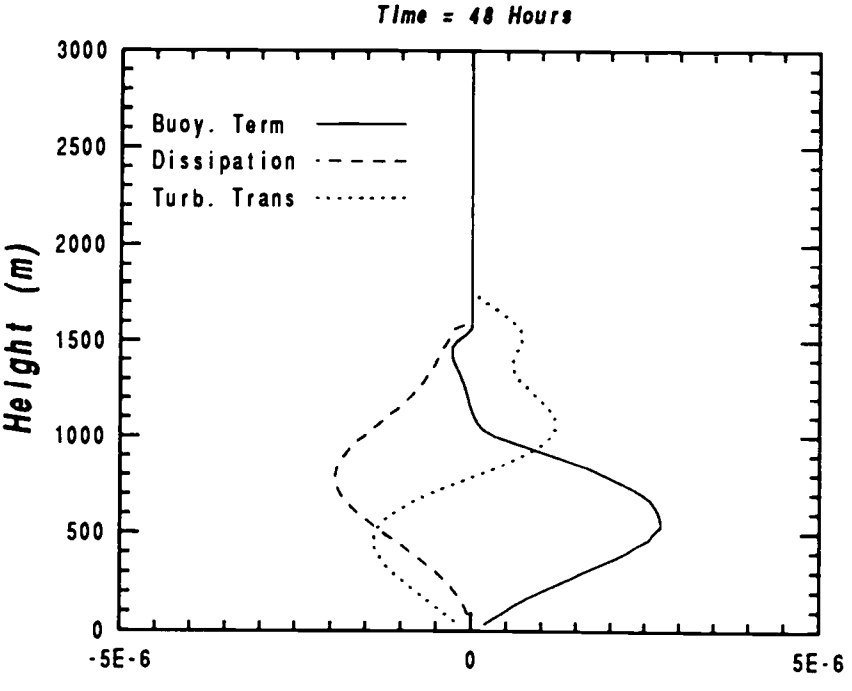

Fig 5.9 Terms of the cloud turbulent kinetic energy equation.

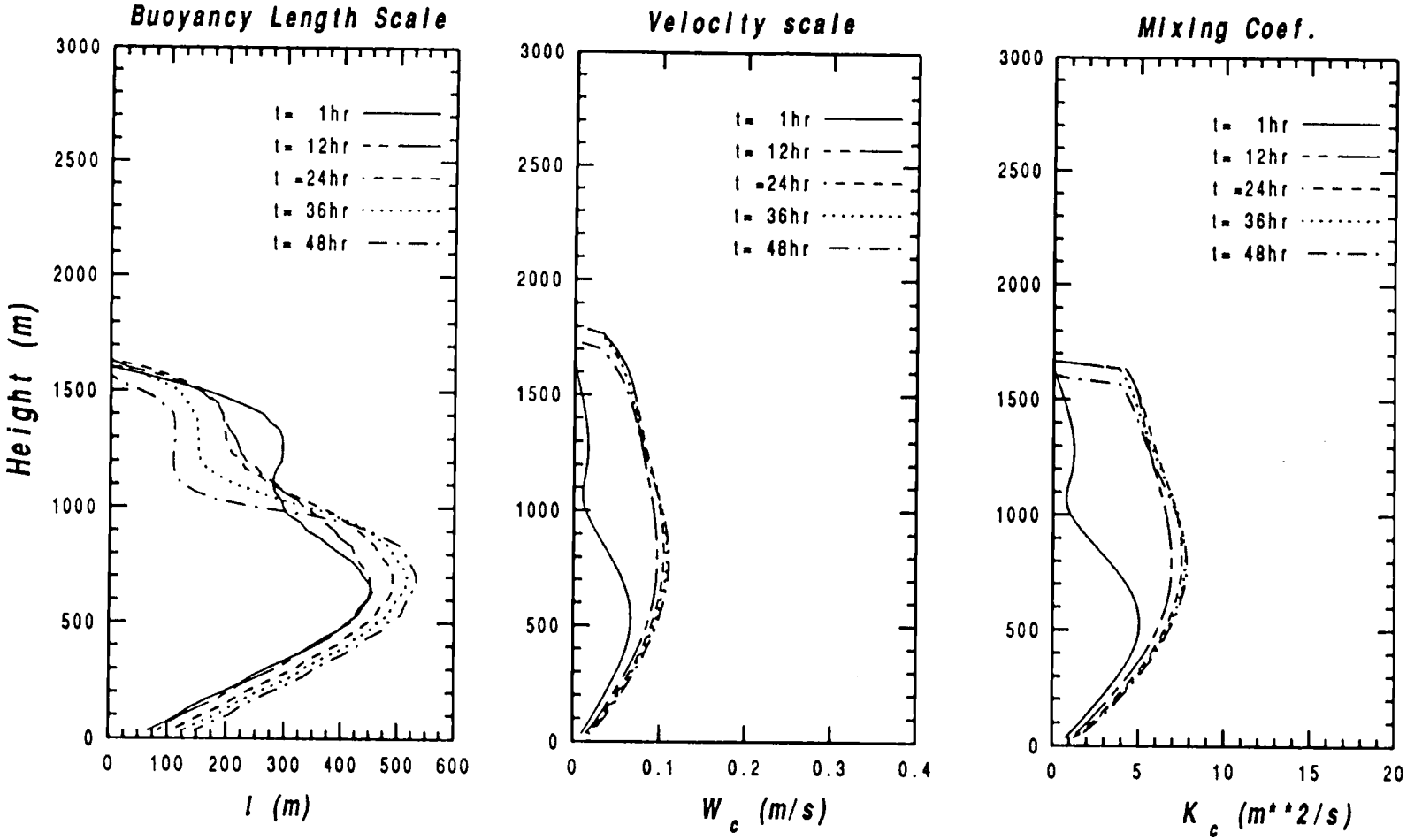

Fig 5.10 Evolution of important boundary layer variables including, a. buoyancy length scale, b. cumulus velocity scale and c. cloud mixing coefficient.

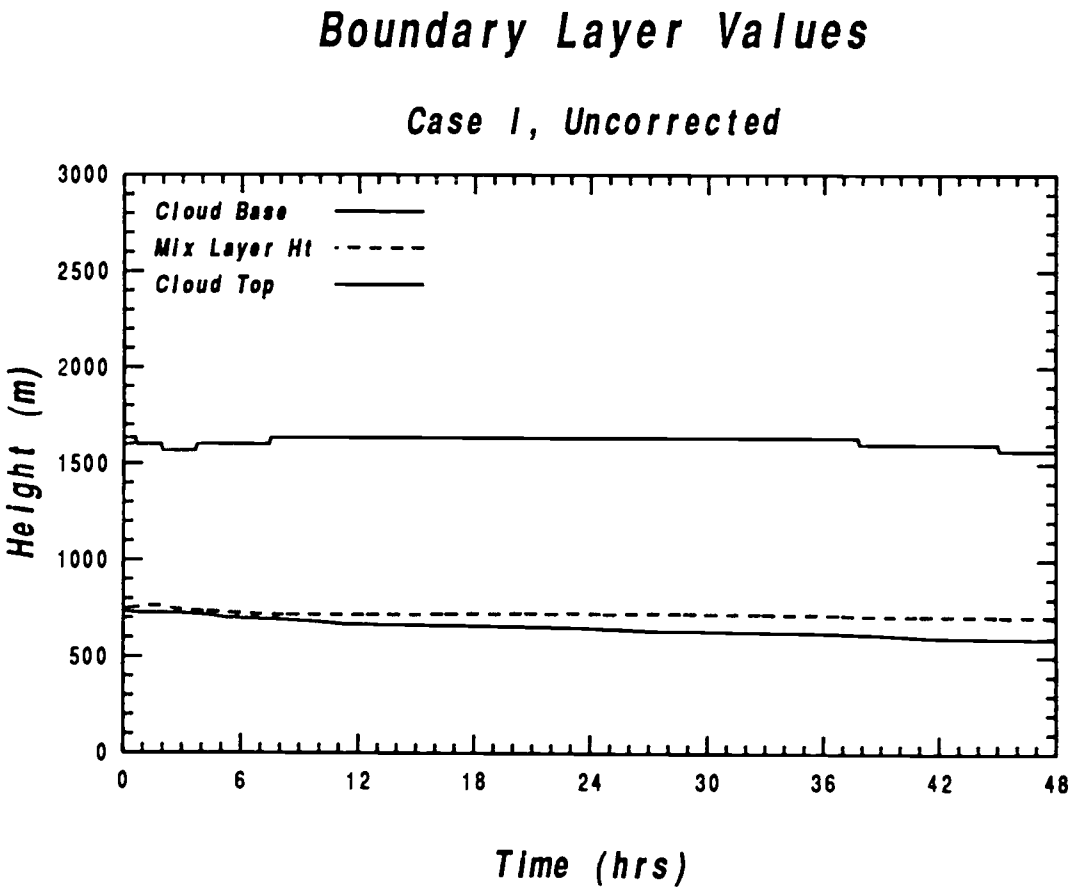

Fig 5.11 Boundary layer values over the 48 hour simulation

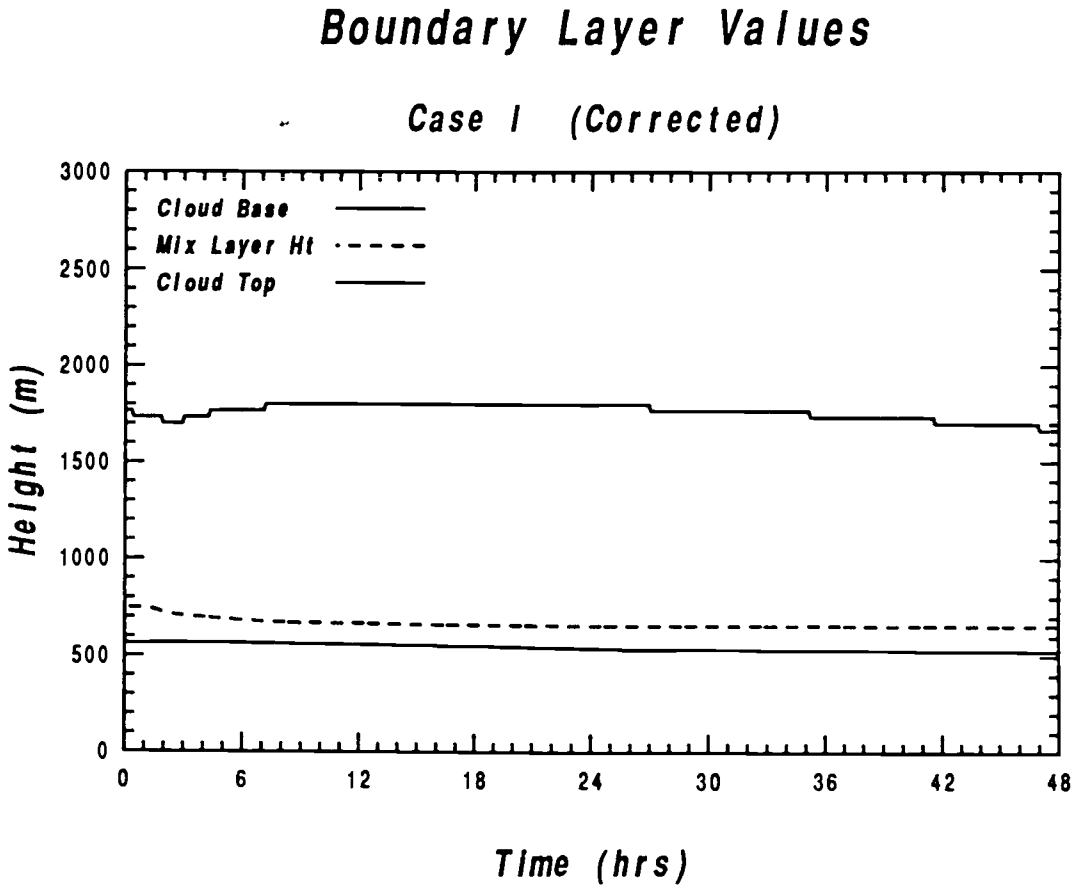

Fig 5.12 Boundary layer values over the 48 hour simulation

changes sign. In this region, buoyancy is acting to retard the generation of cloud kinetic energy. The turbulent transport term is generally removing kinetic energy from the lower regions and distributing it in the upper portion of the cloud layer and up to a few hundred meters into the inversion layer. The model seems to reach a relative balance after less than 1 hr of simulated time and maintains a near constant profile of w_c. The only exception to this is near the top of the cloud layer where the influence of the inversion layer is strong and pressing downward.

Another element of this model simulation that may be of interest is the interaction between the diagnosed mixed layer height and the height of the cloud base. Figures 5.11 and 5.12 show the change in these quantities over the 48 hours covered by this simulation. It is clear that after an initial adjustment period the mixed layer height remains relatively constant and the cloud base lowers slightly as the boundary layer moistens. This overlap appears to be a continuous feature even as the cloud top lowers and it appears that the equilibrium structure involves a mixed layer height slightly above the cloud base height. This is even more clearly defined for the moisture corrected case where a constant separation of about 100m is maintained over the most of the 48 hour simulation (Fig. 5.12).

5.2) Case II

Case 2 was run to assess the models ability to produce a cloud layer under initially dry, unstable conditions over a warm ocean surface. Under such conditions the surface moisture flux is expected to be large and model must respond to this flux by redistributing moisture effectively in the vertical. If the convection scheme fails to respond or if its response is too weak then the mixed layer will eventually become saturated and reduce the surface flux substantially. The model's ability to maintain an unsaturated boundary layer and the structure it produces in doing this says a great deal about its ability to represent convective processes.

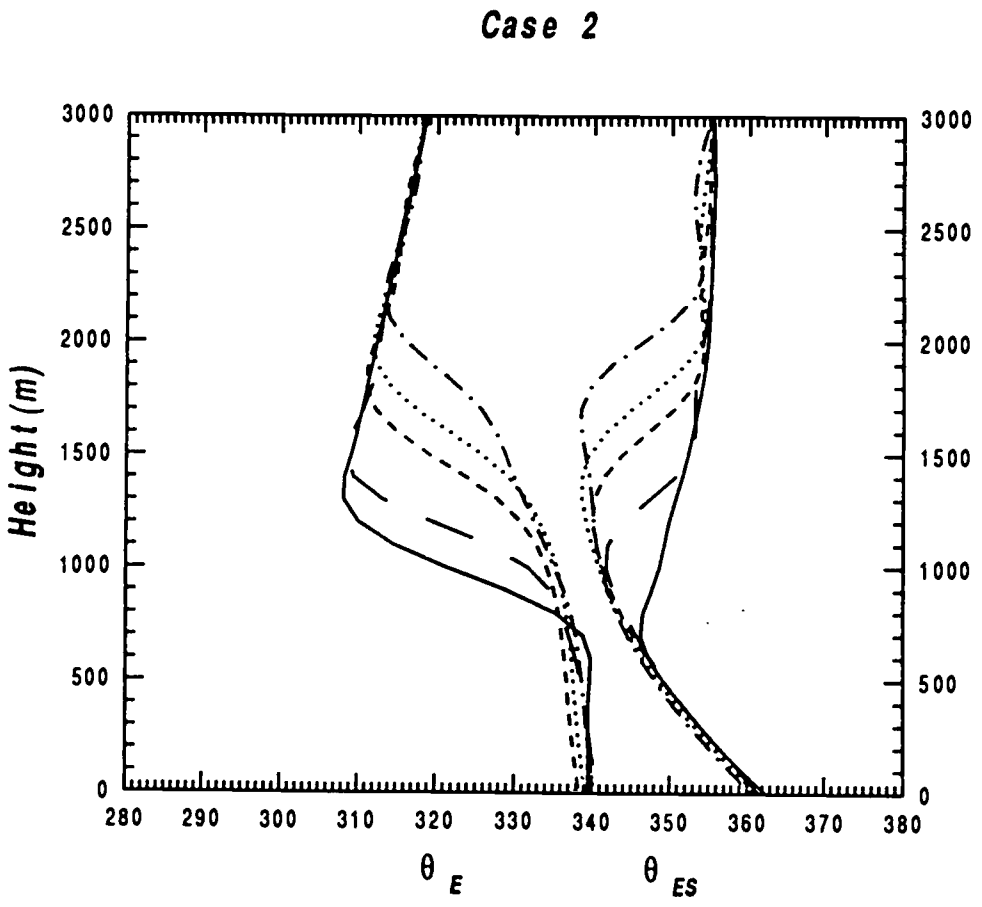

Fig 5.13 Evolution of potential temperature quantities over the 24 hour simulated time for case 2.

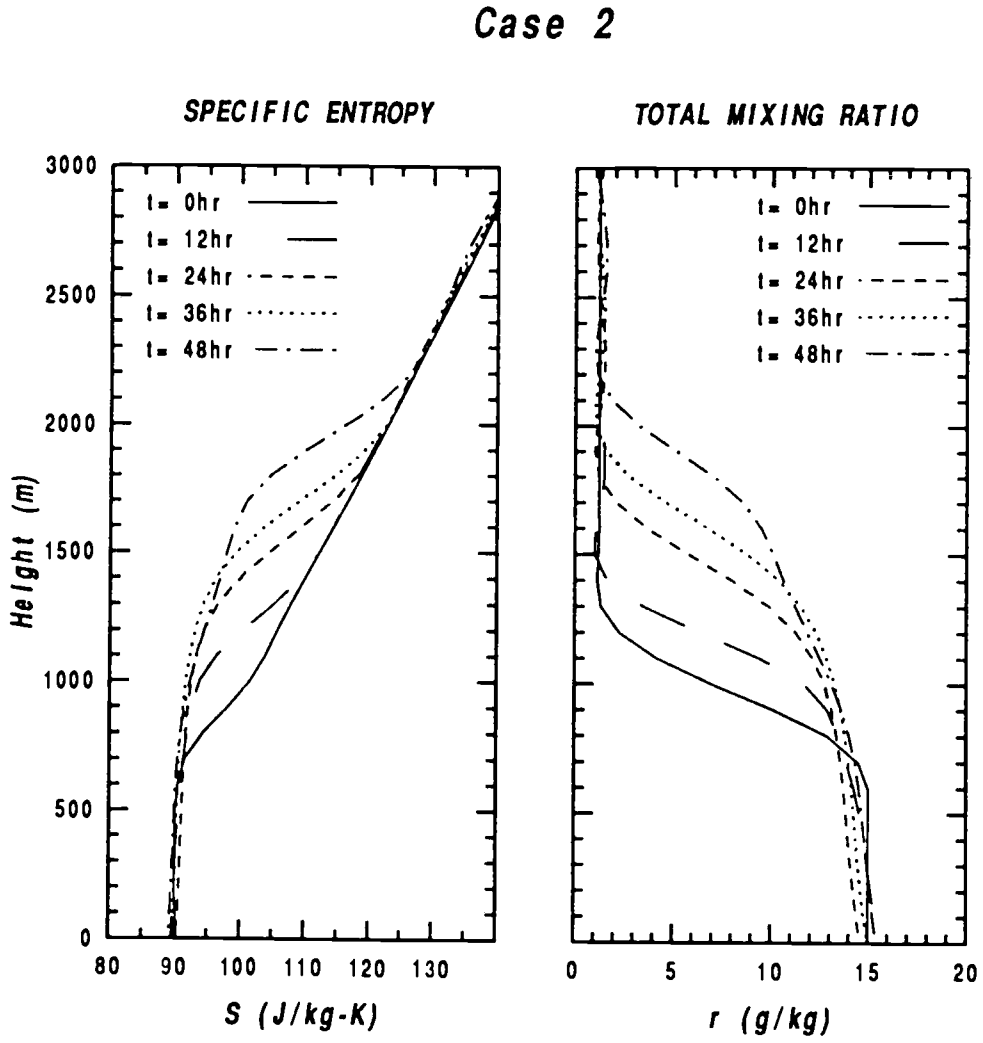

Fig 5.14 Evolution of conserved model quantities over the 24 hour simulation for case 2.

The evolution of model variables for this simulation are presented in Figs. 5.13 and 5.14a-b. From these figures it is apparent that the model was successful in both maintaining an unsaturated boundary layer over time and in producing a growing active cloud layer. It is also apparent that the model was able to produce the characteristic layered structure that includes a mixed layer, a cloud layer and a strong inversion layer. A significant moistening of the upper level is also apparent and is characterized by increases in the mixing ratio of as much as 10g/kg over the 24 hour period of this simulation. Associated with this moisture increase is a significant cooling as illustrated by a drop in θ_{ES} by over 10 deg K.

Figure 5.15 shows the evolution of several important diagnosed boundary layer values representing cloud base, cloud top and the height of the mixed layer. Several features of these curves are in sharp contrast to those of case 1. First, the relationship between the mixed layer and the cloud base heights are quite different. In case 1 they maintained a steady separation of about 100 m. Here the relationship is much more complex. The mixed layer height begins the simulation near 600m and slowly rises in response to the strong surface flux. At the same time the cloud base is relatively high (1000m) due to the dryness of the lower layer. As the mixed layer moistens, the cloud base drops and at three hours into the simulation, the mixed layer height exceeds the cloud base. This condition is necessary for cloud formation and growing cloud layer forms and persists for several hours. After about 9 hours, the mixed layer height and cloud base maintain a similar level and on several occasions the mixed layer drops below the cloud base and the condition for cloud activity is cut-off. This is characterized by the spikes in Fig. 5.15.

The intermittency modeled here is a direct result of the choice of length scales used in defining the conditions necessary for cumulus activity. These periods do not represent a collapse and rebuilding of the cloud layer as the figure might suggest, but rather periods when the buoyant production term is turned off.

Dissipation and transport of cloud kinetic energy occur as long as some kinetic energy is present. These intermittent periods are a result of the cloud scheme removing more moisture than is added at the surface and is only possible because the effects of subsidence have been removed. A complete study of intermittency would require not only a treatment of subsidence but also a reformulation of the cumulus onset condition that allows for a smoother transition. The slight oscillations observed in the mixed layer height are believed to be a result of sharp changes in this condition that turn on and off the production term.

The forcing terms for this simulation are shown in Fig 5.16 through 5.19 and show the magnitudes and structure of the individual parameterized quantities. Figure 5.16 shows the cloud and mixed layer properties at 6 hours. At this point both the cloud and mixed layer are still growing and explains why both parameterized quantities are removing moisture from the lowest layers and transporting it upwards. By 12 hours the mixed layer is no longer growing and we see a good balance in both the moisture and entropy terms below the mixed layer height. Above this moisture is increasing and the entropy is decreasing. By 18 hours (Fig. 5.18) the pattern changes somewhat and although a relative balance is achieved in the mixed layer, a peculiar pattern is developing. This is primarily the result of a negative moisture forcing and positive entropy forcing just above the mixed layer height near 1200m. What this suggests is that the cloud scheme is removing moisture from a level above the level where surface diffusion processes are acting. By 24 hours, this pattern develops into the same two layered forcing pattern found in case 1. This pattern again is characterized by a balance of the forcing terms below the mixed layer height and an additional layered structure above .

In this case, this pattern appears to be associated with the development of a feature of the cloud layer that is characterized by the linear profile of s and r above the mixed layer height. Convection is still removing moisture from the surface only if it is being deposited in the highest level. The second negative

moisture peak near 1500m on Fig. 5.19 is the models attempt to maintain the linear profiles. Given sufficient time to develop, this middle section would most likely be characterized by zero net forcing while the convection would act to remove moisture from the lowest layer and deposit it in a thin layer near the top. This must occur if the cloud layer is to remain unsaturated.

These forcing terms are integrally connected to the terms of the turbulent kinetic energy budget seen in Figs. 5.20 and 5.21 and to the profiles of terms used in the cumulus parameterization scheme (Fig. 5.22). The same pattern is seen developing in all of these terms and the boundary layer grows. Perhaps the most important of these is the structure that develops in the buoyancy length scale *l*. Between t=18hours and t=24 hours, a significant change occurs in the structure of *l* from a distinct peaked pattern to a pattern that levels off after a lower peak. The magnitude is also seen to decrease substantially as some of the moisture from the mid-cloud layer is transported aloft. This same pattern can be seen in both the cumulus velocity scale (fig. 5.22b) and in the cloud mixing coefficient. For these variables the tendency is towards a linear profile through the cloud layer.

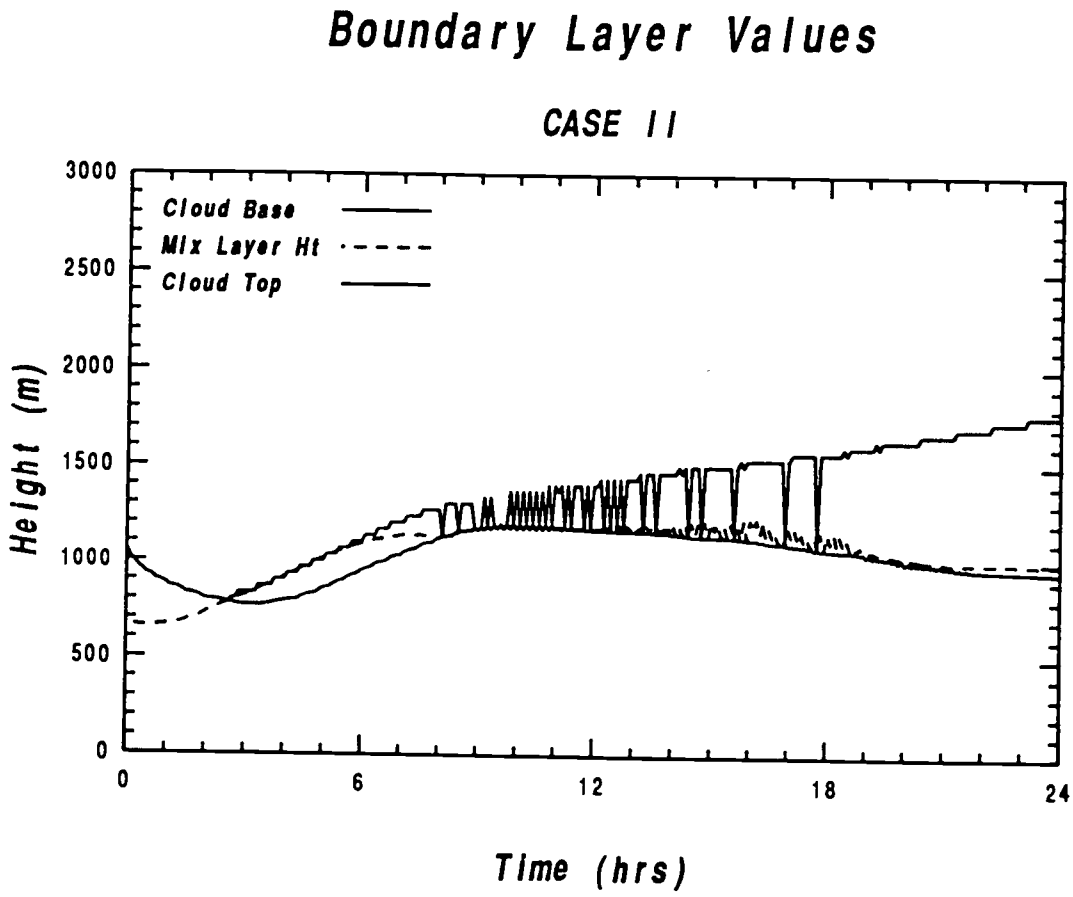

Fig 5.15 Evolution of boundary layer values for case 2.

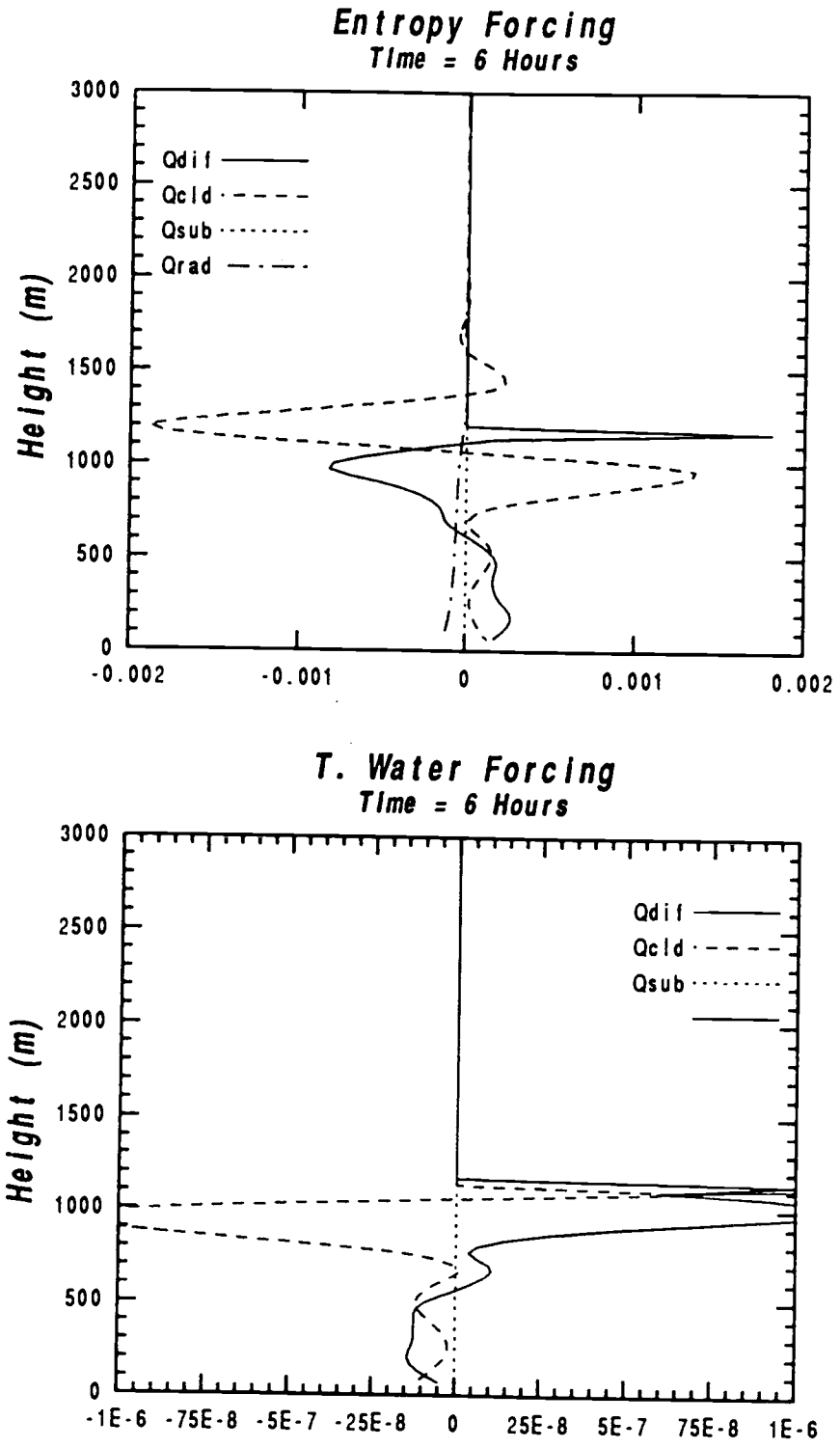

Fig 5.16a-b Parameterized forcing terms of the prognostic equations after 6 hours of simulated time.

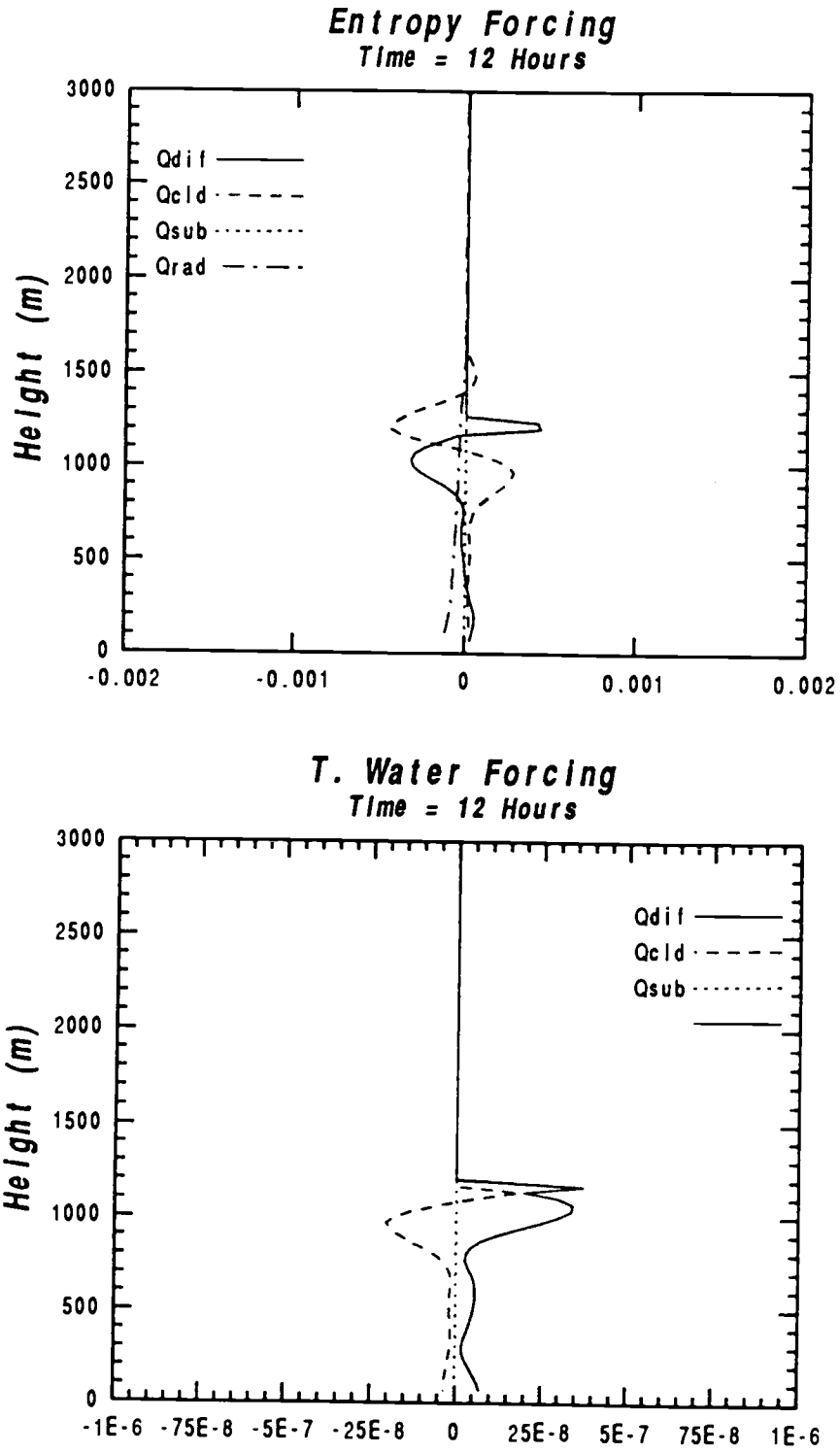

Fig 5.17 a-b Parameterized forcing terms of the prognostic equations after 12 hours of simulated time.

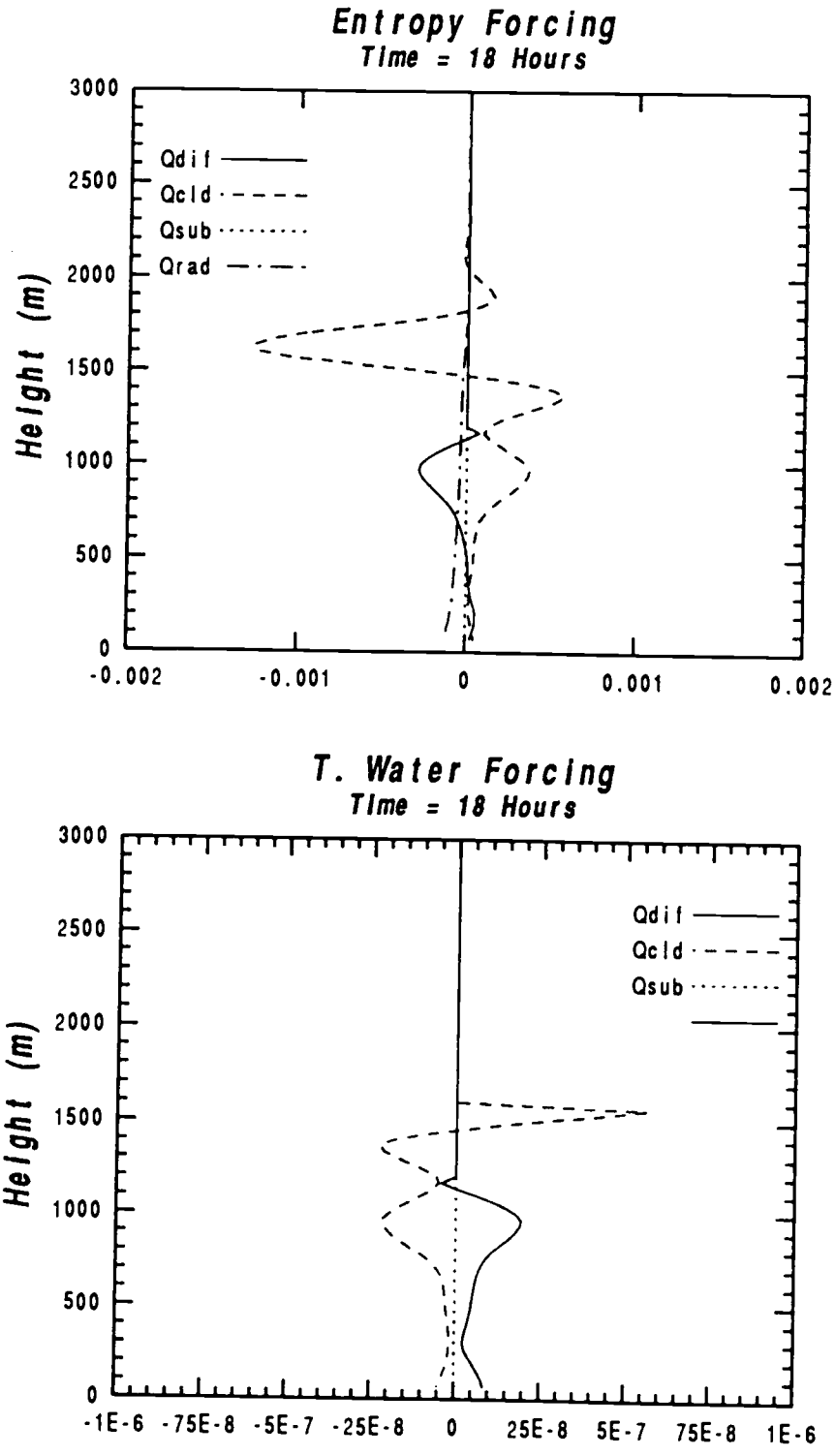

Fig 5.18a-b Parameterized forcing terms of the prognostic equations after 18 hours of simulated time.

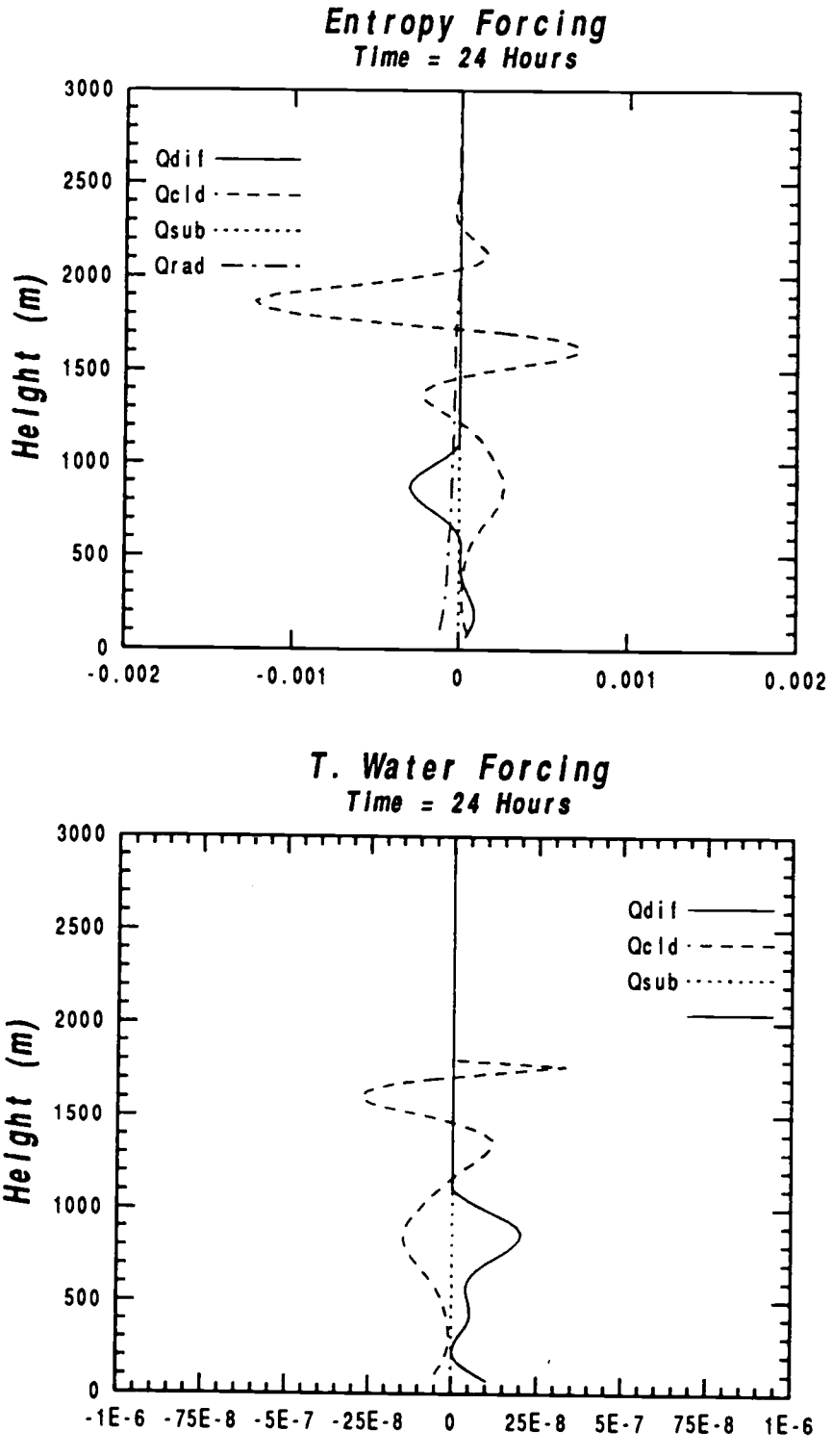

Fig 5.19a-b Parameterized forcing terms of the prognostic equations after 24 hours of simulated time.

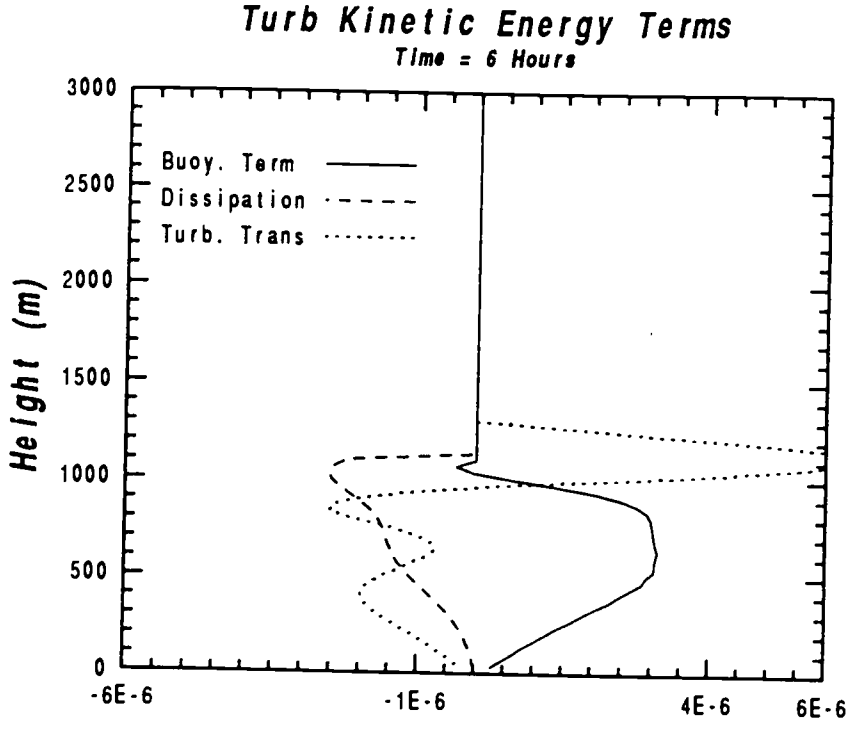

Fig 5.20a Terms of the cloud turbulent kinetic energy equation.

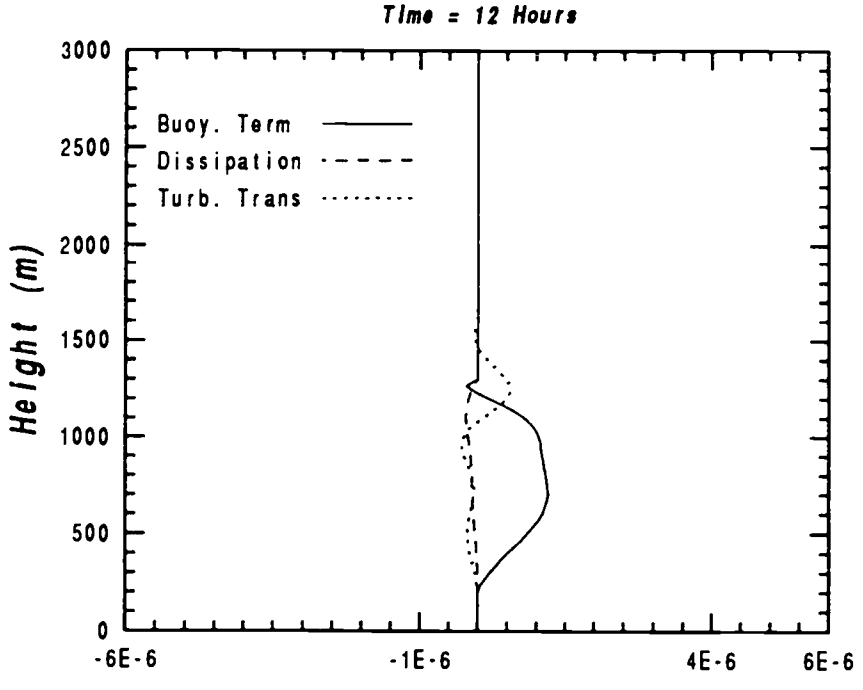

Fig 5.20b Terms of the cloud turbulent kinetic energy equation.

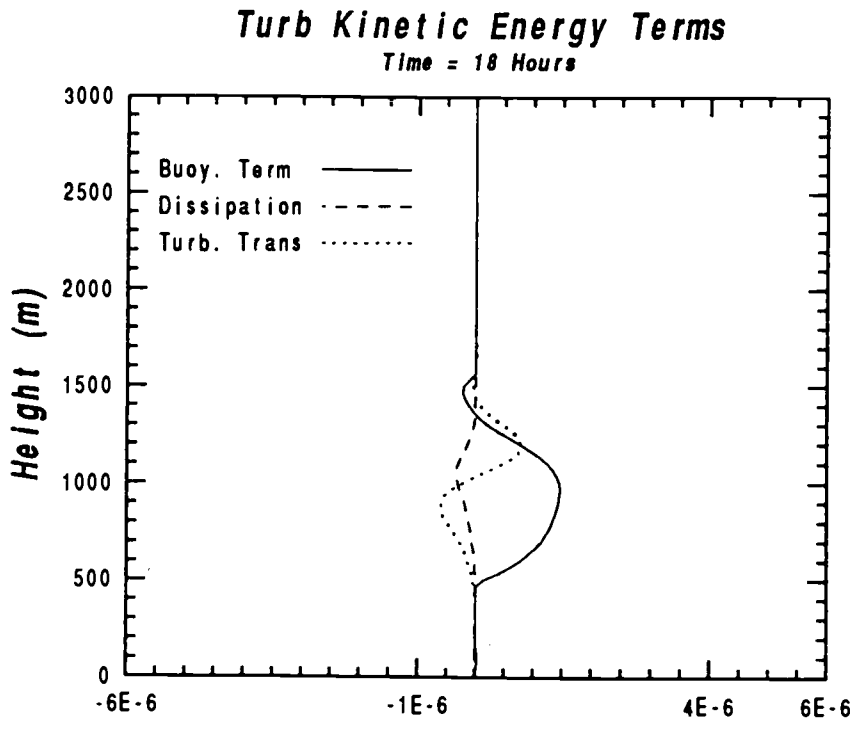

Fig 5.21a Terms of the cloud turbulent kinetic energy equation.

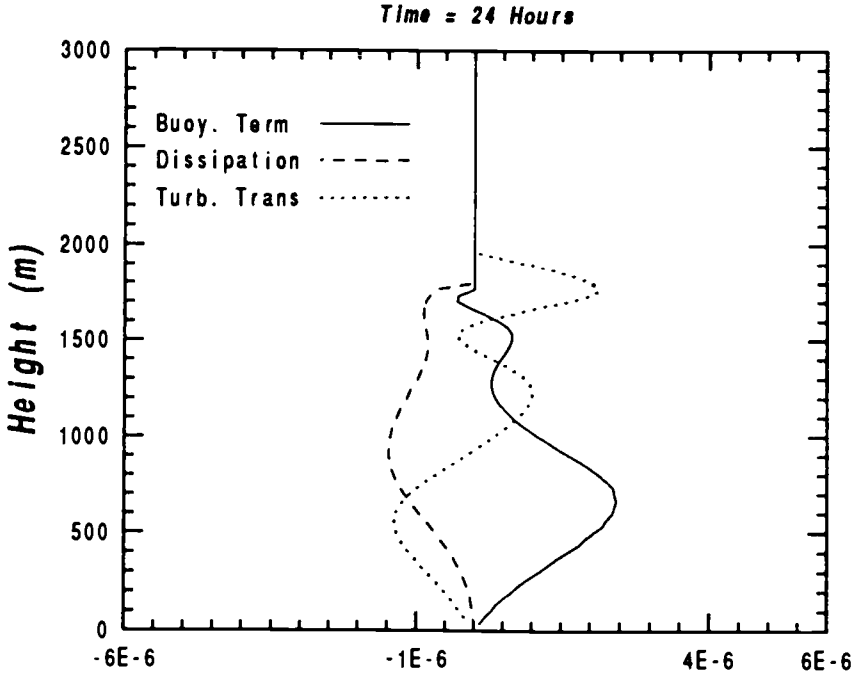

Fig 5.21b Terms of the cloud turbulent kinetic energy equation.

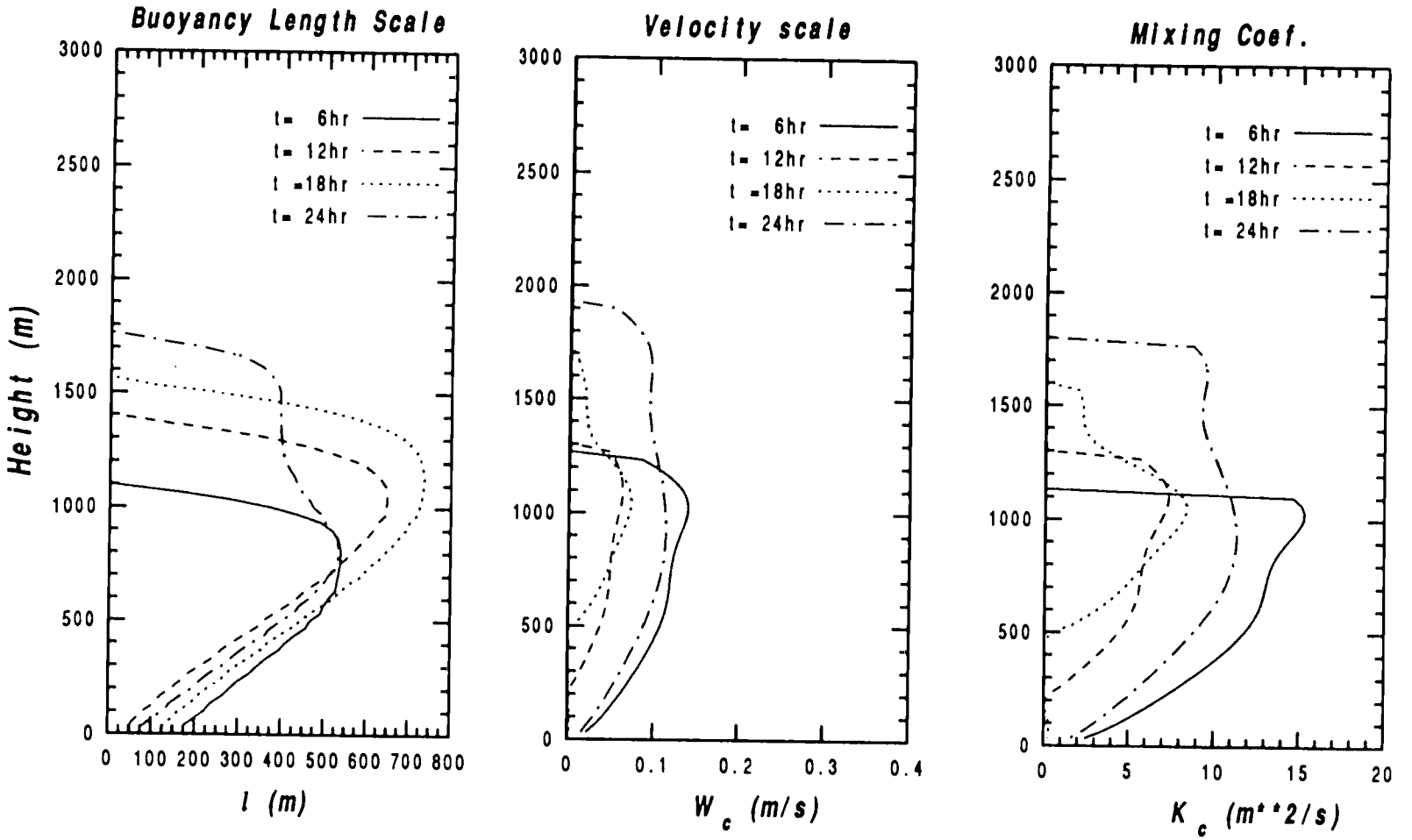

Fig 5.22 Evolution of important boundary layer variables including, a. buoyancy length scale, b. cumulus velocity scale and c. cloud mixing coefficient.

6. SUMMARY AND CONCLUSIONS

A physically based model has been developed to represent the equilibrium structure of the trade wind boundary layer. This model combines several unique concepts including the use of conserved variables to represent boundary layer processes and the use of a kinetic energy prediction equation to parameterize the effects of convective mixing. In addition, several new ideas concerning cloud mixing properties are introduced. The most fundamental of these revolves around the notion that for shallow cumulus layers, the intensity of convective mixing depends primarily on local properties rather than properties of the cloud layer as a whole. A local measure of conditional instability is used along with a special buoyancy length scale to compute the generation of the convective energy due to buoyancy. Two model simulations were performed and the results examined to assess the role of these assumptions in successfully modeling the tropical convective boundary layer.

Results of these model simulations indicate that the model performs well in responding to the effects of large-scale forcing, producing and maintaining a realistic convective boundary layer structure. While some problems were apparent, these simulations demonstrated the usefulness of the model and the relative success of cumulus parameterization scheme. The use of conserved variables also appears to provide a convenient way of both treating the thermodynamic processes associated with convective mixing and representing the characteristic layered structure of the convective boundary layer.

Results from the first simulation indicate that this model is capable of representing and maintaining an equilibrium boundary layer structure for the period of a day. The local mixing assumptions used in the development of the model and the cumulus parameterization scheme appear to be adequate to represent convective transports associated with shallow convection. Some problems

however, exist in the regions of the inversion layer where a strong imbalance of forces was observed. This behavior is thought to be mainly a result of the fact that other scales of convective activity may also contribute to the maintenance of the boundary layer structure, at least for the case studied. The model is not able to represent these other scales in its present form. It is apparent however, that the model does a reasonable job of representing that portion of the convective activity that is local in nature.

Case 1 provided a good opportunity to assess the use of several features of the model. The first is the use of a prognostic form of a kinetic energy equation to determine a velocity scale to represent convective transports. This method proved to be an effective and convenient way of determining the magnitude and strength of the convective turbulence. Although changes in the turbulent kinetic energy equation might be appropriate, the general approach appears to have merit if used consistently with the K-closure approach.

The use of a K-closure approach is based on the concept that shallow clouds are local in nature and that their mixing is dependent upon both the local gradient and the length scale of the mixing elements. The formulation used here however, has several elements that are not strictly local. For example, the buoyant length scale is used to help estimate the convective velocity scale, a measure of the intensity of the local mixing. If this length scale were to become large, then the local assumptions used and the K-closure approach might become invalid. How large the length scale would have to be in order for this to occur is difficult to say. For the simulations performed here the buoyant length scale remained relatively small and did not appear to be a problem.

The introduction of a turbulent transport term also represents a departure from a strict local approach and could also lead to a situation where the local assumptions are invalidated. This term however, was seen as necessary in order to represent the turbulent kinetic energy structure of the lower inversion layer and appeared to be effective in helping maintain the layered structure of the upper

boundary layer.

One quantity that is extremely local in nature is the conditional instability argument used in the buoyancy production term. While this term provides an effective means of representing the strength of kinetic energy production within the cloud layer it is incapable of representing any production associated convective elements overshooting the inversion base. As a result, the only source for kinetic energy above the inversion base is through turbulent transport. The use of a value averaged or integrated over a thin layer might improve the models performance.

A second length scale was used to represent the mixing length of a typical shallow convective eddy (L_c). This length scale was chosen to be on the order of the mixed layer depth. Although some evidence was presented for this choice, in truth, very little strong evidence is available. The value used appears to have worked out quite well. It not only gave reasonable values for the convective fluxes but also provided a convenient way of coupling the cloud layer and the mixed layer allowing each to have some influence over the other. During case one, a constant overlap was maintained between the depth of the mixed layer and the depth of the cloud base. It appears that the use of this length scale helped the model maintain a steady interaction between the two layers.

Results from the second simulation illustrated the ability of the model to develop a physically realistic trade wind boundary layer structure from an initial state consisting of a cloud-free mixed layer with a dry layer aloft. Some problems became apparent during this simulation and were traced to the use of a convective switch condition that turned on and off the buoyancy production term when the cloud base was diagnosed above the mixed layer height. While the condition itself seems to be a reasonable way to represent the decoulpling of the two layers, the sudden adjustment lead to some strong oscillations. Over the 24 hours of simulated time in case 2, the oscillation weakend and no signs of a growing instability was apparent. The use of a less sudden transition time may be more appropriate.

In spite of the relative success of these model simulations one key point in

particular has been neglected. This is the question of whether conserved variables alone are sufficient to model processes in partially cloudy boundary layers over a wide range of conditions. In a one dimensional model, a single combination of mean variable can represent an infinite number of actual conditions ranging from 10% to 90% cloud cover. Only when the layer is completely saturated or completely unsaturated can the partition between vapor and liquid be known for certain. The consequences of this are unclear and further work needs to be done to address this problem.

From the results of these two simulations and from the discussions presented here it is apparent that this model provides practical alternative to parameterizing and modeling the tropical trade wind boundary layer. Many of the arguments presented and used in this model are new and their exact nature not fully understood. Because most of these arguments are based on physical assumptions about the nature of convective processes, their validity and usefulness can eventually be tested To do this, more must be known about convective boundary layers and about clouds themselves. This will require more analysis, more field studies and new technology that will make it possible to accurately measure convective properties.

BIBLIOGRAPHY

Albrecht, B. A., A. K. Betts, W. H. Schubert, and S. K. Cox, 1979: A model of the thermodynamic structure of the trade-wind boundary layer: Part I. Theoretical formulation and sensitivity tests. *J. Atmos. Sci.*, **36**, 73-89.

Albrecht, B. A., 1984: A model study of downstream variations of the thermodynamic structure of the trade winds. *Tellus*, **36A**, 187-202.

Arakawa, A., and W. H. Schubert, 1974: Interaction of a cumulus cloud ensemble with the large-scale environment. Part 1. *J. Atmos. Sci.* **31**., 674-701

Augstein et al., 1973: Mass and energy transports in an undisturbed Atlantic trade wind flow. *Mon. Wea. Rev.*,**101**, 101-111.

Austin, Baker, Blyth and Jensen, 198*: Small-scale variability in warm contenental cumulus clouds. *J. Atmos. Sci.*, **42**, 1123-1138.

Beniston M. G. and G. Sommeria, 1981: Use of a detailed planetary boundary layer model for parameterization purposes. *J. Atmos. Sci.*, **38**, 780-797.

Betts A. K., and W. Ridgway, 1989: Climatic equilibrium of the Atmospheric Boundary Layer over a tropical ocean. *J. Atmos. Sci.*, **46**, 2621-2641.

Betts A. K., and B. A. Albrecht, 1987: Conserved variable analysis of the convective boundary layer thermodynamic structure over thetropical oceans. *J. Atmos. Sci.*, **44**, 83-99.

Betts A. K., 1986: A new convective adjustment scheme. Part I Observational and theoretical basis, *Quart. J. Roy. Meteor. Soc.*, **112**, 677-691.

Betts A. K., 1982: Cloud thermodynamic models in saturation point coordinates., *J. Atmos. Sci.* **39**, 2182-2191.

Betts A. K.,1975: Parametric interpretation of trade-wind cumulus budget studies. *J. Atmos. Sci.*, **32**, 1934-1945.

Betts A. K.,1973: Non-precipitating cumulus convection and its parameterization. *Quart. J. Roy. Meteor. Soc.* , **99**, 178-196

Bougeault, Ph., 1981: Modeling the trade-wind cumulus boundary layer. Part I: Testing the ensemble cloud relations against numerical data. *J. Atmos. Sci.*, **38**, 2414-2428

Blyth, A. M., W. A. Cooper and J. B. Jensen, 1988: A study of the source of entrained air in Montana cumuli. *J. Atmos. Sci.*, **45**, 3944-3963

Blyth, A. M., and Latham, 1985: An Airborn Study of Vertical Structure and Microphysical Variability Within a Small Cumulus. *Quart. J. Roy. Meteor. Soc.*, **111**, 773-792

Brummer, B., 1978: Mass and Energy Budgets of a 1 Km High Box Over the GATE C-Scale Triangle During Undisturbed and Disturbed Weather Conditions. *J. Atmos. Sci.*, **35**, 997-1010.

Cotton, C. and R. A. Anthes, 1989: Storm and cloud dynamics. Academic Press Inc., 883pp.

Deardorf, J. W., 1972: Numerical investigation of neutral and unstable planetary boundary layers. *J. Atmos. Sci.*, 29, 91-115

Ek, M. and M. Mahrt, 1989: A users guide to the OSU one-dimensional planetary boundary layer model. *Dept. Atmos. Sci, Oregon State*

Emanuel, K. A. and R. Rotunno, 1989: Polar lows as arctic hurricanes. *Tellus*, **41A**, 1-17

Emanuel, K. A., 1981: A Similarity Theory for Unsaturated Downdrafts Within Clouds. *J. Atmos. Sci.*, **38**, 1541-1557.

Emmitt, G., 1978: Tropical Cumulus Interaction with and Modification of the Subcloud Region. *J. Atmos. Sci.*, **35**, 1485-1502.

Esbensen 1975: An Analysis of Sub-Cloud layer Heat and Moisture Budgets in the Western Atlantic Trades. *J. Atmos. Sci.*, **32** , 1921-

Esbensen, 1978: Bulk Thermodynamic Effects and Properties of Small Tropical Cumuli. *J. Atmos. Sci.*, **35**, 826-

Firestone and Albrecht, 1986: The Structure of the Atmospheric Boundary Layer in the Central Equitorial Pacific During Jan., Feb. of FGGE. *Mon. Wea. Rev.*, **114**, 2219-

Fritsch and Chappell, 1980: Numerical Prediction of Convectivly Driven Mesoscale Pressure Systems Part I: Convective Parameterization. *J. Atmos. Sci.*, **37**, 1722-

Holland and Rasmusson, 1973: Measurements of the Atmospheric Mass, Momentum and Energy Budgets over a 500 km Square of Tropical Ocean. *Mon. Wea. Rev.*, **101**, 44-55

Holton, J. R., 1979: An introduction to dynamic meteorology. Academic press, 391pp.

Holtslag, A. A. M. and H. A. R. de Bruin, 1988: Applied modeling of the nighttime surace energy balance over land. *J. Appl. Meteor.*, **27**, 689-704

Iribarne, J. V. and W. L. Godson, 1981: Atmospheric thermodynamics. 2nd ed. Reidel Publ Co. 259pp.

Klemp, J. B., and R. B. Wilhelmson, 1978: The simulation of three-

dimensonal convective storm dynamics. *J. Atmos. Sci.*, **35**, 1070-1096

LeMone and Pennell, 1976: The Relationship of Trad Wind Cumulus Distribution to Subcloud Layer Fluxes and Structure. *Mon. Wea. Rev.*, **104**, 524-539

Malkus, J. S. 1956: On the Maintenance of the Tradewinds. *Tellus*, **8**, 335-350

Nicholls, S., and M. A. LeMone, 1980: The Fair Weather Boundary Layer in GATE: The Relationship of Subcloud Fluxes and Structure to the Distribution and Enhancement of Cumulus Clouds. *J. Atmos. Sci*, **37**, 2051-2067.

Nicholls, S., M.A. LeMone, and G. Sommeria, 1982: The Simulation of a Fair Weather Mariene Boundary Layer in GATE using a Three Dimensional Model. *Quart. J. Roy. Meteor. Soc.*, 48, 167-190.

Nita and Esbensen, 1974: Heat and Moisture Budget Analysis Using BOMEX Data. *Mon. Wea. Rev.*, **102**, 17-28

Nitta, T., 1975: Observational Determination of Cloud Mass Flux Distributions. *J. Atmos. Sci.*, **32**, 73-91

Ogura Y., and J, Russell and H-R Cho, 1977: A semi-empirical model of the tradewind inversion. *J. Met. Soc. Japan*, **55**, 209-222

Ooyama, K. V., 1990: A thermodynamic foundation for modeling the moist atmosphere. *J. Atmos. Sci.*, 2580-2593

Paluch, 1979: The Entrainment Mechanism in Colorado Cumuli. *J. Atmos. Sci.*, **36**, 2467-2478

Phillips, N. A., 1957: A coordinate system haveing some special advantages for numerical forecasting. *J. Meteor.*, **14**, 184-185

Pennell and LeMone, 1974: An Experimental Study of Turbulence Structure in the Fair Weather Trade Wind Boundary Layer. *J. Atmos. Sci.*, **31**, 1308-1323

Raymond, D. J. and A. M. Blyth, 1986: A Stochastic Mixing Model for Nonprecipitating Cumulus Clouds. *J. Atmos. Sci.*, **43**, 2708-2718.

Raymond, D. J., 1979: A Two-Scale Model of Moist Non-Precipitating Convection. *J. Atmos. Sci.*, **36**, 816-831

Reihl, H. and J. S. Malkus, 1957: On the heat balance and maintenance of circulation in the trades. *Quart. J. Roy. Meteor. Soc.*, **83**, 21-29

Reihl, H., T. C Yeh, J.S. Malkus, and N. E. La Seur, 1951: The North-east trade of the Pacific Ocean. *Quart. J. Roy. Meteor. Soc.*, **77**, 598-626

Rosenthal, S. L., 1978: Numerical simulations of tropical cyclone development with latent heat release by the resolvable scales I: Model description and preliminary results. *J. Atmos. Sci.*, **35**, 258-271

Sarachik, E. S. 1978: Tropical sea surface temperature: An interactive one-dimensional atmosphere-ocean model. *Dynamics of Atmospheres and Oceans*, **2**, 455-469

Sasamori, T., 1972: A linear harmonic analysis of atmospheric motion with radiative dissipation. *J. meteor. Soc. Japan,* **50**, 505-518

Sommeria, G., 1976: Three-Dimensional Simulation of Turbulent Processes in an Undisturbed Trade Wind Boundary Layer. *J. Atmos. Sci.,* **33**, 216-241.

Sommeria, G. and M. A. LeMone, 1978: Direct testing of a three - dimensional model of the planitary boundary layer against experimental data. *J. Atmos. Sci.,* **35**, 25-39.

Taylor, G. R. and M. B. Baker, 1991: Entrainment and detrainment in cumulus clouds. *J. Atmos. Sci.,* **48**, 112-121.

Tiedtke, M., W. A. Heckley and J. Slingo, 1988: Tropical forecasting at ECMWF: The influence of physical parametrization on the mean structure of forecasts and analyses. *Quart. J. Roy. Meteor. Soc.,* **114**, 639-664.

Troen, I. and L. Mahrt, 1986: A simple model of the atmospheric boundary layer; sensitivity to surface evaporation. *Bound. Layer Meteor.* **37**, 129-148

Yamamoto, G., M. Tanaka and S. Asano, 1970: Radiative transfer in water clouds in the infrared region. *J. Atmos. Sci.,* **27**, 282-292

Yanai, M., J. H. Chu, T. E. Stark and T. Nitta, 1976: Response of deep and shallow tropical maritime cumuli to large scale processes. *J. Atmos. Sci.,* **33**, 976-991

Appendices

Appendix 1 List or Terms

m	-	Total mass of air-water system
m_a	-	Mass of dry air
m_v	-	Mass of water vapor
m_m	-	Mass of water substances
m_c	-	Mass of airborne condesate
m_w	-	Mass of airborne liquid water
T	-	Temperature (same for all constituants)
V	-	Volume of system
P	-	Total pressure of system
P_a	-	Pressure exerted by dry air
P_v	-	Pressure exerted by water vapor
$E_w(T)$	-	Saturation vapor pressure with respect to water
ρ	-	Total density of system (dry air + water)
ξ	-	Density of dry air (m_a/V)
η	-	Density of water substances (m_v/V)
ρ_v	-	Density of water vapor
ρ_c	-	Density of condensate
r	-	Mixing ratio of total water substance (m_m/m_a)
r_v	-	Mixing ratio of water vapor (m_v/m_a)
ε	-	Molecular weight ratio of vapor and dry air
R_a	-	Specific gas constant for dry air
R_v	-	Specific gas constant for water vapor
C_{pa}	-	Specific heat of dry air at constant pressure
C_{va}	-	Specific heat of dry air at constant volume ($C_{pa} = C_{va}+R_a$)

C_{pv}	-	Specific heat of water vapor at constant pressure
C_{vv}	-	Specific heat of water vapor at constant volume
$L(T)$	-	Latent heat of liquid-vapor phase change
$L_i(T)$	-	Latent heat if liquid-ice phase change
s	-	Specific entropy
h	-	Height of the mixed layer
L_c	-	Convective mixing length scale
w_c	-	Convective mixing velocity scale
w_s	-	Subsidence velocity parameter
E	-	Cloud turbulent kinetic energy
A_p	-	Buoyant production of cloud turbulent kinetic energy
l	-	Buoyancy length scale

Appendix 2. Derivation of Entropy Equation

Gibbs theorem states that the total entropy of a system is the sum of the partial entropies of the individual constituents. This can be expressed as

$$dS = \sum_i dS_i$$

where the subscript i represents the phase of each constituent present. Thus i will be either a, for dry air, v for water vapor or c for condensate. The total differential expansion for each individual component takes the form

$$dS_i = \frac{\partial S_i}{\partial T})_{P,m} dT + \frac{\partial S_i}{\partial P})_{T,m} dP + s_i dm_i$$

For each of the three components of air this total differential will become

$$dS_a = \frac{\partial S_a}{\partial T})_{P,m} dT + \frac{\partial S_a}{\partial P})_{T,m} dP + s_a dm_a$$

$$dS_v = \frac{\partial S_v}{\partial T})_{P,m} dT + \frac{\partial S_v}{\partial P})_{T,m} dP + s_v dm_v$$

$$dS_c = \frac{\partial S_c}{\partial T})_{P,m} dT + \frac{\partial S_c}{\partial P})_{T,m} dP + s_c dm_c$$

Several thermodynamic relationships exist that can greatly simplify these expressions. These relationships take the form

$$S_i = s_i m_i \qquad dm_a = 0$$

$$\frac{\partial s_a}{\partial T})_{P,m} = \frac{c_{Pa}}{T} \qquad \frac{\partial s_a}{\partial P})_{,Tm} = -\frac{R_a}{P_a}$$

$$\frac{\partial s_v}{\partial T})_{P,m} = \frac{c_{Pv}}{T} \qquad \frac{\partial s_a}{\partial P})_{,Tm} = -\frac{R_v}{P_v}$$

$$\frac{\partial s_c}{\partial T})_{P,m} = \frac{c_c}{T} \qquad \frac{\partial s_c}{\partial P})_{,Tm} \equiv 0. \qquad dm_c = -dm_v$$

Using these relationships the component differential entropy equations become

$$dS_a = m_a c_{Pa} d\ln T - m_a R_a d\ln P_a$$

$$dS_v = m_v c_{Pv} d\ln T - m_v R_v d\ln P_v + s_v dm_v$$

$$dS_c = m_c c_c d\ln T + s_c dm_c$$

With these entropy equations it is now possible to combine partial entropies using Gibbs theorem. It will then be possible to define a reference state and integrate over the change from this reference state to a final state. The saturation condition of this final state leads to the necessity to compute two forms of the entropy equation; one for unsaturated conditions (S_1) and one for saturated conditions (S_2) where condensate is present. The reference state of both will be the same and consist of a marginally saturated state at temperature T_0, dry air pressure P_a, vapor pressure E(T), mass of dry air m_a and a mass of total moisture m_m. This moisture will be entirely in the form of vapor ($m_v = m_m$)

Unsaturated Air.

$$dS_1 = dS_a + dS_v$$

$$dS_1 = m_a c_{p_a} d\ln T - m_a R_a d\ln P_a + m_v c_{p_v} d\ln T - m_v R_v d\ln P_v + s_v dm_v$$

For the unsaturated case, no condensate is formed so the masses of dry air and water vapor remained fixed and the integrated form of the entropy equation becomes,

$$S_1 = (m_a c_{p_a} + m_v c_{p_v}) \ln \frac{T}{T_0} - m_a R_a \ln \frac{P_a}{P_{a_0}} - m_v R_v \ln \frac{P_v}{P_{v_0}} + S_0$$

To put this in terms of the prognostic variables, the two equations of state are used to eliminate the pressure terms and the resulting expression is simplified by using the relationships $c_{v_a} = c_{p_a} - R_a$ and $c_{v_v} = c_{p_v} - R_v$, and the whole equation is divided by the volume to put the mass term in the form of densities. With these changes and the assumption that the reference state entropy is zero (S_0=0),the unsaturated form of the entropy equation is

$$\sigma_1 = \xi \left(c_{v_a} \ln \frac{T}{T_0} - R_a \ln \frac{\xi}{\xi_0} \right) + \eta \left(c_{v_v} \ln \frac{T}{T_0} - R_v \ln \frac{\eta}{\eta_0} \right)$$

Saturated Air.

$$dS_2 = dS_a + dS_v + dS_c$$

$$dS_2 = (m_a c_{Pa} + m_v c_{Pv} + m_c c_c) d\ln T - m_a R_a d\ln P_a - m_v R_v d\ln P_v + s_v dm_v + s_c dm_c$$

Using the same initial state as in the unsaturated case, this expression can be simplified by recognising the following relationships

$m_c = 0$	no condensate present
$m_v = m_m$	all moisture exists a vapor
$dm_c = dm_v$	depletion of vapor becomes condensate

$$(s_v - s_c) = \frac{L(T)}{T}$$

These simplifications along with the property that m_m and m_a are constant, give an integrated form of the saturated entropy equation of the form

$$S_2 = m_a\left(c_{Pa}\ln\frac{T}{T_0} - R_a\ln\frac{P_a}{P_{a0}}\right) + m_m c_{Pv}\ln\frac{T}{T_0} - m_m R_v \ln\frac{E(T)}{E(T_0 T}$$

$$+ \frac{L(T)}{T}(m_v - m_m)$$

This can be put in terms of the model prognostic variables by using the equation of state for dry air to eliminate Pa and by using the Clausius Clapyron and Kichoffs equations to get the expression,

$$R_v \ln\frac{E(T)}{E(T_0)} = c_{Pv}\ln\frac{T}{T_0} - C(T) + \frac{L(T)}{T} - \frac{L(T_0)}{T_0}$$

Upon substitution of this, the equation of state for dry air, and after dividing through by the volume, the saturated form of the entropy density equation becomes

$$\sigma_2 = \xi\left(c_{va}\ln\frac{T}{T_0} - R_a\ln\frac{\xi}{\xi_0}\right) + \eta C(T) + \eta^* \frac{L(T)}{T} - \eta\frac{L(T_0)}{T_0}$$

where

$$C(T) = \int_{T_0}^{T}\frac{c_c}{T}dT = c_c\ln\frac{T}{T_0}$$

Appendix 3 Numerical Solutions

3.1). Temperature

This sections presents the details of the iteration scheme used to determine the temperature (T_2) from the saturated form of the entropy equation. This process involves solving the following equation for T.

$$\sigma_2 = \xi\left(c_{v_a}\ln\frac{T}{T_0} - R_a\ln\frac{\xi}{\xi_0}\right) + \eta^*\frac{L(T)}{T} - \eta\frac{L(T_0)}{T_0} + \eta c_c\ln\frac{T}{T_0}$$

Let $\tau = \ln\dfrac{T}{T_0}$

$$G(\tau) = \frac{dE(T)}{dT}$$

$$x = \xi c_{va} + \eta c_c$$

$$z = \sigma + \xi R_a\ln\frac{\xi}{\xi_0} + \eta\frac{L(T_0)}{T_0}$$

So that the entropy equation becomes

$$x\tau + G(\tau) - z = F(\tau_i;x)$$

We need to find τ such that the condition $F(\tau;x) = 0$ is satisfied. To do this we can use Newtons method in the iterative form

$$\tau_{n+1} = \tau_n - \frac{F(\tau_n;x)}{F'(\tau_n;x)}$$

where

$$F'(\tau_n;x) = x + G'(\tau) = x + \frac{d^2E(T)}{dT^2}$$

The iteration is performed until

$$| \tau_{n+1} - \tau_n | \leq \text{tolerance}$$

3.2). Vertical Velocity

To determine the vertical velocity under the conditions set forth in the current form of the model it is necessary to solve the following equation for w at each model level.

$$\frac{\partial}{\partial z}\left[\rho c_N^2 \frac{\partial w}{\partial z} \right] = \frac{\partial}{\partial z}(P_\xi Q_\xi + P_\eta Q_\eta + P_\sigma Q_\sigma) + g(Q_\xi + Q_\eta)$$

To do this in a manner consistent with the configuration of the model, a Galerkin method is used to reduce the set of n equations to a matrix form. To do this let

$$F(Q) = \frac{1}{\rho C_N^2}\frac{\partial}{\partial z}(P_\xi Q_\xi + P_\eta Q_\eta + P_\sigma Q_\sigma) + g(Q_\xi + Q_\eta)$$

$$K1(z) = \frac{1}{\rho C_N^2}\frac{\partial}{\partial z}(\rho C_N^2)$$

so that the equation may be written as

$$[\, w_{zz} + K1(z) w_z - F(Q) \,] = 0.$$

Following the Galerkin method, multiply this by the basis function at each model level and integrate over the domain to obtain

$$[\, w_{zz} + K1(z) w_z - F(Q) \,|\, \phi_n = 0.$$

$$\int_a^b [\, w_{zz} + K1(z) w_z - F(Q) \,|\, \phi_n = 0.$$

and, following the numerical representation of the model, the vertical velocity can be represented as

$$w = \sum_{m=1}^{M+1} a_m \phi_m$$

Substituting this expression into the above representation we obtain

$$\sum_{m=1}^{M+1} a_m \left\{ \int_a^b \phi_m'' \phi_n dz + \int_a^b K1(z) \phi_m' \phi_n dz \right\} = \int_a^b F(Q) \phi_n dz$$

where the first integral can be integrated by parts to reduce the order of the derivative. If the boundary conditions are assigned such that w(a)= w(b) = 0, then this expression simplifies to

$$\sum_{m=1}^{M+1} a_m \left\{ -\int_a^b \phi_m' \phi_n' dz + \int_a^b K1(z) \phi_m' \phi_n dz \right\} = \int_a^b F(Q) \phi_n dz$$

This can be represented in matrix notation as

$$[-M + R] \vec{a}_m = \vec{b}$$

where the integral elements of the matrix are

$$M = \int_a^b \phi_m' \phi_n' dz$$

$$R = \int_a^b K1(z) \phi_m' \phi_n dz$$

$$b = \int_a^b F(Q) \phi_n dz$$

To determine the matrix elements, analytically derived values are use for the components of M while values for b and R must be determined numerically each each time the equation is solved due to the presence of time dependent coefficients inside the integrals. Upon solution of the matrix system for the spline amplitudes, the vertical velocity can be obtained using the summation representation shown above. It is important to note that using this form of the derivation, the boundary conditions on the vertical velocity must always remain zero.